

**Gene expression analysis of neuronal precursors  
from adult mouse brain and differential screen for  
neural stem cell markers**

**Inaugural-Dissertation  
zur Erlangung des Doktorgrades  
der Mathematisch-Naturwissenschaftlichen Fakultät  
der Universität zu Köln**

**vorgelegt von  
Sandra Pennartz  
aus Krefeld**

**Köln, 2004**

Berichtersteller: Prof. Dr. Sigrun Korsching  
Prof. Dr. Jens Brüning  
Dr. Harold Cremer

Tag der mündlichen Prüfung: 03.11.2004

## Zusammenfassung

Im adulten Maushirn gehen in der subventrikulären Zone (SVZ) fortwährend neuronale Vorläuferzellen aus neuralen Stammzellen (NSZ) hervor und migrieren in den *Bulbus olfactorius* (OB), wo sie in GABAerge Interneuronen differenzieren. PSA-NCAM (*Polysialic acid-Neural cell adhesion molecule*) wird während des Migrationsprozesses spezifisch von den unreifen neuronalen Zellen (PSA<sup>+</sup> Zellen) exprimiert. Diese Tatsache wurde im Rahmen dieser Doktorarbeit genutzt, um eine homogene Population von neuronalen Vorläuferzellen per FACS (*Fluorescence-activated cell sorting*) zu isolieren. Die Genexpression der PSA<sup>+</sup> Zellen wurde umfassend mit Hilfe der Seriellen Analyse der Genexpression (SAGE) untersucht. Der Vergleich der SAGE-Daten von PSA<sup>+</sup> Zellen und adultem Gesamthirn (ATB) führte zur Identifizierung von Genen, die in den Vorläuferzellen überexprimiert sind. Für ausgewählte Gene wurden die SAGE-Ergebnisse mittels *cDNA Microarray* und quantitativer *Real-time PCR* validiert und die zelluläre Expression im Maushirn mit Hilfe von *in situ* Hybridisierungen analysiert. Zuvor in diesem Zusammenhang beschriebene Gene wie der Proliferationsinhibitor CD24, die Sialyltransferase STX und der Reelin-Rezeptor ApoER2 bestätigten die Identität der Vorläuferzellen und die Präzision der SAGE. Einzelne bereits charakterisierte, aber in der PSA<sup>+</sup> Zellpopulation noch unbekannte Gene wurden identifiziert ebenso wie die konzertierte Expression funktioneller Gengruppen. Das Vorkommen von Transkriptionsfaktoren der Sox- und Dlx- Familie, Pax6 und Meis2 weist daraufhin, dass die sekundäre Neurogenese weitgehend von den gleichen Faktoren kontrolliert wird wie die primäre in der Embryogenese. Gene für Apoptose und Proliferation werden beide stark exprimiert. Die auffallend hohe Expression chemotaktischer Faktoren legt nahe, dass diese bei der neuronalen Migration eine Rolle spielen könnten. Außerdem wurden gänzlich uncharakterisierte Gene wie zum Beispiel RIKEN 3110003A17 beobachtet. Im Rahmen unserer Kollaboration mit dem *Developmental Biology Institute of Marseille* entstehen erste auf der SAGE basierende funktionelle Daten.

Das Defizit an Markergenen für NSZ beeinträchtigt den Fortschritt in der Stammzellforschung. Daher war ein weiteres Ziel dieser Arbeit, potentielle NSZ-Marker durch den Vergleich von SAGE-Daten für embryonale Stammzellen (ES-Zellen), PSA<sup>+</sup> Zellen und ATB zu identifizieren. Hierzu wurde eine SAGE-Datenbank für Bruce-4 ES-Zellen erstellt. Die verwendete Selektionsstrategie basierte auf zwei Annahmen: Erstens, das Entwicklungspotential nimmt von ES-Zellen über NSZ, über neuronale Vorläuferzellen bis hin zu adulten Neuronen und Glia ab. Zweitens, die genetischen Programme von ES-Zellen und NSZ überlappen. Unter diesen Voraussetzungen sollten einige der Gene, die in ES-Zellen stark exprimiert werden, aber nur schwach oder gar nicht in PSA<sup>+</sup> Vorläuferzellen und ATB, in den wenigen NSZ im Gehirn aktiv sein. Acht Gene, die für Zelloberflächenproteine kodieren, wurden von der resultierenden Kandidatenliste ausgewählt und untersucht:

Aufgrund eines fehlerhaften Eintrags in einer öffentlichen Datenbank wurde die Expression für den Glutamattransporter GLT1 mit Hilfe von *in situ* Hybridisierungen untersucht und in *Embryoid bodies*, in *Neurospheres* und bemerkenswerterweise in der SVZ, der neurogenen Zone im adulten Gehirn, nachgewiesen.

Im Rahmen dieser Arbeit wurde das erste Genexpressionsprofil PSA<sup>+</sup> neuronaler Vorläuferzellen erstellt, welches gemeinsam mit den SAGE-Daten der Bruce-4 ES-Zellen eine Ausgangsbasis für zukünftige funktionelle Analysen darstellt.

## Abstract

In the adult mouse brain, neuronal precursor cells continuously emanate from neural stem cells (NSC) in the subventricular zone (SVZ) and migrate into the olfactory bulb (OB) where they differentiate to serve as replenishment for GABAergic interneurons. During the migration process, PSA-NCAM (Polysialic acid-Neural cell adhesion molecule) specifically marks the neuronal precursors (PSA<sup>+</sup> cells). This phenomenon was exploited in the framework of this doctoral thesis to isolate a homogeneous cell population of neuronal precursor cells using Fluorescence-activated cell sorting. Here, the first comprehensive picture of the gene expression in PSA<sup>+</sup> precursors was generated using Serial Analysis of Gene Expression (SAGE). Comparison of SAGE data for PSA<sup>+</sup> cells and for adult total brain (ATB) led to the identification of precursor-enriched genes. For selected genes, the results were validated using cDNA microarrays and quantitative real-time PCR, and the expression was analyzed at the cellular level in mouse brain using *in situ* hybridizations. Genes previously described in this context like the proliferation inhibitor CD24, the sialyltransferase STX and the Reelin receptor ApoER2 confirmed the identity of the precursor cells and the accuracy of the SAGE. Individual characterized genes that were so far unknown in the PSA<sup>+</sup> cell population were identified as well as functional groups of genes by means of cluster analysis of SAGE data. The presence of transcription factors of the Sox and Dlx families, Pax6 and Meis2 indicated that secondary neurogenesis might be largely controlled by the same factors that are active during development. Clusters for apoptosis and proliferation are both upregulated. The high expression of chemotactic factors in the neuronal precursors suggests that they might be involved in neuronal cell migration. In addition, novel genes like RIKEN 3110003A17 were observed. First functional data based on the SAGE are being generated in the framework of our collaboration with the Developmental Biology Institute of Marseille.

Given that a lack of markers for NSC considerably impedes progress in NSC biology, the second part of this work aimed at identifying potential NSC markers by comparing SAGE data for embryonic stem (ES) cells, PSA<sup>+</sup> cells and ATB. The selection strategy was based on two assumptions. First, in a hierarchical order of developmental potential, ES cells are positioned above NSC, which are above restricted precursors that in turn are above adult neurons and glia. Second, the genetic programs of ES cells and NSC overlap. Thus, genes that are highly expressed in ES cells and downregulated or absent in PSA<sup>+</sup> neuronal precursors and ATB should in part also be expressed by the few stem cells in the adult brain. Eight candidates coding for cell surface proteins were identified from the resulting list of candidates and were investigated.

Due to a public database mistake *in situ* hybridizations were performed for the glutamate transporter GLT1 and demonstrated expression in embryoid bodies, neurospheres and, strikingly, in the SVZ, the neurogenic area of the mouse forebrain.

Taken together, this doctoral thesis generated the first gene expression profile for PSA<sup>+</sup> neuronal precursors, which -together with the SAGE library for Bruce-4 ES cells- will serve as a starting basis for future functional analysis.

## Abbreviations

Ara-C	Cytosine- $\beta$ -D-arabinofuranoside
aRNA	Amplified RNA
ATB	Adult total brain
bp	Base pair(s)
BrdU	5-Bromo-2-deoxyuridine
BSA	Bovine serum albumin
cDNA	Copy DNA
CGCP	Cerebellar granule cell precursor cell(s)
CNS	Central nervous system
dATP	Deoxyadenosine triphosphate
dCTP	Deoxycytosine triphosphate
dGTP	Deoxyguanosine triphosphate
DiI	1,19-dioctadecyl-6,69-di(4-sulfophenyl)-3,3,39,39-tetramethyl-indocarbocyanine
DMEM	Dulbecco's modified Eagle's medium
DNA	Deoxyribonucleic acid
dNTPs	Deoxyribonucleotid triphosphate
dTTP	Deoxythymidine triphosphate
E	Embryonic day
EC	Embryonic carcinoma
ECM	Extracellular matrix
ES	Embryonic stem
FACS	Fluorescence-activated cell sorting
FCS	Fetal calf serum
GFAP	Glial fibrillary acid protein
GO (A)	Gene Ontology (Annotation)
h	Hours
HBSS	Hank's Balanced Salt Solution
LV	Lateral ventricle
min	Minutes
NSC	Neural stem cell(s)
Nt	Nucleotides
OB	Olfactory bulb
P	Postnatal day
PBS	Phosphate-buffered saline
PCR	Polymerase chain reaction
PIQOR	Parallel Identification and quantification of RNAs
qPCR	Quantitative real-time PCR
RMS	Rostral migratory stream
RNA	Ribonucleic acid
RT	Room temperature
SAGE	Serial analysis of gene expression
sec	Seconds
SGZ	Subgranular zone
SSC	Saline sodium citrate
SVZ	Subventricular zone
Tk	Thymidine kinase
VZ	Ventricular zone

**CONTENTS**

**1 INTRODUCTION.....1**

**1.1 Neurogenesis in the adult mammalian brain ..... 1**

1.1.1 Neuronal precursors are born in the adult SVZ and become olfactory bulb interneurons ..... 1

1.1.2 The hippocampal subgranular zone produces new granule neurons ..... 7

1.1.3 Adult neural stem cells and the search for marker genes ..... 8

1.1.3.1 Specific genetic markers for NSC have not been identified..... 10

**1.2 Aim of the study ..... 13**

**2 MATERIALS AND METHODS..... 15**

**2.1 Gene expression analyses ..... 15**

2.1.1 SVZ dissection and dissociation..... 15

2.1.2 Purification of PSA<sup>+</sup> cells by FACS..... 15

2.1.3 RNA isolation ..... 16

2.1.4 Serial analysis of gene expression (SAGE)..... 16

2.1.5 Microarrays..... 17

2.1.6 Quantitative real-time PCR (qPCR) ..... 18

**2.2 Cell culture ..... 19**

2.2.1 General cell culture conditions ..... 19

2.2.2 TE 671 cell line ..... 19

2.2.3 ES cell line Bruce-4..... 19

2.2.4 Preparation of embryoid bodies..... 20

2.2.5 Preparation of neurospheres ..... 20

**2.3 Histological analyses..... 21**

2.3.1 Preparation of cryosections ..... 21

2.3.2 *In situ* hybridizations ..... 22

2.3.2.1 Generation of Digoxigenin-labeled RNA probes ..... 22

2.3.2.2 Hybridization ..... 23

2.3.3	Immunohistochemistry .....	24
2.3.3.1	Staining with a peroxidase system.....	24
2.3.3.2	Immunofluorescence .....	25
2.3.3.3	Primary antibodies.....	25
2.3.3.4	Secondary antibodies.....	25
2.3.4	Microscopy .....	26
<b>3</b>	<b>RESULTS .....</b>	<b>27</b>
<b>3.1</b>	<b>Choice of SAGE libraries.....</b>	<b>27</b>
3.1.1	Isolation of PSA <sup>+</sup> neuronal precursor cells from the adult mouse brain .....	27
3.1.1.1	Control experiments with the human cell line TE 671 .....	29
3.1.2	Isolation of Bruce-4 ES cells.....	29
<b>3.2</b>	<b>Generation of SAGE libraries for PSA<sup>+</sup> precursors and ES cells.....</b>	<b>30</b>
<b>3.3</b>	<b>PSA<sup>+</sup> cell-enriched genes identified by SAGE .....</b>	<b>31</b>
3.3.1	Clustering of SAGE data .....	36
3.3.2	Validation of SAGE results using microarrays and qPCR.....	40
3.3.3	<i>In situ</i> hybridizations for selected genes in mouse brain.....	42
3.3.4	Analysis of the rostral migratory stream in PlexinA3-deficient mice.....	45
<b>3.4</b>	<b>Genes identified in ES cells by SAGE.....</b>	<b>46</b>
3.4.1	Characteristic genes for pluripotent cells .....	46
3.4.2	Selection of potential NSC marker genes.....	49
3.4.3	Investigation of potential NSC marker genes.....	51
3.4.3.1	Expression in embryoid bodies and neurospheres.....	51
3.4.3.2	Expression in mouse brain.....	52
<b>3.5</b>	<b>Analysis of GLT1 expression.....</b>	<b>54</b>
<b>4</b>	<b>DISCUSSION.....</b>	<b>62</b>
<b>4.1</b>	<b>Gene expression analyses .....</b>	<b>62</b>
<b>4.2</b>	<b>Transcriptome analysis of PSA<sup>+</sup> neuronal precursor cells .....</b>	<b>63</b>
4.2.1	Already known genes confirm the SAGE results.....	63

## Contents

---

4.2.2	Novel genes were identified in the PSA <sup>+</sup> cell population .....	63
4.2.3	First functional data based on the SAGE results are generated.....	68
<b>4.3</b>	<b>Analysis of ES cell-enriched genes and potential NSC markers .....</b>	<b>69</b>
4.3.1	Characteristic genes confirm pluripotency of ES cells.....	69
4.3.2	Potential NSC markers were selected from the SAGE data.....	71
<b>4.4</b>	<b>Intense GLT1 expression was found in a neurogenic area .....</b>	<b>73</b>
4.4.1	Future experiments for GLT1 .....	76
<b>4.5</b>	<b>Conclusions and outlook .....</b>	<b>76</b>
<b>5</b>	<b>REFERENCES.....</b>	<b>78</b>
	<b>ACKNOWLEDGMENT.....</b>	<b>97</b>
	<b>ERKLÄRUNG.....</b>	<b>98</b>
	<b>LEBENS LAUF.....</b>	<b>99</b>



## 1 Introduction

### 1.1 Neurogenesis in the adult mammalian brain

Neurogenic forces were assumed to die down around birth resulting in an adult mammalian brain without regenerative capacity. The scarcity of mitoses in the adult CNS, an event never observed in differentiated neurons, significantly contributed to the formation and obstinate preservation of this view. The dogma of lacking neurogenesis in the adult brain was first challenged by Joseph Altman in the 1960s (Altman, 1962; Altman, 1969; Altman, 1963). Using autoradiographic analyses, he observed cell proliferation and migration in postnatal mammalian brains, but failed to demonstrate the neuronal identity of these cells. The concept of nonexistent adult neurogenesis prevailed until the 1980s, when Nottebohm *et al.* discovered newborn neurons in adult canary brains (Burd and Nottebohm, 1985; Goldman and Nottebohm, 1983). In the mammalian brain, evidence for the phenomenon accumulated, but the breakthrough was achieved only in 1992 by Weiss *et al.* with the demonstration of EGF-induced proliferation of isolated brain cells and the generation of new neurons (Alvarez-Buylla and Lois, 1995; Bayer *et al.*, 1980; Reynolds and Weiss, 1992). Further experiments in mice showed precisely that only a subset of neurons is replaced and that highly neurogenic capacity is restricted to small regions, namely the subventricular zone (SVZ) (Doetsch *et al.*, 1999a; Morshead *et al.*, 1994; Reynolds and Weiss, 1996) and the dentate gyrus of the hippocampus (Cameron *et al.*, 1993; Seri *et al.*, 2001). Today, the existence of multipotent neural stem cells (NSC), the source of neurogenesis, in the adult brain is indisputable, although they have not been identified at cellular level yet. The presence of NSC was also confirmed in the SVZ and hippocampus of the human brain where their activity seems to be substantially reduced (Eriksson *et al.*, 1998; Sanai *et al.*, 2004).

#### 1.1.1 Neuronal precursors are born in the adult SVZ and become olfactory bulb interneurons

Neurogenesis in the SVZ of adult mouse brain produces neuronal precursor cells, which migrate along the rostral migratory stream (RMS) into the olfactory bulb (OB) (Altman, 1969; Lois and Alvarez-Buylla, 1994; Luskin, 1993). Upon arrival, they differentiate into GABAergic interneurons and contribute to the regulation of the olfactory system (Carleton *et al.*, 2003; Gheusi *et al.*, 2000).

The SVZ forms during development, at E11.5, adjacent to the ventricular zone (VZ) (Zimmer et al., 2004). While the latter diminishes and vanishes at birth, the former persists into adulthood. The SVZ then extends along the lateral wall of the lateral ventricle (LV), which is lined by the ependyma, an epithelial monolayer representing the vestiges of the VZ. The roof of the LV and the medial wall facing the septum are largely devoid of SVZ. Doetsch *et al.* described the cellular composition and architecture of the SVZ based on ultrastructural and immunocytochemical characteristics (Doetsch et al., 1997). Four main cell types constitute the SVZ: ependymal cells (28%), astrocytes (B cells, 23%), rapidly dividing transit-amplifying C cells (11%) and migrating neuronal precursors (A cells, 33%) (Fig. 1).

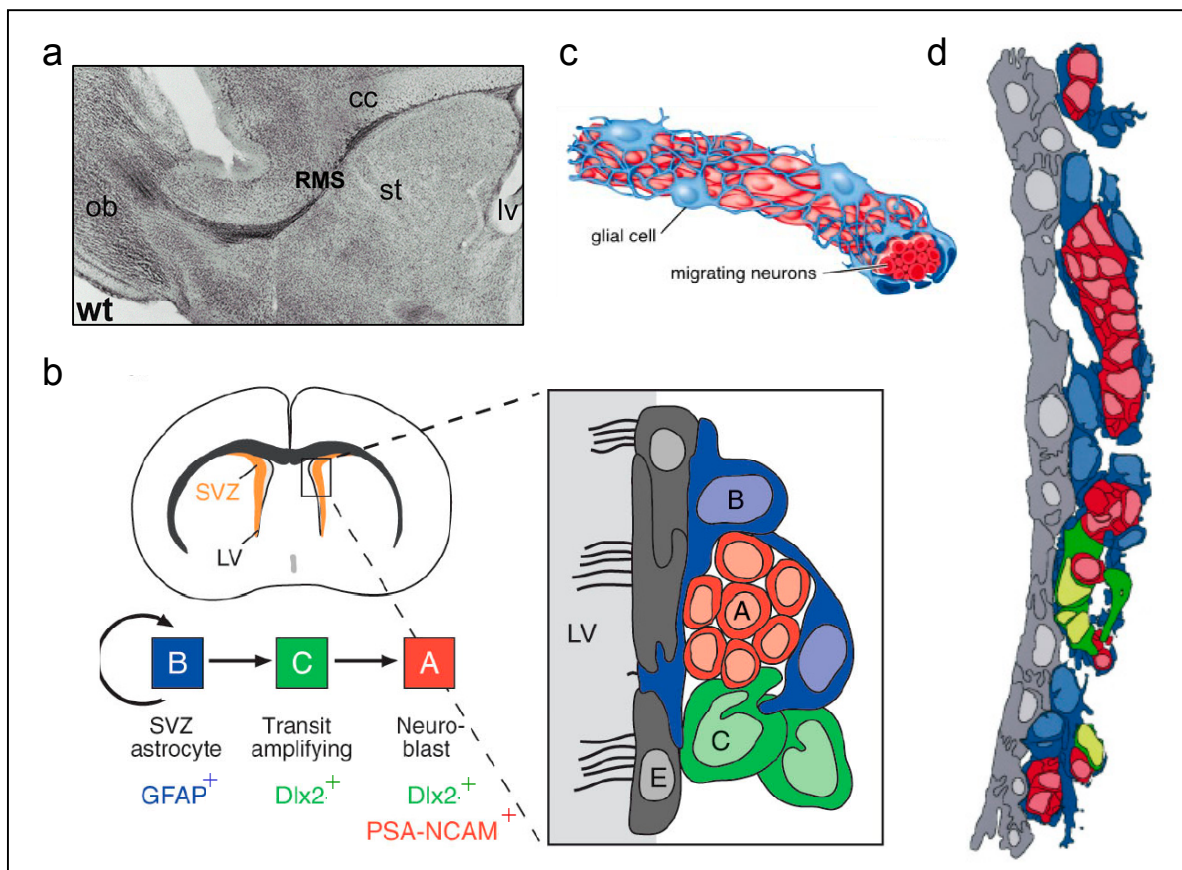


Fig. 1 Localization and cellular composition of the adult SVZ and RMS. (a) Nissl staining of adult mouse brain (sagittal section) clearly brings out the RMS that is created by migrating PSA<sup>+</sup> neuronal precursor cells and connects LV and OB. (b) A schematic representation of a coronally sectioned adult mouse brain shows the location of the SVZ adjacent to the LV. SVZ astrocytes (B cells) give rise to transit-amplifying C cells, which produce the PSA<sup>+</sup> cells (A cells). Next to the layer of ependymal cells (grey), A cells migrate through tunnels of astrocytes. Occasionally, an astrocyte contacts the LV with a single cilium. (c) The RMS consists mainly of PSA<sup>+</sup> cells (red) ensheathed by astrocytes (blue). (d) This schematic SVZ representation was interpreted from serial section reconstructions at the electron microscope and illustrates how the different cell types are distributed along the LV. cc: corpus callosum, LV: lateral ventricle, OB: olfactory bulb, RMS: rostral migratory stream, ST: striatum, wt: wild type. Adapted from Chazal et al, 2000 ; Doetsch et al., 2000 ; Lie et al., 2004 ; Doetsch et al., 1997.

Ependymal cells are terminally differentiated and mitotically inactive cells. They possess multiple cilia reaching into the lumen and are immunoreactive for CD24 (leukocyte cluster of differentiation 24) (Tab. 1). The star-shaped astrocytes express glial fibrillary acid protein (GFAP) and are subdivided into B1 and B2 astrocytes: B1 cells separate the A cells from the ependyma, while B2 cells are located between A cells and striatum. An interesting feature of B1 cells is the occasional contact of the LV via a single cilium that is distinct from those of the ependymal cells in that it lacks a central pair of microtubules and is six times shorter (Doetsch et al., 1999b). Lineage tracing studies using the antimitotic drug Ara-C followed by labeling with  $^3\text{H}$ -thymidine or replication-deficient retroviruses showed that B cells give rise to C cells, which in turn produce A cells (Doetsch et al., 1999a; Doetsch et al., 1999b). The highly mitotic C cells occur in small clusters contacting the A cells (Doetsch et al., 1997) (Fig. 1). C cells can be isolated by sorting for  $\text{Dlx2}^+$  (Distal-less homeobox2),  $\text{PSA-NCAM}^-$  (Polysialic acid-Neural cell adhesion molecule) cells (Doetsch et al., 2002). The neuronal precursors form a large network of chains ensheathed by tunnels of astrocytes throughout the SVZ, primarily in the anterior part, and coalesce in the RMS (Doetsch and Alvarez-Buylla, 1996). They can be readily identified and isolated by the expression of PSA-NCAM and will also be referred to as  $\text{PSA}^+$  cells (Pennartz et al., 2004; Rousselot et al., 1995) (Tab. 1). In addition, they express the proliferation inhibitor CD24 (Belvindrah et al., 2002) and Doublecortin (Dcx), a marker for migrating neurons in the postnatal brain (Gleeson et al., 1999). All four cell types express the intermediate filament Nestin, which was originally found as a neuroepithelial stem cell marker (Doetsch et al., 1997; Lendahl et al., 1990).

Tab. 1 Markers for different SVZ cell types.

	Neuroblast (Type A)	Transit Amplifying (Type C)	SVZ Astrocyte (Type B)	Ependymal cells
PSA-NCAM	+	-	-	-
Dlx2	+	+	-	-
GFAP (mono)	-	-	+	-
mCD24 (HSA)	+	-	-	+
Nestin	+	+	+	+

The four principle cell types of the SVZ can be distinguished by immunostaining for the selected markers in this table. “mono” indicates that a monoclonal antibody was used against GFAP. Modified from Doetsch et al., 2002.

The RMS is predominantly populated with  $\text{PSA}^+$  cells (almost 80 %), contains only one type of B cell and is devoid of C cells (Doetsch et al., 1997). The immature  $\text{PSA}^+$  cells are surrounded by a tunnel of astrocytes and migrate tangentially towards the OB (Fig. 1c).

Within the RMS, they continue to use their characteristic chain migration (Lois et al., 1996) without the usual means of migration, the guidance of radial glia (Rakic, 1972) or axons (Gray and Sanes, 1991). Chain migration is astrocyte-independent and can be reconstituted *in vitro* using an artificial extracellular matrix (ECM) (Wichterle et al., 1997). Some of the molecular cues regulating the migration process have been unraveled. In NCAM-deficient mice, migration is inhibited, and the neuronal precursors accumulate in the SVZ, which results in a drastically reduced OB (Chazal et al., 2000; Cremer et al., 1994). Further experiments revealed that the enzymatic removal of PSA disrupts chain migration *in vitro* and *in vivo* indicating that the PSA moiety ( $\alpha$ -2,8 linked polysialic acid) attached to NCAM is the essential factor for chain migration (Hu, 2000; Ono et al., 1994). PSA is mainly transferred to NCAM by the sialyltransferases ST8SiaII (STX) (Livingston and Paulson, 1993) and ST8SiaIV (PST) (Eckhardt et al., 2000; Yoshida et al., 1995). While STX is responsible for polysialylation of NCAM during embryogenesis and until shortly after birth, PST expression is low during development and prevails in adult animals (Kurosawa et al., 1997; Ong et al., 1998). In contrast to the developing brain, where PSA-NCAM is widely expressed, in the postnatal brain, it is found only on immature precursors in SVZ and RMS as well as in the dentate gyrus (Durbec and Cremer, 2001; Rutishauser and Landmesser, 1996). As the neuronal precursors switch to radial migration in the OB and continue to differentiate, expression of PSA-NCAM ceases (Rousselot et al., 1995).

Moreover, Eph/ephrin signaling is involved in PSA<sup>+</sup> cell migration and regulation of cell proliferation (Conover et al., 2000). The chemorepellents Slit1 and Slit2 repulse the neuronal precursors away from the SVZ (Hu, 1999; Nguyen-Ba-Charvet et al., 2004; Wu et al., 1999). Netrin-1/DCC interaction helps to attract the PSA<sup>+</sup> cells in the OB by regulating the formation of directed protrusions (Murase and Horwitz, 2002). Mitral cells and granule cells secrete the ECM glycoproteins Reelin and Tenascin-R, respectively, which initiate the switch from tangential to radial migration in the OB and serve as detachment signals leading to the disassembly of the chains (Hack et al., 2002; Saghatelian et al., 2004). Expression of the Reelin receptor, apolipoprotein E receptor2 (ApoER2), in PSA<sup>+</sup> cells has been proven.

After completing radial migration, the cells differentiate into two classes of GABAergic interneurons in the OB, the center of odor processing (Fig. 2) (Lois and Alvarez-Buylla, 1994; Luskin, 1993). Here, odor-evoked action potentials propagated along olfactory axons converge in the glomeruli where excitatory synapses confer the signal to projection neurons, the tufted and mitral cells (Carleton et al., 2002). The long axons of the projection neurons transmit the signal to the olfactory cortex. Each sensory neuron expresses only one odorant

receptor gene and projects a single axon to a glomerulus. About 1000 sensory axons of the same kind converge on the dendritic arbor of a mitral cell, which results in an amplification of sensory signals. Lateral inhibition through GABA release by interneurons at two levels is thought to refine odor discrimination (Carleton et al., 2002; Gheusi et al., 2000). A few PSA<sup>+</sup> cells become periglomerular interneurons, which are located between the glomeruli and form reciprocal dendrodendritic synapses with mitral and tufted cells (Lowe, 2003).

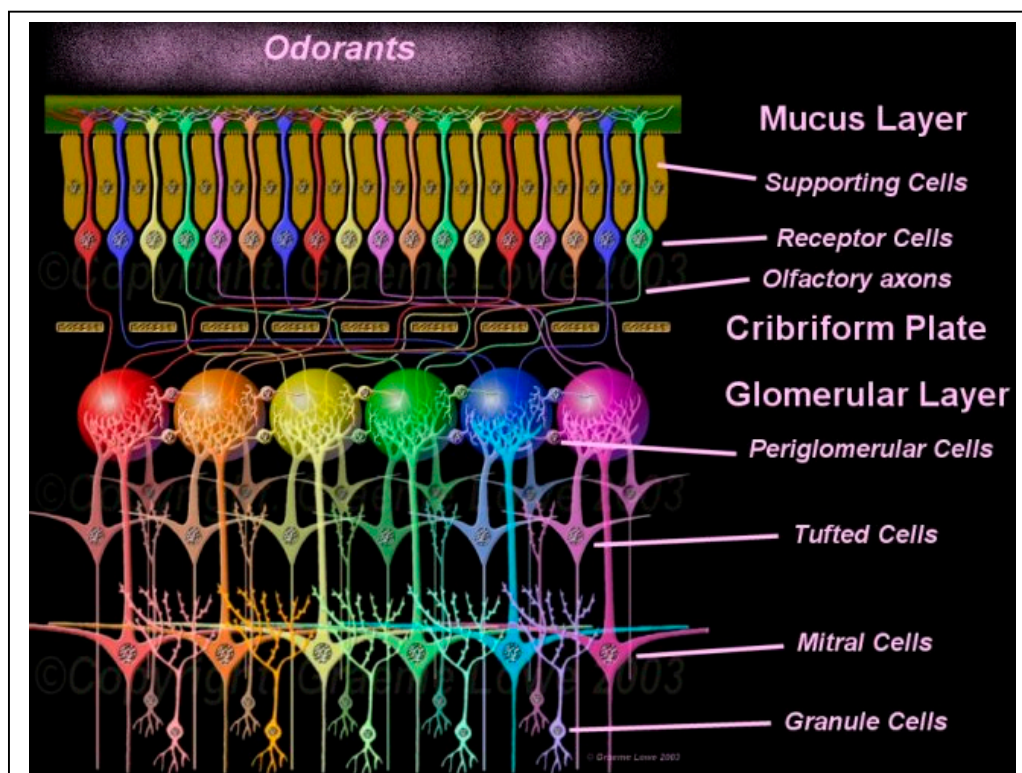


Fig. 2 Organization of the olfactory system. The glomeruli of the olfactory bulb are convergence sites for input from olfactory axons of receptor cells in the olfactory epithelium. Each tufted and mitral cell has a single dendrite that terminates within a glomerulus. Signals are relayed from the sensory neurons via the axons of tufted and mitral cells to the olfactory cortex. Signal modulation through lateral inhibition occurs at two sites. Periglomerular interneurons between the glomeruli release GABA in response to glutamate release from primary dendrites of mitral and tufted cells. Granule interneurons are depolarized by glutamate from mitral cells and in turn inhibit mitral and tufted cells by GABA release. Periglomerular and granule cells are constantly replaced by newly arriving PSA<sup>+</sup> neuronal precursors. With kind permission of Graeme Lowe ©Copyright 2003 (<http://flavor.monell.org/~loweg/index.htm>)

Most precursors become anaxonic granule interneurons, which are located deeper in the OB beneath the glomerular layer and interlink the secondary dendrites of mitral and tufted cells again by making dendrodendritic synapses. Activity in a mitral or tufted cell innervating one glomerulus leads to suppression of mitral or tufted cells innervating neighboring glomeruli (Yokoi et al., 1995). The factors that decide on the differentiation into granule or periglomerular cells have not been determined yet. While the majority of the cells is

GABAergic, a minor subset becomes dopaminergic (Baker et al., 2001). Petreanu *et al.* divided the maturation process of new granule interneurons into five stages according to their morphology and location (Petreanu and Alvarez-Buylla, 2002). Carleton et al. labeled the precursors with GFP using a replication-deficient retrovirus to explore the temporal sequence of electrophysiological changes (Carleton et al., 2003). Class 1 cells are the migrating cells in RMS, which display immature properties (Stewart et al., 1999) and express PSA-NCAM. They do not form synapses (Lois et al., 1996), many express GABA<sub>A</sub> receptors and then AMPA receptors (Carleton et al., 2003). Radially migrating granule cells in the OB that express NMDA receptors belong to class 2. Class 3 comprises maturing granule cells that have completed migration and do not extend beyond the mitral cell layer. First synaptic connections and ongoing growth of dendrites can be observed. Class 4 granule cells develop dendritic arbors in the external plexiform layer beneath the glomerular layer and possess very few first spines. Unlike developing neurons in embryogenesis, these cells acquire the ability to generate action potentials only late as class 5 granule cells, which exhibit dendritic trees with many spines. PSA-NCAM expression has ceased. The mature cells show electrophysiological characteristics indistinguishable from old granule cells. The order of acquired electrophysiological properties of the newcomers differs from the order of events seen in primary neurogenesis where NMDA receptors precede AMPA receptors (Carleton et al., 2003). Carleton *et al.* concluded that the delayed maturation of excitability in secondary neurogenesis might be ascribed to a mechanism protecting preexisting functional circuits from uncontrolled neurotransmitter release and disruption by new cells. The period from birth in the SVZ to functional integration in the OB lasts about two weeks. Over half of the newly integrated cells die within 4 weeks. These analyses prove the functional contribution of new neurons to the adult OB. However, why the continuous supply of new neurons is a necessity throughout life is still unclear. The steady elimination and integration of cells is supposed to permit a high degree of circuit adaptation and plasticity in the neuronal network. NCAM-deficient mice, in which the OB receives no supply of new interneurons, show impaired odor discrimination but normal odor detection and odor memory (Gheusi et al., 2000).

Another interesting feature of PSA<sup>+</sup> cells is their strong mitotic activity. By contrast, neurons during development are already postmitotic at the time of migration (Frazier-Cierpial and Brunjes, 1989). PSA<sup>+</sup> cells are committed to become neurons before exiting the cell cycle (Menezes et al., 1995). While the cells keep proliferating throughout the RMS, the majority of them never reaches the OB but undergoes apoptosis (Morshead and van der Kooy, 1992). The factors that control cell numbers in the RMS are unknown.

Transplantation of postnatal PSA<sup>+</sup> cells showed that the precursors are incorporated into diverse CNS regions but not, for example, into cortex and hippocampus (Lim et al., 1997). The transplanted cells were never observed to form projection neurons, only interneurons. These results indicate that the neuronal precursors have a more restricted potential than NSC, which was further demonstrated by their disability to form Neurospheres (1.1.3) (Gritti et al., 2002). However, the potential of PSA<sup>+</sup> cells is not restricted to the neuronal lineage. Upon lesions in the corpus callosum, small chains of PSA<sup>+</sup> cells migrate there and form oligodendrocytes and astrocytes (Nait-Oumesmar et al., 1999). The report by Sanai *et al.* that, in the human brain, the presence of these neuronal precursors and the RMS is difficult to verify, has disillusioned scientists in view of a direct therapeutical application of PSA<sup>+</sup> cells (Sanai et al., 2004). Nonetheless, insights from the investigation of the murine precursors can be exploited to improve cell replacement strategies. Knowledge about the genes underlying migration and differentiation is essential for brain repair. Replacement of neurons in the adult brain signifies integrating new cells into preexisting circuits, of which the possibility is generally controversial for humans (Rakic, 2004). Since there are differences in the maturation process between embryonic precursors and those in adult neurogenesis, PSA<sup>+</sup> cells can serve as a model for brain repair (Carleton et al., 2003).

PSA<sup>+</sup> cells represent an interesting intermediate state in neural differentiation between NSC and mature neurons. Although some of the factors controlling the fate of the cells, their special mode of migration and their targeting to the OB were discovered, they represent only small pieces of a molecular jigsaw. A gene expression analysis could contribute to the identification of the missing “pieces” that would allow subsequent functional analyses to determine how they fit into the molecular picture.

### 1.1.2 The hippocampal subgranular zone produces new granule neurons

Even though the present study focuses on the SVZ, the hippocampus, the second neurogenic area, should be briefly delineated. The subgranular zone (SGZ) of the dentate gyrus lies between the granule cell layer and the hilus. Here, neurogenesis was also demonstrated in the human adult brain (Eriksson et al., 1998). The functional integration of newly generated granule neurons into the hippocampus was shown by electrophysiological studies in mice (Song et al., 2002; van Praag et al., 2002). According to the group of Alvarez-Buylla, GFAP<sup>+</sup> astrocytes (B cells) function as NSC and give rise to intermediate cells (D cells), which divide with a lower frequency and are more differentiated than the C cells of the SVZ. D cells in turn

produce new granule cells (G cells) that migrate only a short distance to integrate into the hippocampal granule cell layer (Fig. 3) (Doetsch, 2003; Seri et al., 2001).

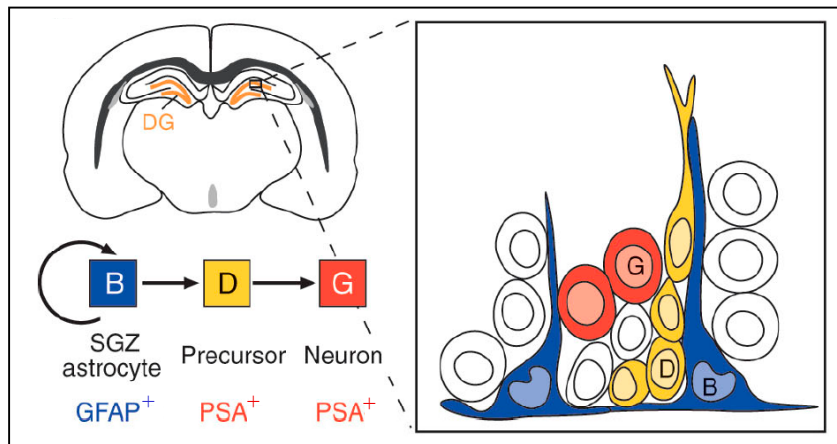


Fig. 3 Cell types in the SGZ of the hippocampus. This schematic representation of a coronal brain section shows the site of secondary neurogenesis in the hippocampus. SGZ astrocytes (B cells) give rise to intermediate precursors (D cells), which produce granule neurons (G cells). (Taken from Doetsch, 2003)

Van der Kooy holds another view claiming that the hippocampus contains committed neural and glial progenitor cells, but not NSC (Morshead and van der Kooy, 2004; Seaberg and van der Kooy, 2002). However, his conclusions were drawn from experiments *in vitro* and might be ascribed to the lack of a factor necessary for NSC from the SGZ but not from the SVZ. A recent study suggested that cells differentiating into GABAergic interneurons in the hippocampus are recruited from the posterior SVZ (Aguirre et al., 2004). Hippocampal neurogenesis might be involved in learning and memory (Kempermann, 2002). Physical exercise and higher demands through an enriched environment increased neurogenesis in mice (van Praag et al., 1999).

### 1.1.3 Adult neural stem cells and the search for marker genes

NSC are defined by their capacity to self-renew and by multipotency, the ability to give rise to the three major cell types of the CNS: neurons, astrocytes and oligodendrocytes (Gage, 2000; Pevny and Rao, 2003; Zappone et al., 2000). NSC can be identified solely retrospectively in culture where they proliferate in the presence of epidermal growth factor (EGF) and basic fibroblast growth factor (bFGF) and form floating clonal aggregates, named neurospheres, which contain a small percentage of NSC (Gritti et al., 1999; Reynolds and Weiss, 1992). It is conceivable that the lineage relationship in neurospheres resembles the one observed *in vivo* (NSC→C cells→A cells) (Morshead and van der Kooy, 2004). BrdU incorporation studies as



well as elimination of mitotically active cells in the SVZ and subsequent labeling or neurosphere cultures indicated that NSC are slowly dividing, quiescent cells (Gritti et al., 2002; Morshead et al., 1994). They are characterized by their extremely low frequency in the mammalian brain, which renders their examination so difficult. Whereas amphibians, reptiles and birds have a remarkable capacity for brain regeneration, which is due to neurogenic radial glia in the adult VZ, neurogenesis is dramatically reduced in mammalian adult brains (Garcia-Verdugo et al., 2002). Although NSC have been found in the entire rostrocaudal axis and other CNS regions (Gritti et al., 2002; Palmer et al., 1999), new cells are generated exclusively in the SVZ and (maybe) the SGZ of dentate gyrus where NSC are relatively concentrated. According to rough estimations, 0.2-0.4% of SVZ cells function as NSC (Morshead et al., 1998; Rietze et al., 2001).

The restriction of neurogenesis to these areas can be explained by the local environment. In SVZ and hippocampus, NSC reside in a stem cell “niche”, a specialized microenvironment, which comprises cell-cell-interactions, the vasculature and the ECM (Doetsch, 2003; Palmer et al., 2000; Spradling et al., 2001). Ependymal cells, for example, express bone morphogenetic proteins (BMP) antagonist Noggin (Lim et al., 2000). As BMP inhibit neurogenesis, Noggin contributes to the creation of a neurogenic environment by blocking BMP signaling. Astrocytes populations in neurogenic and nonneurogenic regions were shown to be distinct (Lim and Alvarez-Buylla, 1999; Song et al., 2002). While hippocampal and SVZ astrocytes promoted neurogenesis, spinal cord-derived astrocytes had no impact. The close proximity to the basal lamina of blood vessels that was only recently discovered in the SVZ by Mercier *et al.* has gained in importance (Alvarez-Buylla and Lim, 2004; Mercier et al., 2002). Endothelial cells around the vessels secrete factors that elicit NSC proliferation and neuron production (Shen et al., 2004).

The NSC present in the adult SVZ can be distinguished from fetal NSC (neuroepithelial stem cells), which can be isolated from the VZ during development (Cai et al., 2002; Ciccolini, 2001; Pevny and Rao, 2003). In this work, the general term “NSC” refers to adult NSC unless otherwise indicated. Fetal NSC are morphologically distinct from adult NSC, are GFAP-negative (Imura et al., 2003) and respond only to bFGF but not EGF because they lack the EGF receptor. They generate projection neurons while adult NSC generate primarily interneurons. Both types form neurospheres, express Nestin and lack the expression of lineage-specific markers. Adult NSC can be isolated from E14 onwards. Apparently, the properties of NSC change in the course of development (Murayama et al., 2002). While

strongly proliferating stem cells in fetal development conduct corticogenesis, few quiescent stem cells represent the remnants of development in the adult brain (Cai et al., 2002).

Given that the adult mammalian brain and spinal cord do not recover from injury, the regenerative capacity of NSC has been investigated also in regard of treatment for neurodegenerative diseases. The ultimate goal is to mobilize endogenous NSC or to derive them from the very patient for subsequent transplantation. In any case, NSC would not provoke rejection by the immune system contrary to ES (embryonic stem) cells and their (neuronal) derivatives. ES cells were shown to form teratomas upon injection (Lovell-Badge, 2001). In addition, isolation of NSC is ethically unobjectionable.

Multipotent NSC can be propagated *in vitro* as neurospheres, tagged with markers and grafted into the brain where they adapt to the region: NSC in the form of neurospheres from the SGZ were shown to differentiate into GABAergic interneurons upon transplantation into the SVZ (Gage et al., 1995; Suhonen et al., 1996). A potential beyond the generation of brain cells was revealed when NSC were injected into blastocysts and contributed to multiple organs of all three germ layers (Clarke et al., 2000). Several studies have reported augmented neurogenesis in response to mechanical lesions, ischemia or seizure in rodent brains (Jin et al., 2001; Kee et al., 2001). The effect was much weaker in nonneurogenic regions distant from the SVZ. Concomitant infusion of growth factors into the LV produced more new neurons and led to moderate behavioral recovery (Fallon et al., 2000; Nakatomi et al., 2002). NSC might be suitable for neuronal cell replacement, but the functional properties of the new neurons are still unclear and lost cells have not been sufficiently replaced yet (Lie et al., 2004).

#### **1.1.3.1 Specific genetic markers for NSC have not been identified**

The present lack of markers for NSC impedes their isolation, further characterization and therapeutic use. It also keeps their exact cellular localization in the adult brain in the dark. Johansson *et al.* suggested that the ependymal cells of the SVZ function as NSC (Johansson et al., 1999). The study was based on the fluorescent label DiI, which was supposed to be specific for ependymal cells but obviously must have been transferred to neighboring cells, given that the results were disproved. The opposing notion was established by the group of Alvarez-Buylla with the demonstration that SVZ astrocytes contain the NSC (Doetsch et al., 1999a). The infusion of Ara-C into the SVZ for 6 days eliminated rapidly dividing cells, the C and A cells. The astrocytes were reduced in number as compared to untreated mice suggesting that during the 6 days some of them underwent division and died (Doetsch et al., 1999b). BrdU and <sup>3</sup>H-thymidine showed that C cells reappeared after 2 days and A cells after 4 days.

Within 14 days, the SVZ was regenerated completely. Specific labeling of astrocytes using a replication-deficient retrovirus demonstrated that the newly generated cells were GFAP-positive, thus derived from astrocytes. Doetsch *et al.* found that the DiI experiment was not reproducible (Doetsch *et al.*, 1999a).

Further studies corroborated the idea that NSC are a subpopulation of astrocytes and reported that ependymal cells from adult or early postnatal mice are capable of generating neurospheres, which did not display features of multipotency and self-renewal classifying them as unipotent (Chiasson *et al.*, 1999; Laywell *et al.*, 2000). Specific elimination of astrocytes in combination with neurosphere assays proved that all NSC are GFAP-positive and thereby ruled out the possibility that an unidentified cell type functions as NSC giving rise to GFAP<sup>+</sup> cells (Imura *et al.*, 2003; Morshead *et al.*, 2003). Alvarez-Buylla extended the hypothesis to the existence of a neuroepithelial-radial glia-astrocyte lineage that contains the NSC (Alvarez-Buylla *et al.*, 2001; Doetsch, 2003). This view formed due to several observations; for example, radial glia convert into astrocytes in newborn mammals (Voigt, 1989) while they persist in non-mammalian vertebrate adult brains to function as primary precursors for neurons (Garcia-Verdugo *et al.*, 2002). Furthermore, a single cilium contacting the ventricle lumen is present on neuroepithelial stem cells, radial glia and on a few SVZ astrocytes and shows identical characteristic features in all three cell types (Alvarez-Buylla *et al.*, 2001; Doetsch, 2003).

Despite all the evidence, GFAP expression in NSC is still controversial. In any case, consensus is that GFAP by itself is not indicative of a NSC. For the NSC state, it is neither necessary, since it is not found in retinal stem cells (and fetal NSC), nor sufficient as it is expressed in nonneurogenic cells (Morshead and van der Kooy, 2004).

FACS isolation of CD133<sup>+</sup>, CD24<sup>-/lo</sup> cells from human fetal brain tissue resulted in a cell population of which 4.3% gave rise to neurospheres (Uchida *et al.*, 2000). Combining sequential selection steps based on large cell size and absence of peanut agglutinin (PNA) and CD24 led to 80 % enrichment of murine SVZ NSC (Rietze *et al.*, 2001). However, only 63% of the total neurosphere-forming activity was contained in this population leaving behind NSC with different characteristics. Immunocytochemistry failed to demonstrate GFAP expression on the selected cells. The selection criteria were criticized by later studies (Morshead and van der Kooy, 2004; Murayama *et al.*, 2002).

Capela *et al.* achieved a 25-fold enrichment of NSC when they isolated 4% of SVZ cells using LeX (Capela and Temple, 2002). LeX is a carbohydrate that is also known as CD15 (leukocyte cluster of differentiation 15) or SSEA-1 (stage-specific embryonic antigen1). LeX

was previously found on the surface of mouse ES cells and other pluripotent cells, in embryonic germinal zones and on subpopulations of cells in the adult CNS. Strikingly, LeX<sup>+</sup> cells were found in the SVZ and encompass all neurosphere-forming cells of the SVZ. 6% of the 12% SVZ astrocytes are LeX-positive, thus, 0.7% of all SVZ cells are LeX-expressing astrocytes. 18% LeX<sup>+</sup> cells express GFAP. If it is true that C cells are capable of generating neurospheres (Doetsch et al., 2002) and LeX labeling comprises all neurospheres-forming cells (Capela and Temple, 2002), then LeX is likely to be expressed also by C cells (which has not been ascertained yet). LeX expression is also found in association with blood vessels and close to the pial surface, i.e. in regions where a basal lamina is present (Alvarez-Buylla and Lim, 2004). Capela *et al.* refuted Johansson's results by showing that ependymal cells selected by CD24 expression or presence of cilia did not generate proper neurospheres that are multipotent and capable of self-renewal (Capela and Temple, 2002).

The transcription factor Sox2 is expressed in ES cells, neural progenitors and is found in the SVZ and the RMS (Graham et al., 2003; Zappone et al., 2000). Sox2 regulatory sequences (SRR) were suggested to interact with octamer transcription factors and to be involved in multipotency-specific expression in ES cells and NSC. Transgenic mice expressing GFP under the control of SRR2 have been used to isolate cells, of which some were multipotent (Miyagi et al., 2004; Pevny and Rao, 2003).

The expression of the nuclear orphan receptor TLX was reported to maintain NSC in an undifferentiated, proliferative state and to be intimately linked to GFAP expression despite high expression in adult brain (Shi et al., 2004). Using a  $\beta$ -galactosidase reporter under the control of the TLX promoter, Shi *et al.* showed that TLX expression co-localized in part with BrdU and Nestin (Tab. 1) in the SVZ. TLX<sup>+</sup> cells isolated by FACS are multipotent and self-renewing but do not express GFAP (Shi et al., 2004) challenging the prevailing hypothesis that all NSC are GFAP-positive. Interestingly, in TLX mutant mice, BrdU labeling was found neither in the SVZ nor in the hippocampus. However, TLX is not a cell surface protein and was not able to isolate a pure NSC population.

The ABCG2 (Bcrp1) transporter mediates the efflux of the fluorescent DNA-binding dye Hoechst 33342 and has been exploited for the isolation of hematopoietic stem cells by sorting for a population with low Hoechst fluorescence, which was termed "side population" (SP) (Goodell et al., 1996; Scharenberg et al., 2002). Although ABCG2 was detectable at E10.5 (absent at E14.5) no isolation of fetal NSC from embryonic brain was feasible (Cai et al., 2002). When this sorting method was used to isolate cells from neurospheres of embryonic and adult origin, (only) the adult SP cells lacked expression of ABGC2 (Kim and Morshead,

2003). The SP method is neither powerful enough for isolation of cells from primary tissue nor suitable to tackle the question of NSC localization *in vivo*. In addition, Hoechst dye was shown to exert a cytotoxic effect (Kim and Morshead, 2003).

To date, no isolation strategy has been able to generate a pure NSC population, and a true NSC marker -ideally a transmembrane protein convenient for isolation- is still missing.

## **1.2 Aim of the study**

PSA<sup>+</sup> cells represent migratory neuronal precursors between NSC-derived transit-amplifying precursors and differentiated neurons. Therefore, they are of great interest for the analysis of developmental processes, neuronal migration and differentiation. The neuronal precursors are the product of secondary neurogenesis in the SVZ and can teach how newly generated cells find their place in the adult brain. Previously, only single genes have been examined in PSA<sup>+</sup> cells; therefore, in the framework of the present doctoral thesis, a comprehensive analysis of transcriptome using SAGE (Serial analysis of gene expression) was to be performed to gain insight into their molecular nature. A homogeneous population of PSA<sup>+</sup> precursors was to be isolated from the adult brain using Fluorescence-activated cell sorting (FACS). In order to identify precursor cell-enriched genes, the SAGE library of PSA<sup>+</sup> cells was to be contrasted with SAGE data of adult total brain (ATB) representing mature neuronal and glial cells. Subsequently, this study intended to demonstrate the expression of these genes selectively at cellular level in SVZ and RMS. The first part of the work was supposed to generate a list of candidate genes in PSA<sup>+</sup> neuronal precursors providing a basis for future functional studies.

The ability to identify and isolate NSC *in vivo* would contribute significantly to the understanding of the regulation of their self-renewal and proliferation, the mechanisms for neural differentiation and answer why neurogenesis has been limited to such small regions in the rodent adult brain and might be even dormant in human adults. Their regenerative potential could be exploited to replace lost cells by mobilization of endogenous NSC or by culturing and transplanting them to alleviate or even cure neurodegenerative disease. The lack of a specific marker represents a tremendous obstacle in NSC biology.

The second part of this thesis aimed at identifying potential NSC markers using a strategy based on the SAGE data generated for the homogeneous population of neuronal precursors in the first part. In a hierarchy of developmental potential, NSC are positioned above committed

neuronal precursors, which in turn are above differentiated neurons and glia (Gage, 2000), the ATB SAGE library (Fig. 4).

As NSC are not accessible due to the lack of markers, neurospheres were considered as a substitute. The possibility was discarded because neurospheres do not fulfill the requirement of homogeneity and are prone to modifications in culture. By contrast, cultured ES cells represent a homogeneous population, are above NSC in the hierarchy of developmental potential, and their high similarity to NSC in terms of self-renewal and differentiation potential suggests comparable underlying gene expression programs (Clarke et al., 2000). A global overlap between genes expressed in ES cells and NSC has been demonstrated (Ivanova et al., 2002; Ramalho-Santos et al., 2002).

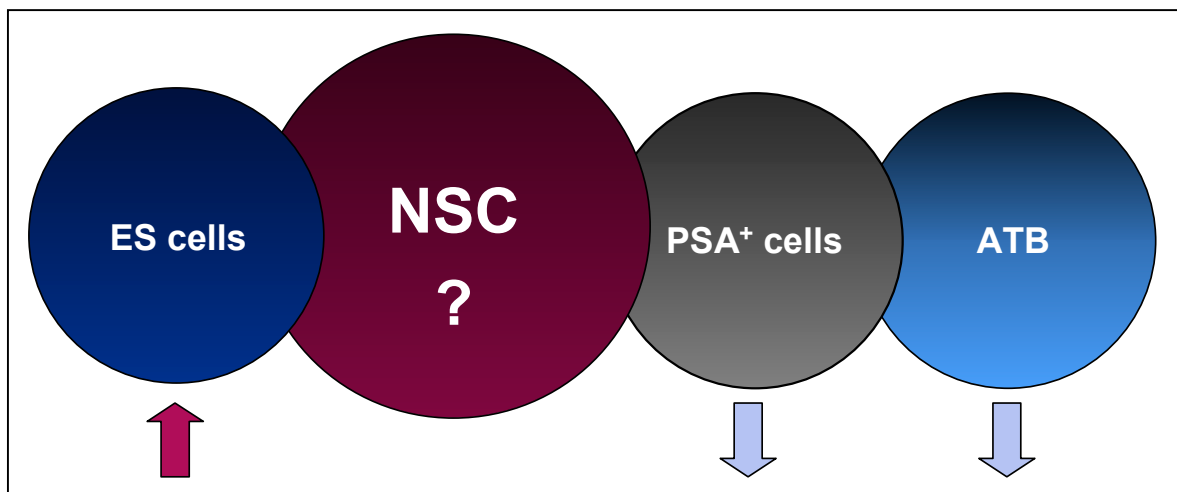


Fig. 4 Selection strategy for potential NSC markers. ES cells, NSC, PSA<sup>+</sup> cells and ATB are shown in a hierarchical order in terms of developmental potential starting with the greatest one on the left. All cell types are accessible and can be isolated homogeneously, except for the NSC because of a lack of marker genes. Given that there is an overlap in the genetic programs of ES cells and NSC, genes that are highly expressed in ES cells and downregulated or absent in PSA<sup>+</sup> cells and ATB should contain a subset of genes which are also expressed by the vanishingly small number of stem cells in the brain.

Provided that this overlap exists and that the number of NSC in ATB is negligibly small, the selection of genes from SAGE data that are highly expressed in ES cells and downregulated or absent in PSA<sup>+</sup> neuronal precursors and ATB should lead to the identification of genes that are potentially expressed by NSC (Fig. 4). The candidate genes were to be further analyzed to determine if their cellular localization is compatible with the localization of neurogenic areas, i.e. the SVZ.

## 2 Materials and methods

### 2.1 Gene expression analyses

#### 2.1.1 SVZ dissection and dissociation

4-6 weeks old male C57BL/6J mice were killed by rapid decapitation. Brains were removed, 400  $\mu\text{m}$  sections were cut in cold 1 x PBS using a vibratome (Leica) and placed in cold HBSS (Hank's Balanced Salt Solution, Invitrogen, Karlsruhe). The SVZ from the lateral wall of the anterior horn of the LV was dissected from the appropriate slices with tweezers (Biologie tip, 0.05 mm x 0.02 mm, Dumostar, Fine Science Tools, Foster City, USA). The small tissue pieces were collected in cold HBSS, pelleted by centrifugation for 3 min at 700 x g, incubated in 1 ml trypsin (5 mg/ml in HBSS, Sigma-Aldrich, Taufkirchen) for 12 min at 37°C with gentle agitation every 3 min, followed by inactivation of trypsin with 5 ml DMEM (Dulbecco's Modified Eagle Medium, Invitrogen), 10% FCS. After centrifugation for 3 min at 700 x g, the explants were washed with 5 ml 37°C HBSS and centrifuged for 3 min at 500 x g. After resuspension in 2 ml 37°C PBS cells were dissociated mechanically with a 1000  $\mu\text{l}$  Eppendorf pipette.

#### 2.1.2 Purification of PSA<sup>+</sup> cells by FACS

Individualized PSA<sup>+</sup> cells were split up in 3 samples: the first one (100  $\mu\text{l}$ ) without antibodies, the second one (100  $\mu\text{l}$ ) served as a control with secondary antibody only, the third one (1.8 ml) was incubated with  $\alpha$ -PSA mAb menB (1:100) (Rougon et al., 1986) for 30 min at 37°C, followed by washing once before incubation with anti-mouse IgM-FITC (1:100, Immunotech, Marseille, France) for 15 min at 37°C. Cell sorting was performed using the high-speed cell sorter FACS Vantage SE (Becton Dickinson, San Jose, USA). PSA<sup>+</sup> cells, located in regions R1 and M1, were sorted at  $3 \times 10^3$  cells/sec. In the R1 population, PSA<sup>+</sup> cells were selected by green fluorescence (530 nm  $\pm$  30). The marker M1 was set to obtain a high percentage of PSA<sup>+</sup> cells.

PSA-expressing TE 671 cells were used to survey if antibody binding or the FACS procedure affect gene expression. TE 671 were incubated with and without the antibody at 37°C for 30 min and the RNA isolated from both samples. Following incubation with  $\alpha$ -PSA mAb for 30 min and anti-mouse IgM-FITC (1:100) for 15 min at 37°C, 400,000 cells were sorted by

FACS and RNA isolated. Gene expression profiles were generated using PIQOR™ cDNA microarrays (Memorec Biotec, Cologne).

### 2.1.3 RNA isolation

Isolation of total RNA from PSA<sup>+</sup> cells, Bruce-4 ES cells and adult total brain (ATB) was performed using the RNeasy Mini Kit (Qiagen, Hilden) according to the manufacturer's instructions. The RNA was quantified by photometrical measurement or NanoDrop® ND-1000 UV-Vis Spectrophotometer (NanoDrop Technologies, Inc., Rockland, USA) and the integrity checked by the 2100 Bioanalyzer (Agilent Technologies, Palo Alto, USA) or agarose gels. Amplification of RNA samples for microarray and quantitative real-time PCR (qPCR) experiments was performed with T7 polymerase using a modified protocol according to Eberwine (Van Gelder et al., 1990).

### 2.1.4 Serial analysis of gene expression (SAGE)

SAGE is based on the concept that short DNA fragments generated at defined positions can specifically identify the transcript of origin. A given RNA is reverse-transcribed into cDNA and 11 bp DNA fragments, called SAGE tags, are generated at the NlaIII restriction site closest to the 3' end (Velculescu et al., 1995). The SAGE tags are ligated to form concatemers, which are sequenced to count, identify and annotate the tags. The number of tags correlates directly with the number of transcripts in the sample. The "MicroSAGE Detailed Protocol" is based on the original version developed by Velculescu (St Croix et al., 2000; Velculescu et al., 1995). The SAGE libraries were generated with total RNA using the "MicroSAGE Detailed Protocol" (available at [www.sagenet.org](http://www.sagenet.org)) with minor modifications as follows. Elongase (Invitrogen) in combination with Platinum Taq Antibody (Invitrogen) was used for the PCR instead of Platinum Taq polymerase. Phenol/chloroform extraction was performed using PLG Light tubes (Eppendorf). Precipitations were done with 10M ammonium acetate. Concatemers were excised from an agarose instead of polyacrylamide gel to obtain higher yields.

SAGE data analysis was carried out using the Memorec SAGE Analysis Package (Memorec Biotec GmbH). Here, an extensive proprietary tag database works with automatic annotations derived from EST/genomic data and, in addition, contains several hundred manually annotated tags elusive to the automatic mapping. The program extracts 11 base pair (bp) SAGE tags and guarantees a more reliable assignment to UniGene clusters than programs working with 10 bp tags. Proprietary filtering algorithms eliminate SAGE artifacts resulting



from polymorphic tags, ribosomal RNA, mitochondrial RNA, linker tags and LINE/SINE tags. The calculation of statistical significance levels for differential gene expression is based on a formula by Audic and Claverie (Audic and Claverie, 1997). For the purpose of comparison, all SAGE libraries have been normalized to 100,000 tags.

### 2.1.5 Microarrays

PIQOR<sup>TM</sup> (Parallel Identification and quantification of RNAs) cDNA microarrays (Memorec Biotec GmbH, Cologne) were used to generate expression profiles of the controls with TE 671 cells and for the validation of SAGE results. cDNA microarray production, hybridization and evaluation were carried out as previously described (Bosio et al., 2002). Briefly, cDNA microarray probes were generated by RT-PCR with specific primers for selected gene regions (Tomiuk and Hofmann, 2001). The 200-400 bp cDNA fragments were cloned into the pGEM-T Vector (Promega, Mannheim) and sequence-verified. Amplification (Taq PCR Master Mix, Qiagen) of the vector inserts was performed with vector sequence-derived primers with a 5'-amino-modification on one primer. After purification (QIAquick 96 PCR BioRobot Kit, Qiagen) PCR products were quality-controlled on an agarose gel. Probes were spotted in two or four replicates depending on the total number of probes.

100 µg total RNA per sample for control experiments with TE 671 cells or 1 µg of amplified RNA for validation experiments were labeled and hybridized. Because of limited material, the described hybridizations for PSA<sup>+</sup> cells, ES cells and ATB were performed once. Total RNA was combined with a control RNA consisting of an *in-vitro* transcribed *Escherichia coli* genomic DNA fragment with a 30 nucleotides (nt) poly (A)<sup>+</sup> tail (CR1) before mRNA isolation (Oligotex mRNA Mini Kit, Qiagen). The mRNA was diluted to 17 µl and 2 µl of control RNA 2 (CR2) were added, a mixture of three different transcripts to control the efficiency of the labeling step. Reverse-transcription was achieved by adding the mRNA to a mix of 8 µl 5x first-strand buffer (Invitrogen), 2 µl Primer-Mix (oligo(dT) and randomeres, Memorec Biotec), 2 µl low C dNTPs (dATP, dGTP, dTTP 10mM each; dCTP 4 mM), 2 µl FluoroLink<sup>TM</sup> Cy3/Cy5-dCTP (Amersham Pharmacia Biotech, Freiburg) 4 µl 0.1 M DDT and 1 µl RNasin (20-40 U) (Promega). 1 µl (200 U) of SSII enzyme was added, incubated at 42°C for 30 min. This step was repeated once. 0.5 µL of RNase H was added and incubated at 37°C for 20 min to hydrolyze RNA. Cy3- and Cy5-labeled samples were combined and cleaned up using QIAquick<sup>TM</sup> (Qiagen). 50 µl of 2x hybridization solution (Memorec Biotec) at 42°C were added to 50 µl eluent. The cDNA array was incubated in distilled water at 95°C for 2 min to denature the double-stranded cDNA molecules leaving only the strand that is

covalently bound to the slide surface. The array was transferred into 96% ethanol for 30 sec and dried with pressured air. Hybridization was performed according to the manufacturer's instructions (Memorec Biotec) using a GeneTAC™ hybridization station (Perkin Elmer, Langen). Quality controls, external controls and hybridization procedures and parameters comply with the MIAME standards (Brazma et al., 2001).

The hybridized microarrays were scanned with the ScanArray Lite (Packard Bioscience, Dreieich ) and analyzed using the Imogene software version 4.1 (Bio-Discovery, Los Angeles, USA). The signal of each spot was measured in a fixed circle of 350 µm diameters and the background outside the circle within rings 40 µm distant to the signal and 40 µm wide. Local background was subtracted from the signal to obtain the net signal intensity and the ratio if Cy5/Cy3. The ratios were normalized to the median of all ratios using only those spots for which the fluorescent intensity in one of the two channels was 2-fold higher than the negative control (salt and herring sperm). The mean was determined of 4 spots representing the same cDNA.

#### 2.1.6 Quantitative real-time PCR (qPCR)

0.96 µg amplified RNA from ATB and 0.2 µg amplified RNA from PSA<sup>+</sup> cells, were reverse transcribed and 7.5 ng of the RT-reaction product were used as template for each qPCR sample. Transcript levels were measured by qPCR using Perkin Elmer Applied Biosystems prism model 7000 sequence detection system (PE ABI 7000 SDS; Perkin Elmer, Langen). Quantification primers were designed using Primer Express (PE ABI).

Specific primers for the following mouse genes were used in these experiments:

TubulinβIII forward 5'-GATGATGACGAGGAATCGGAA-3'

TubulinβIII reverse 5'-CAGATGCTGCTTGTCTTGGC-3'

Manic fringe forward 5'-TCAAGTTTGTCCCAGAGGATGA-3'

Manic fringe reverse 5'-TTGACTGCGATGAAGATGTCG-3'

Dvl2 forward 5'-CTCCTCCTAATCTCCGAGCTCTT-3'

Dvl2 reverse 5'-TGGAGGCATCATAACTACCATCAT-3'

Sox4 forward 5'-ACAAGAAAGTGAAGCACGTCTACCT-3'

Sox4 reverse 5'-TCCATCTTCGTACAACCCAGT-3'

SAGE data and triplicate qPCR assays indicated insignificant variation of the transcript levels of TubulinβIII. Therefore, TubulinβIII was used for the normalization of the qPCR data. For all qPCR experiments, triplicate assays were performed.

Threshold cycle, Ct, which correlates inversely with the target mRNA levels, was measured as the cycle number at which the SYBRgreen emission increases above a threshold level. Specific mRNA transcript levels were expressed as fold difference between PSA<sup>+</sup> precursors and ATB. For the determination of specific expression of Dishevelled2 (Dvl2), Manic fringe and Sox4 by qPCR in mouse, specific primer pairs for Tubulin $\beta$ III, and the respective genes were used with aRNA from FACS-purified PSA<sup>+</sup> cells and from ATB. RNA integrity was controlled on a gel. Linear amplification was performed according to the modified Eberwine protocol (Van Gelder et al., 1990). To remove genomic DNA, each RNA was treated with RNase free DNase1 (Ambion Inc., Austin, Texas) prior to the reverse transcription reaction. The following cycle conditions were used: 95°C 10 min followed by 50 cycles of 95°C 15 sec, 60°C 1 min. Melting curves were determined for each amplified product according to the suppliers guidelines (Applied Biosystems prism model 7000 SDS software). For each run, negative controls were performed by omitting the template. Standard curves of each gene were used to calculate the expression of Dvl2, Manic fringe and Sox4, which is shown as “x-fold differential expression as compared to Tubulin $\beta$ III”.

## **2.2 Cell culture**

### **2.2.1 General cell culture conditions**

All cell types were cultured in a humidified incubator with a 5% CO<sub>2</sub> atmosphere at 37°C. Frozen cells were quickly transferred from liquid nitrogen into a 37°C water bath, thawed, washed with prewarmed growth medium and seeded on tissue culture dishes. For the purpose of freezing, cells were trypsinized, resuspended in growth medium supplemented with 20% fetal calf serum (Invitrogen) and 10% DMSO (Sigma-Aldrich) and slowly cooled to -80°C. After overnight incubation at -80°C, cells were kept in liquid nitrogen for long-term storage.

### **2.2.2 TE 671 cell line**

TE 671 cells were grown in DMEM (61965-026, Invitrogen) containing 10% FCS, 1 mM sodium pyruvate, 100 U/ml penicillin, and 100  $\mu$ g/ml streptomycin.

### **2.2.3 ES cell line Bruce-4**

C57BL/6J derived ES cells (Bruce-4) (Kontgen et al., 1993) were grown on a layer of embryonic fibroblasts in DMEM containing 10% FCS, 1 mM sodium pyruvate, 1% L-glutamine, 100 U/ml penicillin, 100  $\mu$ g/ml streptomycin, 1% nonessential amino acids, LIF

(Leukemia Inhibitory Factor) and 0.01 mM  $\beta$ -mercaptoethanol. To reduce the contamination of embryonic fibroblasts prior to RNA preparation, ES cells were grown on gelatine-coated plates for 24 h, and then passaged to a new plate for 20 min to allow feeder cells to adhere. The ratio of ES cells to fibroblasts was approximately 60:1 after initial plating. After reduction of contaminating fibroblasts by transient plating the ratio was approximately 80:1 (1.25%).

#### 2.2.4 Preparation of embryoid bodies

SV129 embryonic stem cells were grown on gelatine-coated dishes in DMEM (21969, Invitrogen) containing 0.8 mM sodium pyruvate, 15% FCS, 2 mM L-glutamine, 100 U/ml penicillin, 100  $\mu$ g/ml streptomycin, 25 mM HEPES, 300  $\mu$ M monothioglycerol, 1000 U/ml LIF (ESGRO, Chemicon, Hofheim) and essential amino acids (Biochrom, Berlin). Embryoid bodies (EBs) were grown either in suspension or using the hanging drop-method (Hogan, 1994) with  $3.3 \times 10^4$  cells/ml and 15  $\mu$ l per drop. After 24 h EBs were harvested to prepare cryosections.

#### 2.2.5 Preparation of neurospheres

Neurosphere production was based on established protocols (Groszer et al., 2001; Imura et al., 2003; Knoepfler et al., 2002). P2-P4 CD1 mice were killed by cervical dislocation and their brains removed. 400  $\mu$ m sections were cut in cold PBS using a vibratome (Leica) and placed in cold DMEM (61965-026, Invitrogen), 10% FCS, 100 U/ml penicillin, 100  $\mu$ g/ml streptomycin. The SVZ from the lateral wall of the anterior horn of the LV was dissected from the appropriate slices and collected in cold HBSS. The pieces of tissue were incubated in 1 ml trypsin (5 mg/ml in HBSS, Sigma-Aldrich), 15% glucose, 0.25 mg/ml DNase type I (Roche, Mannheim) for 12 min at 37°C with gentle agitation every 3 min. 9 ml of HBSS were added to dilute the trypsin. The pieces were pelleted by centrifugation at 800 x g for 9 min, resuspended in Neurobasal<sup>TM</sup> Medium (21103, Invitrogen), 100 U/ml penicillin, 100  $\mu$ g/ml streptomycin, supplemented with B-27 (Invitrogen), 20ng/ml basic fibroblast growth factor (bFGF, R&D) and 20ng/ml epidermal growth factor (EGF, R&D) and dissociated by triturating with a fire-polished glass pipette. The cells were passed through a 50  $\mu$ m filcon (Dako, Hamburg), counted and plated in uncoated 35 mm dishes (50,000 cells per ml, 3.5 ml per dish) in the same medium. Medium was changed every 3-4 days by centrifuging the neurospheres at 150 x g for 6 min and carefully resuspending them in fresh medium.

To ensure that the primary neurospheres had the capability of self-renewal, they were dissociated to produce secondary neurospheres. After 5-7 days, primary neurospheres were pelleted by centrifugation at 800 x g for 8 min and dissociated by triturating with a fire-polished glass pipette and passed through a 50 µm filcon. After 4-6 days secondary neurospheres were harvested for cryosections.

## **2.3 Histological analyses**

### **2.3.1 Preparation of cryosections**

Neurospheres or EBs were centrifuged at 300 x g for 6 min, washed in 1x PBS, pH 7.4, fixed in 4 % paraformaldehyde at RT for 15 min (for immunocytochemistry) or 30 min (for *in situ* hybridizations), centrifuged at 400 x g for 8 min, washed in 1x PBS and incubated agitating in 5% sucrose at 4°C overnight. After centrifugation at 600 x g for 10 min they were incubated in 15% sucrose at 37°C for 2 h. They were centrifuged at 700 x g for 10 min. Sucrose solution was removed except for 400-500 µl, which were transferred into 1-2 wells of a 96-well plate. The plate was centrifuged at 1000 x g for 2 min and an equal volume of 37°C warm Tissue Tek OCT compound (Sakura Finetek, Zoeterwoude, The Netherlands) was added and mixed with the sucrose solution by stirring gently with a yellow tip avoiding bubbles. The plate was centrifuged at 1000 x g for 3-4 min to concentrate the neurospheres at the bottom of the well. Subsequently, the plate was immersed into -40 to -45°C cold isopentane for 2 min and stored at -80°C. 8 µm cryosections were cut with a LEICA CM3050 cryostat, collected on Superfrost Plus slides (Menzel, Braunschweig) and stored at -80°C.

3-week-old C57BL/6J mice or CD1 mice of postnatal day 6 (P6), P12, P14 were anaesthetized with 1.2 % Avertin (200 µl/10 g body weight; 2,2,2-Tribromethanol; Sigma-Aldrich) and CD1 mice P3–P5 in ice water. The mice were intracardially perfused with 4% paraformaldehyde and their brains incubated in the same solution for 2-3 h. Mice on embryonic day 14 (E14) and E18 were removed from the mother and their heads incubated in 4% paraformaldehyde at 4°C for at least 24 h. Brains were incubated in 20% sucrose overnight and frozen in isopentane at -40 to -45°C. Coronal and sagittal 12 µm and 10 µm sections were cut with the cryostat and air-dried on Superfrost Plus slides.

All sucrose and paraformaldehyde solutions were prepared in 1x PBS, pH 7.4 and the former supplemented with 0.02 % sodium azide for incubation times longer than 24 h.

### 2.3.2 *In situ* hybridizations

#### 2.3.2.1 Generation of Digoxigenin-labeled RNA probes

Antisense and sense RNA probes for *in situ* hybridizations have been derived from a proprietary collection of cDNA clones (Memorec Biotec) consisting of 200-400 bp fragments (Tomiuk and Hofmann, 2001).

Glycerol stocks of bacteria transformed with pGem-T Vector (Promega, Mannheim) containing the different 200-400 bp inserts were inoculated in 5 ml LB medium with Ampicillin (1 mg/ml) and grown vigorously shaking at 37°C over night. The plasmid DNA was prepared using the NucleoSpin Plasmid Kit or the Nucleobond AX Kit (Macherey-Nagel, Düren) according to the manufacturer's instructions. The DNA concentration was measured with the NanoDrop® ND-1000 UV-Vis Spectrophotometer (NanoDrop Technologies, Inc., Rockland, USA) and the length of each fragment checked on agarose gels. DNA gel electrophoresis with 1kb DNA ladder (Invitrogen) was performed in 1x TBE buffer as described (Sambrook, 1989).

Each vector DNA was digested over night with two different restriction enzymes so that, in consideration of the orientation of the insert, the RNA polymerase would transcribe the template starting from one of the two promoters framing the insert and would stop at the opposite end. In the one reaction a cut was produced at the end of the template opposite of the T7 promoter but excluding the SP6 promoter and in the other reaction the vector was cut at the end of the template opposite the SP6 promoter and before the T7 promoter. Restriction enzymes and buffers were obtained from Invitrogen, Boeringer, and New England Biolabs.

The digested DNA was cleaned up using phenol/chloroform extraction (Sambrook, 1989) or the QIAquick PCR Purification Kit (Qiagen).

For *in vitro* transcriptions (IVT), 1.5-2 µg of linearized vector were incubated with 2µl 10x Buffer MAXIscript™ (Ambion, Huntingdon, UK), 2µl DIG RNA Labeling Mix 10x (Roche Diagnostics, Mannheim), 0.5 µl RNasin (Promega) and 2µl SP6 / T7 polymerase (MAXIscript™) in a total volume of 20 µl at 37°C for 2 h. 2 µl of RQ1 RNase-free DNase (Promega) were added to the IVT reaction at 37°C for 25 min. Subsequently, the resulting digoxigenin-labeled RNA was purified using the clean-up protocol of the RNeasy Mini Kit (Qiagen), protected against degradation with 40 U/100 µl of Recombinant RNasin Ribonuclease Inhibitor (Promega), quantified using the NanoDrop® ND-1000 UV-Vis Spectrophotometer and the integrity checked by agarose gels. RNA probes were stored at -80°C.

### **2.3.2.2 Hybridization**

*In situ* hybridization were performed as described previously (Schaeren-Wiemers and Gerfin-Moser, 1993; Tiveron et al., 1996). Digoxigenin-labeled RNA probes were hybridized on frozen sections and revealed with Alkaline phosphatase-coupled antibodies. All buffers were made with autoclaved milliQ water and/or autoclaved after adding powdery chemicals.

#### RIPA buffer

150 mM NaCl, 1% NP-40, 0.5% Na deoxycholate, 0.1% SDS, 1 mM EDTA, 50 mM Tris pH 8.0 (NP40 was added after autoclaving)

#### (Pre)Hybridization solution

50% formamide, 5 X SSC (Saline sodium citrate), 5 X Denhardt's, 500 µg/ml herring sperm DNA, 250 µg/ml yeast RNA (Prehybridization solutions were used several times and kept at -20°C)

#### Washing buffer

50% formamide, 2 X SSC, 0.1% Tween20

#### B1-T buffer

MABT buffer: 100 mM maleic acid pH 7.5 adjusted with NaOH, 150 mM NaCl, 0.05% Tween20 (no autoclaving)

#### B2-T buffer

10% heat-inactivated FCS in buffer B1-T

#### B3 buffer

100 mM Tris pH 9.5, 100 mM NaCl, 50 mM MgCl<sub>2</sub>, 0.05% Tween20

The frozen sections were dried at RT, washed briefly in 1x PBS and incubated in RIPA buffer 3 times for 10 min. The slides were postfixed in freshly-prepared 4% paraformaldehyde, 1x PBS for 15 min at RT and washed in 1x PBS 3 times for 5 min. Acetylation was performed by transfer to 100 mM Triethanolamine pH 8, drop wise addition of acetic anhydride (0.25 % final concentration) and incubation for 15 min (gently rocking). After washing in 1x PBS 3 times for 5 min, the slides were incubated in prehybridization solution, which was previously

heated to 80°C for 3 min and then kept at the same temperature used for subsequent hybridization (depending on the RNA probe 42°-70°C). Prehybridization was performed for at least 1.5 h. 400-1200 ng/ml RNA probe (concentration depending on probe) were added to hybridization solution, heated at 80°C for 3 min, and kept on ice. 230 µl of this solution were added onto the slide and covered with a glass coverslip. The sections were incubated overnight at 42°-70°C in a chamber humidified with 5 X SSC, 50 % formamide in an incubator. After hybridization, the slides were transferred to washing buffer preheated at the same temperature as used for hybridization and incubated twice for 1 h. The sections were incubated briefly in 2x SSC at RT and for at least 30 min in B1-T buffer. Immunological detection started by blocking for at least 45 min in freshly prepared B2-T buffer. Subsequently, 200 µl of buffer B2-T containing anti-DIG antibody (1:2000, Roche) were added to each slide, covered with a coverslip and incubated in a humidified chamber overnight at 4°C.

The slides were washed in B1-T 3 times for 5 min and incubated in freshly prepared B3 buffer for 30 min. In the meanwhile, a Sigma Fast BCIP/NBT Tablet (Sigma-Aldrich) was dissolved in 10 ml of autoclaved water by vigorous shaking. A drop of 10% Tween20 was added, and the solution was sterile-filtered. In the dark, 250 µl were pipetted on each slide, covered with a coverslip and the color reaction allowed to develop in the dark in a humidified chamber at RT for 2 to 24 h. After ending the reaction with 1x PBS, the slides were briefly washed in water, air-dried and mounted in Aquamount (BDH, Poole, UK).

### 2.3.3 Immunohistochemistry

#### 2.3.3.1 Staining with a peroxidase system

Immunohistochemistry following *in situ* hybridization was performed as described in Chazal *et al.* (Chazal et al., 2000). The experiment started with an incubation of the slides in 100% EtOH, 0.5% H<sub>2</sub>O<sub>2</sub> at RT for 30min to block endogenous peroxidases. The sections were washed in 1x PBS, 0.1% Triton 3 times for 5 min and blocked in 1x PBS, 10% FCS at RT for 1 h. Incubation with the primary antibody in 1x PBS, 10% FCS was performed overnight in a humidified chamber at 4°C. After 3 washing steps, 5 min each, in 1x PBS 10% FCS at RT, the secondary antibody in 1x PBS, 10% FCS was applied for 1.5 h at RT. The slides were washed in 1x PBS 0.1% Triton. A Sigma Fast 3,3 Diaminobenzidine Tablet (DAB; Sigma-Aldrich) was dissolved in 5ml autoclaved water and, after addition of a drop of 10% Tween20, and the solution was sterile-filtered. 200µl were applied to each slide, covered with



a coverslip and the reaction stopped after 15-20 min by washing several times with distilled water. Slides were air-dried and mounted in Aquamount (BDH, Poole, UK).

Stainings with mouse primary antibodies were performed using the Vector M.O.M. Peroxidase Kit (Vector Laboratories, Peterborough, UK) according to the manufacturer's instructions. Endogenous peroxidases were blocked by incubation in 100% EtOH, 0.5% H<sub>2</sub>O<sub>2</sub> at RT for 30min. Slides were washed in 1x PBS for 2 min twice incubated in MOM Ig Blocking Reagent for 1 h at RT, washed in 1x PBS for 2 min twice, incubated in MOM diluent for 5 min and with the primary antibody in MOM diluent for 45 min at RT. After two 2 min washing steps in 1x PBS, the MOM biotinylated anti-mouse IgG reagent was added for 12-15 min at RT. After another two 2 min washing steps in 1x PBS, the slides were incubated with the ABC reagent, which has to be prepared 30 min before, for 5 min and washed in 1x PBS twice for 5 min. The revelation was performed using DAB as described above.

#### **2.3.3.2 Immunofluorescence**

Frozen sections were air-dried and rehydrated briefly in 1x PBS. Postfixation was achieved with freshly prepared 4% paraformaldehyde, 1x PBS for 10 min at RT. The sections were washed 3 times in 1x PBS and permeabilized in 1x PBS, 0.3% TritonX100 for 30 min. Blocking buffer consisted of 1x PBS, 0.3% TritonX100, 8% BSA and was applied for at least 1 h. The slides were incubated with the primary antibody in 1x PBS, 0.3% TritonX100 overnight at 4°C in a humidified chamber. After washing with 1x PBS, 0.3% TritonX100 3 times for 5 min, the secondary antibody 1x PBS, 0.3% TritonX100 was applied in the dark for 1.5 h. The sections were washed in 1x PBS, 0.3% TritonX100 3 times for 5 min, then once in 1x PBS, once in distilled water, dried and mounted with Fluoromount-G Mounting Medium (Biozol, Eching).

#### **2.3.3.3 Primary antibodies**

Anti-CD24 mAb, rat IgG, 1:500, Ascites fluid, (Rougon et al., 1991)

Anti-Frz7 pAb, rabbit, 1:66 (Orbigen, San Diego, USA)

Anti-GFAP mAb, mouse IgG, 1:2000 (Sigma)

#### **2.3.3.4 Secondary antibodies**

Peroxidase-conjugated anti-rat IgG, 1:200 (Jackson Immuno Research Laboratories, West Baltimore, USA )

Rhodamine Red<sup>TM</sup>-X-conjugated anti-rabbit IgG, 1:100 (Jackson Immuno Research Laboratories )

#### 2.3.4 Microscopy

*In situ* hybridizations and immunohistochemistry were analyzed using transmitted light brightfield and epi-fluorescence, respectively, of the Axioskop 2 plus microscope (Zeiss, Göttingen). The following objectives were utilized: Plan-Neofluar 2,5x/0,075; Ph2 Plan-Neofluar 20x/0,50; Plan-Neofluar 40x/0,75; Plan-Neofluar 63x/1,25 Oil (Zeiss). Filter set 15 (excitation BP546/12, beamsplitter FT 580, emission LP590) was used for fluorescent microscopy (488015-000, Zeiss). Pictures were taken using the digital camera AxioCam HR (Zeiss).

### 3 Results

#### 3.1 Choice of SAGE libraries

Two SAGE libraries were generated in the present work: one for neuronal precursors from adult mouse brain and one for ES cells. Subsequently, this data were compared to several already existing SAGE libraries.

Since SAGE displays the expression level of genes by absolute tag numbers, different SAGE projects can be directly compared. The reference SAGE library for ATB representing mature neuronal and glial cells, which was used for selection processes, was generated at Memorec Biotech, Cologne. The publicly available database „GSM767: SAGE\_MouseP8\_PGCP“ was chosen for the purpose of comparison. It contains tags from cerebellar granular cell precursor cells (CGCP) isolated from the brain of P8 mice (CGAP: <http://cgap.nci.nih.gov>, GSM767, Wechsler-Reya R, Riggins GJ, Strausberg RL). In contrast to the PSA<sup>+</sup> precursors, these cells are generated during embryogenesis and do not use chain migration. A SAGE library for amygdala tissue existed at Memorec Biotech. Finally, SAGE data of medulloblastoma was obtained from the publicly available database „SAGE\_Medullo\_3871“ (CGAP: <http://cgap.nci.nih.gov>, GSM766, Scott M, Riggins GJ, Strausberg RL). A SAGE library for R1 ES cells (Anisimov et al., 2002) was also used for comparison to Bruce-4 ES cells.

##### 3.1.1 Isolation of PSA<sup>+</sup> neuronal precursor cells from the adult mouse brain

In the adult mouse forebrain, PSA<sup>+</sup> neuronal precursors are generated in the SVZ and migrate along the RMS into the OB where they differentiate into GABA-ergic interneurons (Altman, 1969; Lois and Alvarez-Buylla, 1994; Luskin, 1993). Expression of PSA-NCAM is found exclusively on these migrating precursors in the adult brain (Tab. 1) (Fig. 5a) (Doetsch et al., 1997). Therefore, a specific antibody, the  $\alpha$ -PSA mAb menB (1:100) (Rougon et al., 1986), allowed the pure isolation of this cell population by FACS (Fig. 5b, c). Homogeneous cell populations are a prerequisite for the generation of a reliable gene expression profile for a certain cell type (Serafini, 1999). Great numbers of mice were required to obtain sufficient numbers of precursor cells to isolate enough total RNA of high quality for further experiments. The isolation and FACS procedure was performed several times with mice numbers ranging from 10-45 to improve the protocol (2.1.1; 2.1.2) and to train working swiftly to minimally affect the cells. The SVZ tissue from the lateral wall of the anterior horn

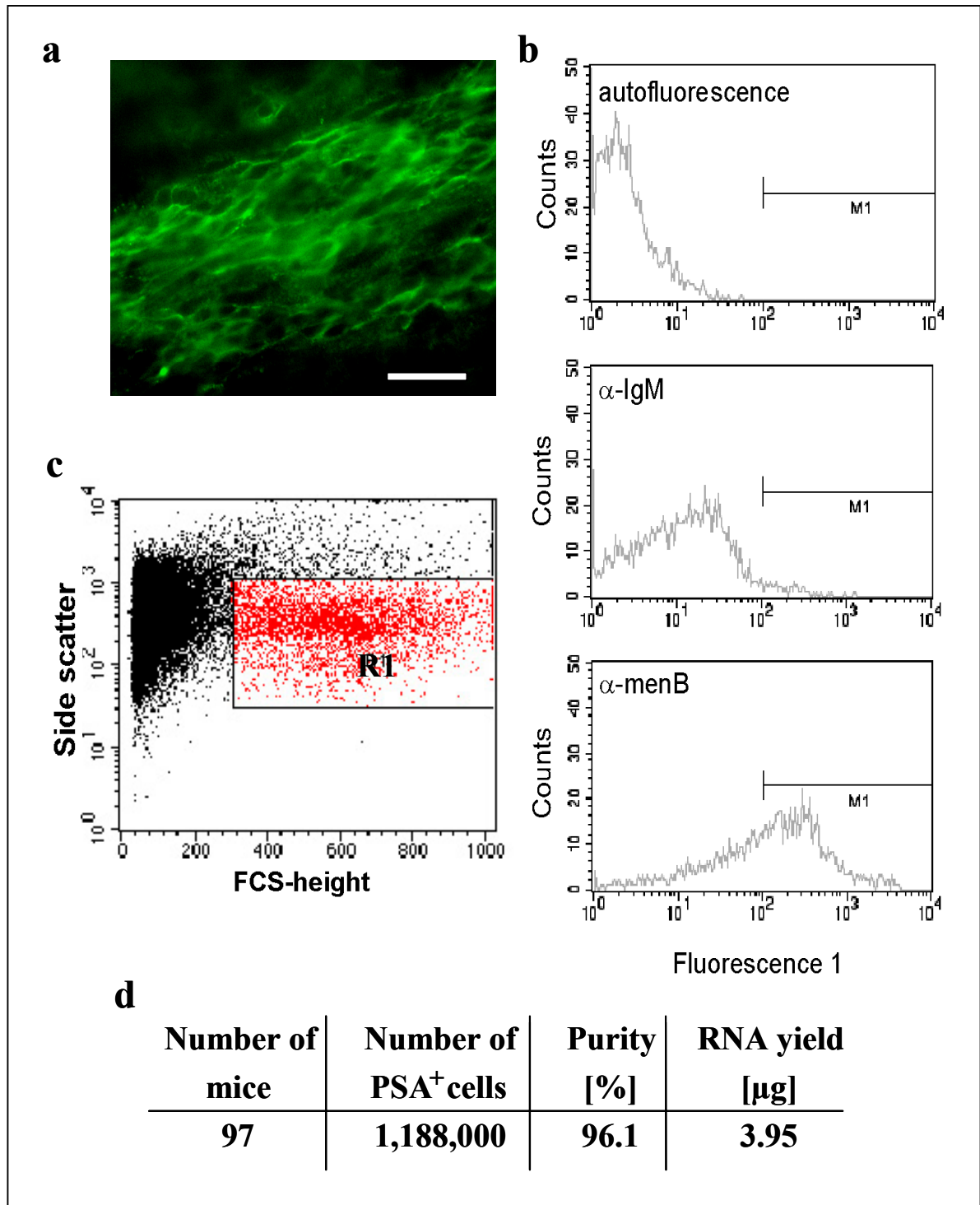


Fig. 5 Isolation of PSA<sup>+</sup> neuronal precursors from the adult mouse forebrain.  $\alpha$ -PSA mAb menB specifically recognizes PSA-NCAM on the surface of the immature neuronal cells in the RMS (a) (Immunostaining kindly provided by Céline Zimmer). Use of this antibody permitted the isolation of a pure population of PSA<sup>+</sup> cells by FACS. R1 marks the population of living cells (b) from which PSA<sup>+</sup> cells were selected in M1 by subtracting the autofluorescence of the cells and the non-specific labeling of the secondary  $\alpha$ -IgM antibody (c). These total yields of PSA<sup>+</sup> cells and RNA were obtained from several FACS experiments performed for the subsequent generation of a SAGE library (d). Scale bar: 25  $\mu$ m.

of the LV was dissected from mouse brain vibratome sections. The cells were individualized, labeled with the  $\alpha$ -PSA mAb and underwent FACS isolation. On average, one mouse yielded 12,000-13,000 PSA<sup>+</sup> cells and 40 ng of total RNA (Fig. 5d). The RNA was immediately isolated after the FACS. Any culture step that might have changed the properties of the cells was omitted. RNA integrity was checked on agarose gels and using the 2100 Bioanalyzer.

### 3.1.1.1 Control experiments with the human cell line TE 671

Since PSA<sup>+</sup> cells could not be isolated without antibody binding and FACS, the best possible control experiment in an attempt to assess their influence on gene expression was performed with a PSA-expressing cell line. PSA-expressing TE 671 cells (monolayer human rhabdomyosarcoma) were used to investigate if the binding of the  $\alpha$ -PSA mAb to PSA-NCAM has any effect on intracellular signaling pathways or if the FACS procedure affects gene expression.

RNA from TE 671 cells incubated with and without the antibody was analyzed using PIQOR<sup>TM</sup> cDNA microarrays. For the second question, cells were sorted by FACS, following incubation with  $\alpha$ -PSA mAb and anti-mouse IgM-FITC, while the control cells were kept on ice. RNA of both samples was prepared. Microarray analysis for both experiments demonstrate that, at least in the case of TE 671 cells, neither the binding of the  $\alpha$ -PSA mAb nor the FACS affect the expression of the 648 genes present on the microarray (Fig. 6).

### 3.1.2 Isolation of Bruce-4 ES cells

A SAGE library for ES cells was required for the identification of potential NSC markers as explained in 1.2. Cultured ES cells are accessible as a homogeneous population, are positioned above NSC in the hierarchy of developmental potential and their gene expression program is believed to overlap with that of NSC (Clarke et al., 2000; Ivanova et al., 2002; Ramalho-Santos et al., 2002) (1.2). Bruce-4 ES cells were chosen because they are derived from the inbred mouse strain C57BL/6J (Kontgen et al., 1993) that was also used for PSA<sup>+</sup> cell isolation. Bruce-4 ES cells have been used in many gene targeting experiments showing excellent germ line transmission, which proves their pluripotent state. Prior to the RNA isolation of ES cells, the ratio of ES cells to contaminating fibroblasts was reduced from 60:1 after initial plating to 80:1 (1.25%).  $5 \times 10^6$  ES cells yielded 88.8  $\mu$ g of total RNA.

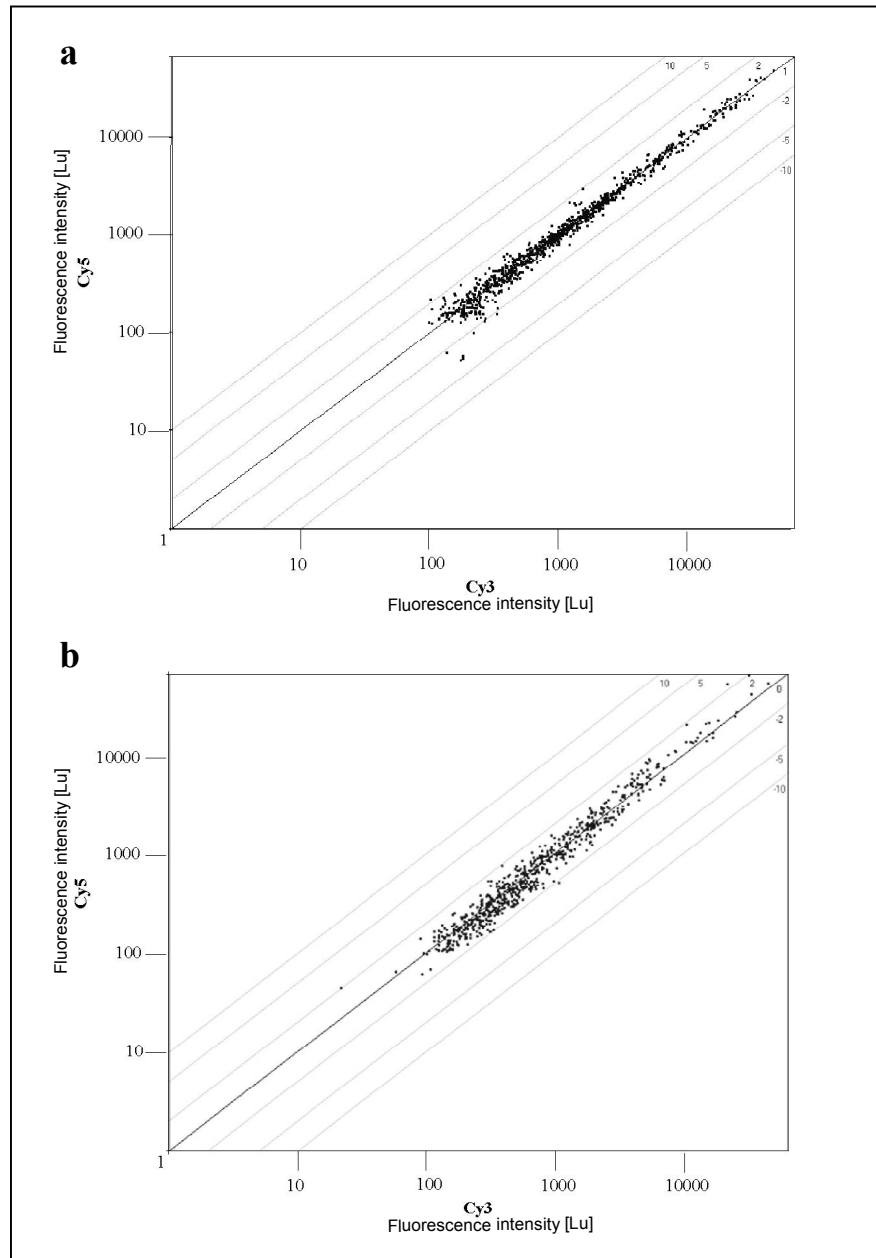


Fig. 6 Scatter plots of microarray control experiments for the isolation of PSA<sup>+</sup> neuronal precursors. Microarray analysis of RNA from PSA<sup>+</sup> TE671 cells in the presence and absence of anti-PSA antibody showed that antibody binding does not affect gene expression (a). Microarray analysis of RNA from PSA<sup>+</sup> TE671 cells with and without FACS after incubation with anti-PSA antibody showed that the FACS procedure does not affect gene expression either (b). The numbers in the upper right corners indicate the x-fold differential expression. Each dot represents a single microarray spot. Lu, Light unit.

### 3.2 Generation of SAGE libraries for PSA<sup>+</sup> precursors and ES cells

To obtain a quantitative measure of the transcriptomes, SAGE was performed for PSA<sup>+</sup> cells and ES cells. 15  $\mu$ g of total RNA obtained from ES cells and 1.4  $\mu$ g from PSA<sup>+</sup> cells were used for the SAGE. Large-scale PCR for the former was done with 30 cycles, for the latter with 32 cycles. 36,093 SAGE tags were sequenced for the PSA<sup>+</sup> cells, 34,947 for the ES cells

(Tab. 2). The mapping of SAGE tags to UniGene and SwissProt was consistent with that observed in other SAGE databases (Gunnarsen et al., 2002). Although tags found only once have been included in the total tag distribution analysis, they have been excluded from gene identification steps. For PSA<sup>+</sup> cells, 20% of the tags belonged to known transcripts, for ES cells 25% (Fig. 7).

Tab. 2 SAGE tag numbers and distribution of tag frequencies for PSA<sup>+</sup> cells and ES cells

	PSA <sup>+</sup> cells	ES cells
Total number of tags sequenced	36,093	34,947
Number of tags after elimination of linker tags	33,046	34,822
Number of unique tags	16,161	10,896
Number of transcripts	14,754	9,921
Tag frequencies		
> 300	3	5
201-300	1	8
101-200	5	25
51-100	22	37
21-50	86	118
11-20	173	259
3-10	1,898	1,583
2	1,908	1,367
1	12,065	7,494

### 3.3 PSA<sup>+</sup> cell-enriched genes identified by SAGE

In order to identify genes enriched in PSA<sup>+</sup> precursors, the relative abundance of transcripts in the PSA<sup>+</sup> cells SAGE data was compared with that in ATB. Genes that were differentially upregulated in PSA<sup>+</sup> cells with a statistical significance of  $p < 0.05$  were selected and sorted by decreasing factor (Tab. 3). All tag numbers have been normalized to 100,000 tags and refer to the combined tag number of a given transcript.

Specificity of the PSA<sup>+</sup> cells SAGE library was demonstrated by the detection of several genes that were previously characterized and known to be expressed by PSA<sup>+</sup> cells. NCAM was expressed (19.3 tags), but was not differential against ATB (16.8 tags), which is consistent with the fact that it is present throughout the brain generally without the PSA modification. However, the sialyltransferase ST8siaII, which is responsible for polysialylation of NCAM on this precursor population (Eckhardt et al., 2000; Kurosawa et al., 1997), was found to be differentially expressed ( $p < 0.05$ ) in the precursor cells (11.1 versus 0.7 tags). High numbers of transcripts were found for the glycosylphosphatidylinositol-anchored molecule CD24 (63.7 versus 1.4 tags), a negative regulator of proliferation, which is highly

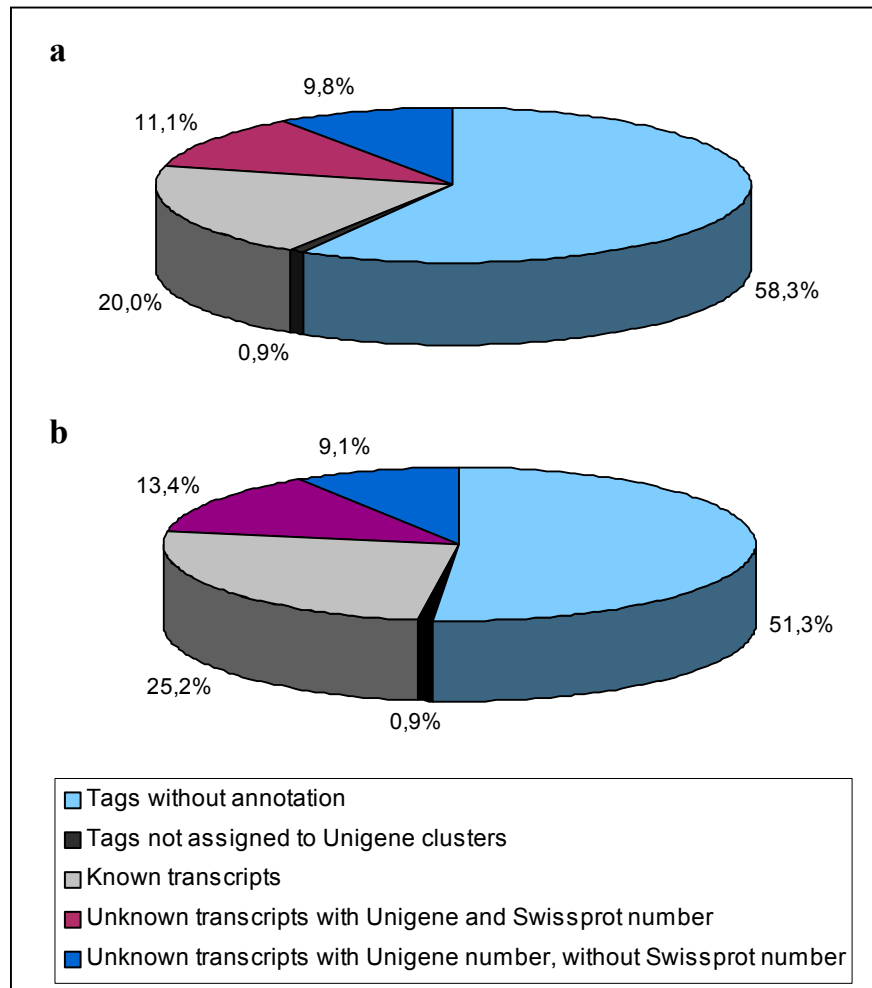


Fig. 7 Mapping of (a) PSA<sup>+</sup> cell SAGE tags and (b) ES cell SAGE tags to UniGene clusters and SwissProt.

expressed by this cell population (Belvindrah et al., 2002) and Doublecortin (Dcx; 38.8 versus 0.7 tags), a microtubule-associated protein, which is expressed by migrating neurons in the postnatal brain (Gleeson et al., 1999). Expression of the Reelin receptor ApoER2 (13.6 versus 4.2 tags) was found (Hack et al., 2002). Transcripts of migration regulators Ephrin-B1 and -B2 (11.1 versus 0.7; 19.4 versus 2.1 tags) were observed in the PSA<sup>+</sup> precursor population (Conover et al., 2000; Hu, 1999; Wu et al., 1999) as well as Nestin (11.1 versus 1.4 tags), which was originally found as a marker for neuroepithelial stem cells and later in almost all SVZ cells (Doetsch et al., 1997; Lendahl et al., 1990), Musashi2 (Sakakibara et al., 2001) and Notch1 (16.6 versus 2.8 tags).

Besides these previously described genes, many significantly differentially expressed genes were identified, which have been characterized in other systems and tissues, as well as novel genes with unknown functions. High transcripts numbers were present of chemokine ligands Ccl4/MIP1 beta (85.9 versus 0 tags), the most strongly expressed gene against ATB,



Ccl3/MIP1 alpha (33.2 versus 0.7 tags), Cxcl16 (11.1 versus 0 tags), C3a anaphylatoxin chemotactic receptor (C3aR1) (16.6 versus 0.7 tags), Chemokine orphan receptor 1 (5.5 versus 0.7 tags), Cxcl10 (5.5 versus 0 tags) and Ccl22 (5.5 versus 0 tags). None of these chemotactic factors was found in the ES cell SAGE data.

The antiapoptotic factor Survivin/IAP4 (16.6 versus 0.7 tags) and cell death promoting Caspases 2 and 6 (each 5.5 versus 0 tags) were strikingly upregulated in this cell population. Significant differential expression was observed for transcription factors implicated in neural development like Sox11 (99.7 versus 2.1 tags), Sox4 (113.6 versus 3.5 tags), Sox2 (11.1 versus 0.7 tags) and Sox9 (13.9 versus 3.5 tags) (Cheung et al., 2000; Li et al., 2002; Spokony et al., 2002; Uwanogho et al., 1995), Pax6 (13.9 versus 0 tags) (Collinson et al., 2003; Talamillo et al., 2003) and Transcription factor 4/ME2 (47.1 versus 13.3 tags) (Chiaramello et al., 1995; Soosaar et al., 1994). The Sox family was represented by members 2, 4, and 11 in ES cells. The homeobox genes Dlx1 (38.8 versus 0 tags), Dlx2 (33.2 versus 0.7 tags) and Dlx5 (11.1 versus 0 tags), which are found in immature neurons during development prior to terminal differentiation, were also prominently expressed (Bulfone et al., 1993; Eisenstat et al., 1999; Simeone et al., 1994).

The SAGE revealed expression of the migration regulator Slit1 (11.1 versus 1.4 tags) in PSA<sup>+</sup> cells. Slit1 was known to be expressed by the septum, and only recently were PSA<sup>+</sup> cells and C cells shown to be immunoreactive for Slit1 (Nguyen-Ba-Charvet et al., 2004; Wu et al., 1999). Slit2 (0 versus 1.4 tags) and the slit receptors Robo2 (2.8 versus 0 tags) and Robo3 (0 versus 0.7 tags) were not differentially expressed.

Abundant transcripts were found for Il-1 alpha (27.7 versus 0 tags) and Il-1 beta (5.5 versus 0 tags) and Pellino1 (13.9 versus 0.7 tags), of cell cycle regulators Cyclins A2 (11.1 versus 0 tags), B1 (8.3 versus 0 tags), G2 (8.3 versus 0 tags), L2 (33.2 versus 2.1 tags), L1 (33.2 versus 3.5 tags), I (52.6 versus 18.9 tags), Cdk8 (8.3 versus 0.7 tags), Cdc20 (11.1 versus 0 tags) and proliferation markers Ki67 (13.9 versus 0 tags) and PCNA (41.6 versus 4.2 tags). Transcripts of disease-related genes WIP (Wiskott-Aldrich syndrome) (8.3 versus 0 tags), Prader-Willi chromosome region1 (8.3 versus 0 tags) and Fragile X mental retardation syndrome1 (8.3 versus 0 tags) were present.

Cell adhesion molecules Cadherin2 (22.2 versus 2.8 tags), Cadherin11 (44.3 versus 11.2 tags) and Adrm1 (8.3 versus 1.4 tags) were also highly expressed in PSA<sup>+</sup> cells. In addition to these genes, for which information was available, a large variety of novel genes was found, like for example, RIKEN cDNA 3110003A17 (30.5 versus 0.7 tags) and RIKEN cDNA 1110038L14 (13.9 versus 0 tags).

## Results

Tab. 3 Top 60 genes and additional selected genes upregulated in PSA<sup>+</sup> cells versus adult total brain.

Position	SAGE tag	Tag number PSA <sup>+</sup> cells	Tag number ATB	UniGene number	Annotation	Microarray fold upregulation
1	CATTTTCATAA	85.9	0.0	Mm.1255	Chemokine ligand Ccl4	
2	TTGCACAAGCT	38.8	0.0	Mm.4543	Dlx1 (manual annotation)	
3	TCCCCCTCAAT	33.2	0.0	Mm.250675	Clone IMAGE:1230530, mRNA	
4	TGGGAAATGAT	33.2	0.0	Mm.34385	RIKEN clone:E430010F15	n.d.
5	GAAATGGCCTT	30.5	0.0	Mm.153457	RIKEN cDNA 2810406C15	
6	TAACTATCAAC	27.7	0.0	Mm.15534	Interleukin 1 alpha	n.d.
7	GCAAACAATCA	22.2	0.0	Mm.27972	Nsap1-pending NS1-associated protein 1	
8	TCCTGTAAATA	22.2	0.0	Mm.12508	Karyopherin alpha 2	
9	CAGAGAATATA (4)	22.2	0.0	Mm.23829	Hypothetical protein LOC238799	
10	TGTGTGAGGTG (3)	38.8	0.7	Mm.12871	Doublecortin	34.1
11	AACTGACAAAT	33.2	0.7	Mm.1282	Chemokine ligand Ccl3	
12	AAGGAAAGGCC	16.6	0.0	Mm.517	Manic fringe	n.d.
13	AATTAATCAAG	16.6	0.0	Mm.45769	RIKEN cDNA 2700083E18	
14	ATTTTATTGGG	16.6	0.0	Mm.3501	Kinesin family member C5A	n.d.
15	GGGGAGAATTC	33.2	0.7	Mm.3896	Dlx2 (manual annotation)	
16	GCCCTATGCTT (2)	16.6	0.0	Mm.27732	Dihydropyrimidinase-like 5	
17	CAAACGCTGG (2)	16.6	0.0	Mm.94021	RIKEN cDNA A230055N17	
18	AGGAAGCTAGA (2)	16.6	0.0	Mm.99	Ribonucleotide reductase M2	
19	TTGAGTTTTA (2)	33.2	0.7	Mm.29014	T-cell lymphoma invasion and metastasis 2	
20	GCACTGTTAAC (5)	99.7	2.1	Mm.257329	Sox11	
21	TTATGGAATTG (3)	63.7	1.4	Mm.6417	mCD24	12.1
22	TCTGTTTTTAT	30.5	0.7	Mm.153803	RIKEN cDNA 2700078F24	
23	TCACCTGAAAC (2)	30.5	0.7	Mm.16767	Heterogeneous nuclear ribonucleoprotein A2/B1	
24	AAAAATGTTGT (2)	30.5	0.7	Mm.28149	RIKEN cDNA 3110003A17	22.4
25	ACGTTTGTGGG	27.7	0.7	Mm.23096	Ppp2r3a	
26	ACTGGTGTACC	13.9	0.0	Mm.28299	Hypothetical protein LOC229363	
27	AGGAAGATCAC	13.9	0.0	Mm.4078	Antigen identified by monoclonal antibody Ki 67	73.6
28	CAGAAGGCCTG	13.9	0.0	Mm.82648	RIKEN cDNA 9030612E09	
29	CGCTGTATTCT	13.9	0.0	Mm.326	RIKEN cDNA 1110038L14	12.0
30	GAAAGGGAGGG	13.9	0.0	Mm.25670	RIKEN clone:4832416J22	
31	GGTTTCTTCCC	13.9	0.0	Mm.16711	Mini chromosome maintenance deficient 2	
32	TAAGTCATAA	13.9	0.0	Mm.24591	RIKEN cDNA D030020G18	
33	GTTGACCTGCT (2)	13.9	0.0	Mm.142095	Calcium regulated heat stable protein 1	
34	TTATATTCTTG (2)	13.9	0.0	Mm.181709	Regulator of G-protein signaling 16	n.d.
35	ACTACATACAG (3)	13.9	0.0	Mm.18637	Tera-pending, teratocarcinoma expressed	1.7
36	CAATCATTTGT (2)	13.9	0.0	Mm.3608	Pax6	1.9
37	CCACTTGGCT (2)	24.9	0.7	Mm.2958	ESTs	
38	ATTGTTTATGA (4)	412.8	12.6	Mm.911	High mobility group nucleosomal binding domain 2	
39	ACAGGCACGAG (6)	113.6	3.5	Mm.18789	Sox4	n.d.
40	AAAATAAAACA	11.1	0.0	Mm.4933	Mini chromosome maintenance deficient 6	
41	AAAGTTATTTA	11.1	0.0	Mm.134794	RIKEN cDNA 2310014H01	
42	AATGAGTTTCA	11.1	0.0	Mm.259561	RIKEN clone:E330024K01 product: DC6 protein homolog	
43	ACTTGTGTTGT	11.1	0.0	Mm.22806	RIKEN cDNA C130018M11	
44	AGGTAGATGTA	11.1	0.0	Mm.320	Polymerase alpha 2	
45	ATGTAATAAAG	11.1	0.0	Mm.8155	TG interacting factor	n.d.
46	CAAATTAACCC	11.1	0.0	Mm.4189	Cyclin A2	n.d.
47	CCAGTGATGGC	11.1	0.0	Mm.234246	RNA binding motif protein 12	
48	CCCAGAGAGGG	11.1	0.0	Mm.4511	RIKEN cDNA 8430437G11	
49	CTGTCTTGAGA	11.1	0.0	Mm.46424	Chemokine ligand Cxcl16	
50	GAAATAAAGAG	11.1	0.0	Mm.3931	Max	

## Results

Tab. 3. (continued)

Position	SAGE tag	Tag number PSA <sup>+</sup> cells	Tag number ATB	UniGene number	Annotation	Microarray fold upregulation
51	GAAGTGAATA	11.1	0.0	Mm.22856	RIKEN cDNA B130052G07	
52	GAGGGAGTTTC	11.1	0.0	Mm.37755	ESTs	
53	GCCAAGGTGGC	11.1	0.0	Mm.29931	Cdc20	n.d.
54	GCTGTGTATTA	11.1	0.0	Mm.37801	Shc SH2-domain binding protein 1	
55	GGCACTGTTGG	11.1	0.0	Mm.1013	Lig1	
56	TAAGATTTAAA	11.1	0.0	Mm.21873	Retroviral integration site 2	
57	TAAGTTATTGC	11.1	0.0	Mm.4873	Dlx5	n.d.
58	TACTCTCCTTT	11.1	0.0	Mm.29133	Budding uninhibited by benzimidazoles 1 beta	
59	TAGCTATGGAG	11.1	0.0	Mm.24629	RIKEN cDNA 2810439F02	
60	TATAGTCTATA	11.1	0.0	Mm.131705	Clone MGC:41439 IMAGE:1314987	
81	CATATACTCCC	8.3	0.0	Mm.22569	Cyclin B1	
92	GGTAAGTGTTG	16.6	0.7	Mm.8552	Survivin/IAP4	60.7
95	TAAATATAATT	8.3	0.0	Mm.3527	Cyclin G2	n.d.
102	TATCTGGAATA	16.6	0.7	Mm.27141	Rac GTPase-activating protein 1	5.1
107	TGCTCTTCTGT	8.3	0.0	Mm.157744	Pwcr1, Prader-Willi chromosome region 1	
112	TTCGCTGAATA	8.3	0.0	Mm.31512	Ring finger protein 2	n.d.
116	TTTTTAAAATC	8.3	0.0	Mm.3451	Fmr1, Fragile X mental retardation syndrome 1	
119	TTGCTGAAAGA (2)	8.3	0.0	Mm.223504	WIP, Wiskott-Aldrich syndrome Protein interacting protein	
133	TGAGCAGGACA (2)	16.6	0.7	Mm.2408	C3aR1, complement component 3a receptor 1	
138	AAGGTTGACTC	13.9	0.7	Mm.9488	CDC like kinase 4	
142	AGTTTTTCTTC	13.9	0.7	Mm.1685	Plexin A3	13.3
147	ATAACTGATCT (2)	13.9	0.7	Mm.28957	Pellino 1	
148	TGGAAAGTGAA	24.9	1.4	Mm.5043	Fos	
149	TCTCTGACTTG (3)	91.4	5.6	Mm.2769	MARCKS-like protein	n.d.
156	AACCATATTGT	5.5	0.0	Mm.6522	Cmkor1, chemokine orphan receptor 1	
164	AATGTTTCCTG	5.5	0.0	Mm.3921	Caspase 2	n.d.
191	CCCAGGCTGCT	5.5	0.0	Mm.877	Cxcl10, chemokine (C-X-C motif) ligand 10	
207	CTTTGAAATGT	5.5	0.0	Mm.196328	Bcl6 interacting corepressor	
219	GATTTAAGCAC	5.5	0.0	Mm.2998	Nedd1, Neural precursor cell expressed, developmentally down-regulated gene 1	
221	GCACATTCTGT	5.5	0.0	Mm.222830	Interleukin 1 beta	n.d.
243	TATATATTTGA	11.1	0.7	Mm.4541	Sox 2	2.9
246	TCCTGAAAGGTC	5.5	0.0	Mm.12895	Ccl22, chemokine (C-C motif) ligand 22	
255	TGCAGCTTTCT	5.5	0.0	Mm.4303	Ezh2, Enhancer of zeste homolog 2	
268	TTCTGTACAGA	5.5	0.0	Mm.1452	Cd86a	n.d.
269	TTGGACGTGGT	5.5	0.0	Mm.28814	Caspase 6	
302	AGACAATGCTG (2)	11.1	0.7	Mm.3374	Ephrin B1	n.d.
307	GGCTGGTTGAC (2)	11.1	0.7	Mm.4954	ST8sialII, Sialyltransferase 8B	1.9
312	TTTAATACAAG (2)	33.2	2.1	Mm.13725	Cyclin L2	5.4
317	GGGTCCTCTTT	19.4	1.4	Mm.31436	Meis 2, myeloid ecotropic viral integration site-related gene 1	
322	TATATTGATTG (2)	55.4	4.2	Mm.16596	Btg1, B-cell translocation gene 1	
336	CTATGGATACT	16.6	1.4	Mm.29558	RIKEN clone:G430091K07 potentially semaphorin 4C	n.d.
373	TTGAGGGTGGG	8.3	0.7	Mm.5114	Dvl2, Dishevelled 2	n.d.
386	CTCACAAATCA (2)	8.3	0.7	Mm.219645	Cdk8	2.3
387	CAATGACTTGT (2)	8.3	0.7	Mm.23684	Axin	
431	AATGTTTCTGC (3)	41.6	4.2	Mm.7141	Pcna, Proliferating cell nuclear antigen	n.d.
433	GCAATAAATGG (3)	97.0	9.8	Mm.19016	Drebrin 1	2.3
434	GGCAAAGATTT (3)	33.2	3.5	Mm.175612	Cyclin L1	
436	ACAGTTAAGCC (2)	19.4	2.1	Mm.4005	Ephrin B2	n.d.
447	ACTGAAGTCAG	16.6	2.1	Mm.3940	Llg1h, Lethal giant larvae homolog	

## Results

Tab. 3. (continued)

Position	SAGE tag	Tag number PSA <sup>+</sup> cells	Tag number ATB	UniGene Number	Annotation	Microarray fold upregulation
452	CCCAGAGGAGC	11.1	1.4	Mm.23742	Nestin	
453	CCCTCTCTCAA	11.1	1.4	Mm.40322	Slit1	n.d.
457	GAAGAATCCGT	11.1	1.4	Mm.22168	Sialic acid synthase	1.9
458	GAATATAAGTA	16.6	2.1	Mm.41650	Staufen 1	n.d.
483	TTAATATCTTT (3)	22.2	2.8	Mm.14897	Cadherin 2	0.9
486	GGATATGTGGT (2)	94.2	11.9	Mm.181959	Egr1, Early growth response 1	n.d.
492	GCCCCCTTCCA	19.4	2.8	Mm.1167	Jun-B	n.d.
537	CAGAACAATGC	8.3	1.4	Mm.181562	Adrm1, Adhesion regulating molecule 1	1.7
567	TTACATAAAGG (2)	8.3	1.4	Mm.10735	Cask	1.7
581	TCGTGCTGCCT (2)	8.3	1.4	Mm.24255	Tle3, Transducin-like enhancer of split 3	
596	CAAACACTGTAG (4)	16.6	2.8	Mm.31255	Notch1	n.d.
652	AAATAAAGTCT (2)	13.9	2.8	Mm.193413	Agrin	1.8
674	GAATAACTTAC (4)	19.4	4.2	Mm.482	Jun/AP1	3.6
696	GAGTGGATTCT	22.2	5.6	Mm.4426	Cd63a	1.0
713	TGGACATAAAT (3)	11.1	2.8	Mm.35930	Msi2h, Musashi 2	
723	GAGGACGATTG (2)	13.9	3.5	Mm.46607	Sox9	
740	AAGCTGAGTGG (2)	44.3	11.2	Mm.1571	Cadherin 11	
753	GTCAGATTTT (4)	47.1	13.3	Mm.4269	Tcf4, Transcription factor 4/ ME2	4.7
757	ATAGAGGCAAT (5)	61.0	17.5	Mm.27218	Morf4l2, Mortality factor 4 like 2	
821	TACTGCTGATA (3)	52.6	18.9	Mm.22711	Cyclin I	
827	TTGATAATTAG (6)	49.9	18.2	Mm.14644	Translin	
828	GATAGAGAGTT	36.0	13.3	Mm.1131	Neural proliferation, differentiation and control gene 1	

Significantly differentially expressed genes ( $p < 0.05$ ) are sorted by decreasing factor for expression in PSA<sup>+</sup> cells versus ATB. Additional genes were selected from the list based on literature stating their involvement in other systems. Tags without UniGene annotation were removed from the list. In cases, where several tags belong to one transcript, the main tag is shown with the number of different tags indicated in parentheses. Total tag numbers are normalized to 100,000. Part of the genes present in the SAGE analysis was also assessed by cDNA microarray experiments. The results are shown as “fold upregulation” or not detected (n.d.).

Various receptors for Tenascin-R are known, but it is unclear which one is responsible for the interaction with PSA<sup>+</sup> cells in the OB (Saghatelyan et al., 2004). Though not differentially expressed, the SAGE showed the presence of Contactin1 (5.5 versus 15.4 tags), Chondroitin sulfate proteoglycan (CSPG) 3 (2.8 versus 2.8 tags), CSPG5 (5.5 versus 10.5 tags) and CSPG6 (5.5 versus 1.4 tags) in the neuronal precursors.

### 3.3.1 Clustering of SAGE data

A cluster analysis which arranges SAGE data in groups according to molecular function and sequence motifs yields additional information since the statistical significance is related to entire groups including also those genes which are not significantly differentially expressed by themselves. Two different data sources were used to group the SAGE data into biologically meaningful categories and to re-calculate the statistics based on the aggregated

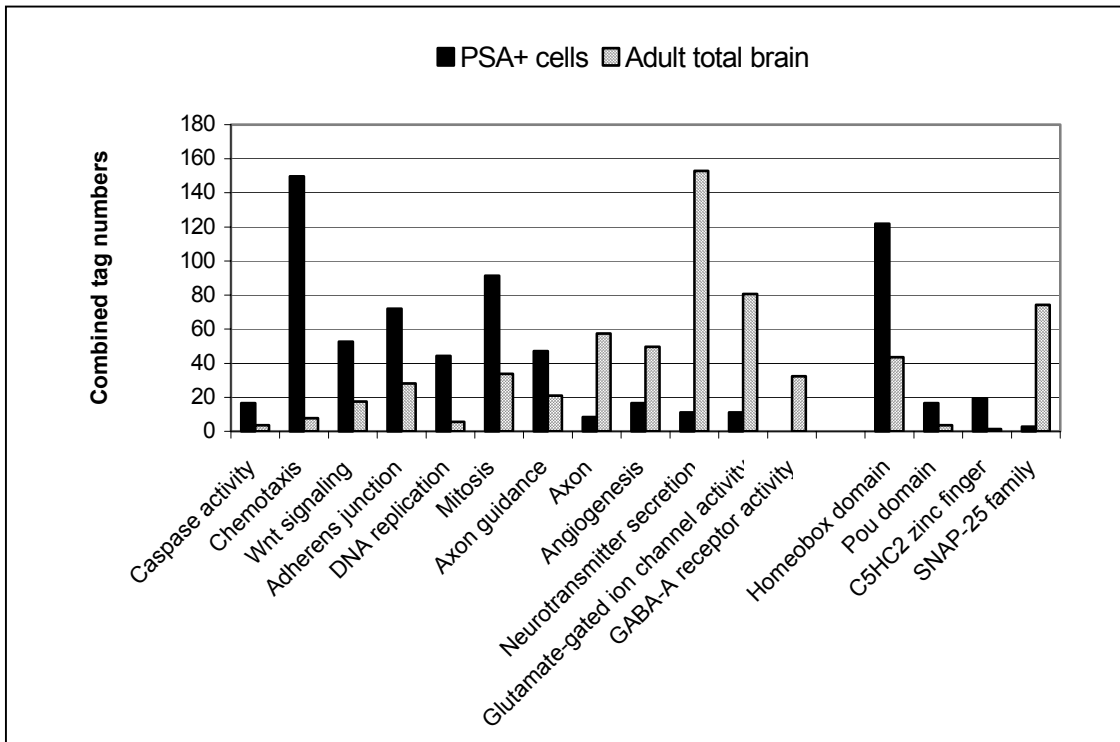
data. The biological function of gene products were annotated by the criteria defined by the Gene Ontology Consortium (GO; The Gene Ontology Consortium, 2000; [www.geneontology.org](http://www.geneontology.org)), using the category-to-gene mapping provided by the GOA project (Camon et al., 2003). The Gene Ontology project provides three controlled vocabularies (ontologies) that can be used to describe gene products in terms of their associated biological processes, cellular components and molecular functions. The GOA project assigns the proteins of the SwissProt/TrEMBL database to the appropriate GO categories. Additionally, gene products were grouped by domain architecture, which was derived from the PROSITE (Falquet et al., 2002), and Pfam databases (Bateman et al., 2002) supplemented by a proprietary motif database developed at Memorec Biotech.

Clusters were selected from the comparison of PSA<sup>+</sup> cells against ATB (Fig. 8a) and against CGCP (Fig. 8b). Prominently upregulated in the PSA<sup>+</sup> precursors in both comparisons was the GO cluster “Chemotaxis”, which comprises alpha and beta chemokines and C3aR1 (Tab. 4 a, b). Cxcl12/SDF1 complements this cluster of genes, in which the other members were individually significantly upregulated in PSA<sup>+</sup> precursors. Not included in these clusters were Cxcl14 (11.1 tags) as well as Cx3cl1 (2.8 tags) and its receptor Cx3cR1 (5.5 tags), which was due to missing GOA annotations. CXCR4, the receptor for SDF-1/Cxcl12, which has been shown to be involved in the control of migration during cerebellum development, was missing in the cluster from the comparison against CGCP (0 versus 34.5 tags) (Lazarini et al., 2003; Zhu et al., 2002).

Although its overall expression was lower compared to the other clusters, it is remarkable that the cluster of caspase activity is increased by a factor 5 and factor 3 in PSA<sup>+</sup> cells compared to ATB (Tab. 4c) and CGCP, respectively. Wnt signaling-implicated genes including  $\beta$ -Catenin and Dishevelled2 (Dvl2) were upregulated as a whole compared to ATB and CGCP. Genes making up the cluster “Adherens junction” like Afadin/Mllt4 and Cadherin2 were more highly expressed in PSA<sup>+</sup> cells than in ATB and CGCP. The clusters “Mitosis” and “DNA replication” were both upregulated in PSA<sup>+</sup> precursors against brain. However, “Mitosis” was even stronger in CGCP. The “Axon guidance” cluster featuring, for example, Er81/Etv1, Slit1 and Ephrins B1 and B3, was significantly differential against ATB and CGCP. Six members of the Ephrin family constituted an individual cluster “Ephrin”, which is upregulated 4-fold against CGCP.

Genes containing homeoboxes were upregulated by a factor 3 in PSA<sup>+</sup> precursors compared to ATB and almost equally expressed by CGCP. Transcription factors with POU domains by

a



b

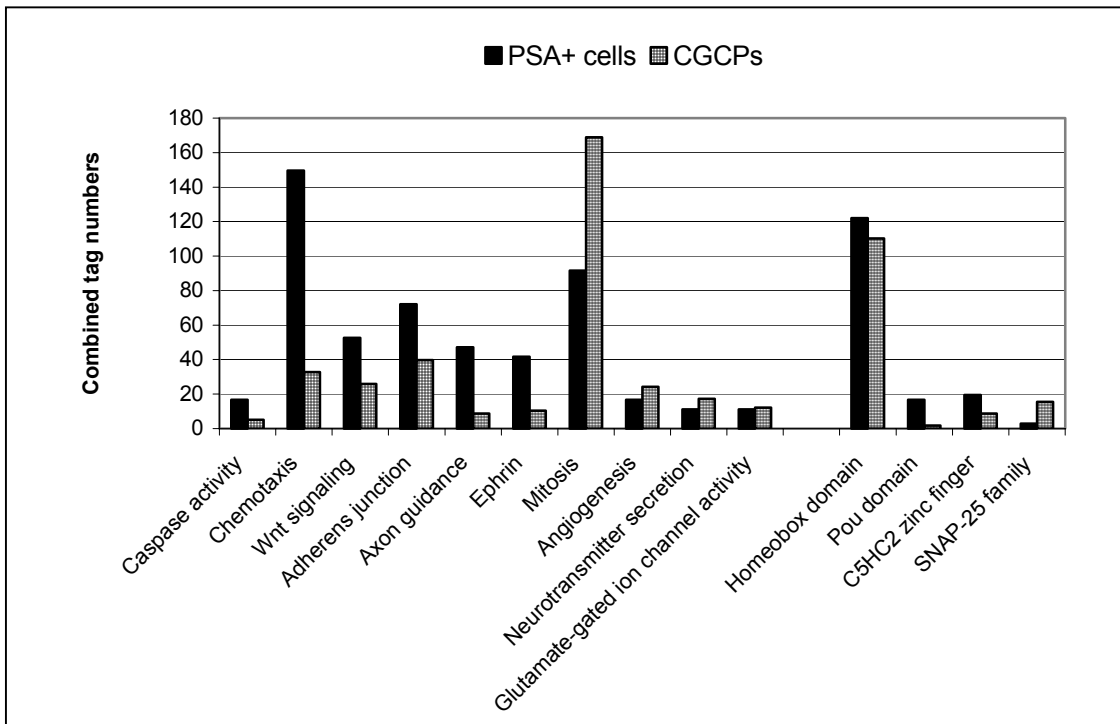


Fig. 8 Clustering of SAGE data into gene groups based on function and sequence motifs. The Gene Ontology Consortium (GO), the Gene Ontology Annotation (GOA) database as well as sequence motif databases were linked to the SAGE results to create clusters of genes with similar molecular functions or sequence motifs upregulated as a whole according to the SAGE. Clusters were selected from the comparisons of PSA<sup>+</sup> cell against ATB (a) and CGCP (b) SAGE data.

## Results

themselves were upregulated 5-fold against brain and 10-fold against CGCP. The C5HC2 zinc finger cluster, which was increased 4-fold, comprised Jumonji, Plu1 and SmcX.

Clusters of genes linked to neuronal differentiation were highly expressed in ATB but low or absent in PSA<sup>+</sup> cells. The cluster of genes related to axon formation was almost 7-fold stronger in ATB than in PSA<sup>+</sup> cells. GABA<sub>A</sub> receptor expression was absent in PSA<sup>+</sup> precursors (Tab. 4d)

Tab. 4 Gene lists for five selected clusters from the clustering analysis of SAGE data.

**a**

SAGE tags	PSA+	ATB	Factor	Signifi-	Annotation
	cells		PSA/ATB	cance	
<b>combined</b>	149.6	7.7	19.4	26.9	<b>9 matches, chemotaxis (GO0006935)</b>
TGAGCAGGACA	11.1	0.7	15.8	2.5	C3ar1, complement component 3a receptor 1 [sp O09047]
TGCAATGAATA	5.5	0.0	15.8	1.8	C3ar1, complement component 3a receptor 1 [sp O09047]
GCGCCCTCCCC	0.0	2.8	-8.0	0.2	Ccl21b, chemokine (C-C motif) ligand 21 [sp O09006]
TCCTGAAGGTC	5.5	0.0	15.8	1.8	Ccl22, chemokine (C-C motif) ligand 22 [sp O88430]
AACTGACAAAT	33.2	0.7	47.4	7.7	Ccl3, chemokine (C-C motif) ligand 3 [sp P10855]
CATTTTCATAA	85.9	0.0	245.0	21.9	Ccl4, chemokine (C-C motif) ligand 4 [sp P14097]
CCCAGGCTGCT	5.5	0.0	15.8	1.8	Cxcl10, chemokine (C-X-C motif) ligand 10 [sp P17515]
CTGTAAAAAAA	0.0	0.7	-2.0	-0.1	Cxcl12, chemokine (C-X-C motif) ligand 12 [sp P40224]
GGTGATTATCT	2.8	2.8	-1.0	-0.1	Cxcl12, chemokine (C-X-C motif) ligand 12 [sp P40224]

**b**

SAGE tags	PSA+	CGCP	Factor	Signifi-	Annotation
	cells		CGCP/PSA	cance	
<b>combined</b>	149.6	32.7	-4.6	9.2	<b>13 matches, chemotaxis (GO0006935)</b>
TGAGCAGGACA	11.1	1.7	-6.4	1.2	C3ar1, complement component 3a receptor 1 [sp O09047]
TGCAATGAATA	5.5	0.0	-4.0	1.0	C3ar1, complement component 3a receptor 1 [sp O09047]
GCGCCCTCCCC	0.0	1.7	1.2	0.1	Ccl21b, chemokine (C-C motif) ligand 21 (leucine) [sp O09006]
GCGCCCTTCCC	0.0	5.2	3.7	0.5	Ccl21b, chemokine (C-C motif) ligand 21 (leucine) [sp O09006]
TCCTGAAGGTC	5.5	0.0	-4.0	1.0	Ccl22, chemokine (C-C motif) ligand 22 [sp O88430]
AACTGACAAAT	33.2	1.7	-19.3	4.2	Ccl3, chemokine (C-C motif) ligand 3 [sp P10855]
CATTTTCATAA	85.9	3.4	-24.9	10.7	Ccl4, chemokine (C-C motif) ligand 4 [sp P14097]
CCCAGGCTGCT	5.5	0.0	-4.0	1.0	Cxcl10, chemokine (C-X-C motif) ligand 10 [sp P17515]
TACTTTATTGA	0.0	1.7	1.2	0.1	Cxcl10, chemokine (C-X-C motif) ligand 10 [sp P17515]
CTGTAAAAAAA	0.0	10.3	7.5	1.2	Cxcl12, chemokine (C-X-C motif) ligand 12 [sp P40224]
CTGTAAACCTC	0.0	5.2	3.7	0.5	Cxcl12, chemokine (C-X-C motif) ligand 12 [sp P40224]
GGTGATTATCT	2.8	0.0	-2.0	0.5	Cxcl12, chemokine (C-X-C motif) ligand 12 [sp P40224]
CTGAATGCTCA	0.0	1.7	1.2	0.1	Lsp1, lymphocyte specific 1 [sp P19973]

**c**

SAGE tags	PSA+	ATB	Factor	Signifi-	Annotation
	cells		PSA/ATB	cance	
<b>combined</b>	16.6	3.5	4.7	2.1	<b>5 matches, caspase activity (GO0004199)</b>
AAAAGTATAGA	2.8	0.0	7.9	1.1	Casp12, caspase 12 [Swissprot: sp O08736]
AATGTTTCCTG	5.5	0.0	15.8	1.8	Casp2, caspase 2 [Swissprot: sp P29594]
CATTATAGCTA	2.8	0.0	7.9	1.1	Casp3, caspase 3, [Swissprot: sp P70677]
TTGGACGTGGT	5.5	0.0	15.8	1.8	Casp6, caspase 6 [Swissprot: sp O08738]
TATTGTTGTGG	0.0	3.5	-10.0	0.3	Casp7, caspase 7 [Swissprot: sp P97864]

d

SAGE tags	PSA+	ATB	Factor	Signifi-	Annotation
	cells		PSA/ATB	cance	
<b>combined</b>	0.0	32.3	-92.0	4.3	<b>10 matches, GABA-A receptor activity (GO0004890)</b>
AGCTATGCCAA	0.0	2.8	-8.0	0.2	Gabra1, GABA-A receptor, subunit alpha 1 [sp P18504]
TCTCACTGTAT	0.0	5.6	-16.0	0.6	Gabra1, GABA-A receptor, subunit alpha 1 [sp P18504]
AGATTTATAAA	0.0	3.5	-10.0	0.3	Gabra4, GABA-A receptor, subunit alpha 4 [sp Q9D6F4]
GAGAAATCAGA	0.0	6.3	-18.0	0.7	Gabra4, GABA-A receptor, subunit alpha 4 [sp Q9D6F4]
CTGGTGGCCTT	0.0	8.4	-24.0	1.0	Gabra6, GABA-A receptor, subunit alpha 6 [sp P16305]
GATTGGTTCAT	0.0	0.7	-2.0	-0.1	Gabra6, GABA-A receptor, subunit alpha 6 [sp P1630]
CCTATTGTTA	0.0	1.4	-4.0	0.0	Gabrg1, GABA-A receptor, subunit gamma 1 [sp Q9R0Y8]
TGTATAACACT	0.0	2.1	-6.0	0.1	Gabrg2, GABA-A receptor, subunit gamma 2 [sp P22723]
TTATCATCAAA	0.0	0.7	-2.0	-0.1	Gabrg2, GABA-A receptor, subunit gamma 2 [sp P22723]
ATATCCAGTT	0.0	0.7	-2.0	-0.1	Gabbr2, GABA-C receptor, subunit rho 2 [sp P56476]

e

SAGE tags	PSA+	ATB	Factor	Signifi-	Annotation
	cells		PSA/ATB	cance	
<b>combined</b>	11.1	152.9	-13.8	15.9	<b>7 matches, neurotransmitter secretion (GO0007269)</b>
AGGAACCAAAG	2.8	9.8	-3.5	0.6	Snap25, synaptosomal-associated protein 25 [sp P13795]
CTCAGTATTGG	0.0	3.5	-10.0	0.3	Snap25, synaptosomal-associated protein 25 [sp P13795]
TATATTAATC	0.0	58.2	-166.0	7.9	Snap25, synaptosomal-associated protein 25 [sp P13795]
CCGCCTGTGGT	8.3	44.9	-5.4	3.4	Syn1, synapsin I [sp O88935]
ACTAGGGTAAA	0.0	4.9	-14.0	0.5	Syn2, synapsin II [tr Q8CE19]
CCATTGATTGG	0.0	7.0	-20.0	0.8	Syn2, synapsin II [tr Q8CE19]
CTGGAGATGTG	0.0	24.5	-70.0	3.2	Syn2, synapsin II [tr Q8CE19]

The clusters “Chemotaxis“ (a), “Caspase activity“ (c), “GABA-A receptor activity“ (d) and “Neurotransmitter secretion“ (ed) are derived from the comparison of SAGE data for PSA<sup>+</sup> cells against ATB and the cluster “Chemotaxis“ (b) from the comparison of PSA<sup>+</sup> cell against CGCP SAGE data. SAGE tag numbers have been normalized to 100,000.

Low tag numbers were detected for Gabra1, Gabra4, Gabra6, Gabrb1, Gabrg1, Gabrg2, Gabrd, Gabrr2 exclusively in ATB. The SNAP25 family implicated in axonal transport and neurotransmitter release was highly expressed in ATB while almost absent in PSA<sup>+</sup> precursors. The clusters “Neurotransmitter secretion” (Tab. 4e) and “Glutamate-gated ion channel activity” were significantly upregulated in brain and equally low in PSA<sup>+</sup> and CGCP. Genes involved in angiogenesis prevail in ATB and were weakly expressed in the CGCP.

### 3.3.2 Validation of SAGE results using microarrays and qPCR

In order to methodically validate the SAGE results, cDNA microarray hybridization and qPCR experiments were performed. Biological validation was achieved by isolating PSA<sup>+</sup> cells and preparing RNA from PSA<sup>+</sup> cells and ATB independently of the RNA preparations for the SAGE experiment. Linear amplification of all RNA samples was performed for the validation experiments. In case of the PSA<sup>+</sup> cells, 0.3 µg total RNA (corresponding to 3-6 ng



mRNA) yielded 2.4 µg aRNA (amplified RNA) -equaling a 400-800-fold amplification-, which were used for microarray and qPCR experiments.

aRNA from PSA<sup>+</sup> cells and ATB was used for hybridization experiments on a PIQOR<sup>TM</sup> cDNA microarray displaying probes representing 2649 genes implicated in neural development, metabolism, signaling and apoptosis in brain. Microarray probes for PIQOR<sup>TM</sup> cDNA microarrays were generated by RT-PCR with specific primers for selected gene regions (Bosio et al., 1999). The probes have a constant length of 200-400 bp to guarantee stable hybridization conditions. A small fraction of the genes represented on this microarray was derived from the SAGE data. Each probe was spotted twice on the arrays. As controls, ES cell aRNA and ATB aRNA were used for hybridization experiments as well as PSA<sup>+</sup> cell aRNA and ES cell aRNA to calculate the ratio for PSA<sup>+</sup> cells against ATB. RNA from ES cells was the same as used for SAGE. Detailed results of these hybridizations are presented as supplemental data: PSA/ATB, Array ID 000123(009); ES cells/ATB, Array ID 000123(010); Array ID PSA/ES cells, 000123(011) (Pennartz et al., 2004).

A strong overall consistency was found between SAGE and microarray results (Tab. 3). For example, Doublecortin: 38.8 versus 0.7 tags per 100,000 tags, microarray 34.1-fold; CD24: 63.7 versus 1.4 tags, microarray 12.1-fold; Survivin: 16.6 versus 0.7 tags, microarray 60.7-fold; PlexinA3: 13.9 versus 0.7 tags, microarray 13.3-fold; RIKEN cDNA 3110003A17: 30.5 versus 0.7 tags, microarray 22.4-fold.

In very few cases, there were discrepant values like for Cadherin2 with 22.2 versus 2.8 tags and 0.9-fold expression on the microarray or Sacsin with 8.3 tags versus 0.7 tags and 0.59 on the microarray. Vice versa, the microarray data indicated upregulation of some genes in PSA<sup>+</sup> cells, which were not found in the SAGE data. For example, Insulin receptor substrate-1 (IRS-1) was upregulated 46.1-fold. The corresponding tag was identified and counted 0.7 times in ATB but not in PSA<sup>+</sup> cells. No SAGE tags were found, for example, for Deleted in colorectal carcinoma (DCC), which showed 28.5-fold upregulation, on the microarray.

In the next step, qPCR was performed for three selected genes, which were not detected by the microarrays, but, according to the SAGE data, were significantly upregulated in PSA<sup>+</sup> cells compared to ATB: Manic fringe (16.6 versus 0 tags), Dvl2 (8.3 versus 0.7 tags) and Sox4 (113.6 versus 3.5 tags). Specific expression in PSA<sup>+</sup> cells was determined by qPCR with aRNA from FACS-purified PSA<sup>+</sup> cells and from ATB (Fig. 9). Manic fringe, Dvl2 and Sox4 were 3-, 4-, 21 times overexpressed, respectively, in PSA<sup>+</sup> precursors. Thus, the SAGE data was validated exemplarily methodically and biologically, i.e. by using independent techniques with independently prepared RNA samples. A complete list of genes, the set of

quantifications of the arrays and the raw data was provided as supplemental material (Pennartz et al., 2004).

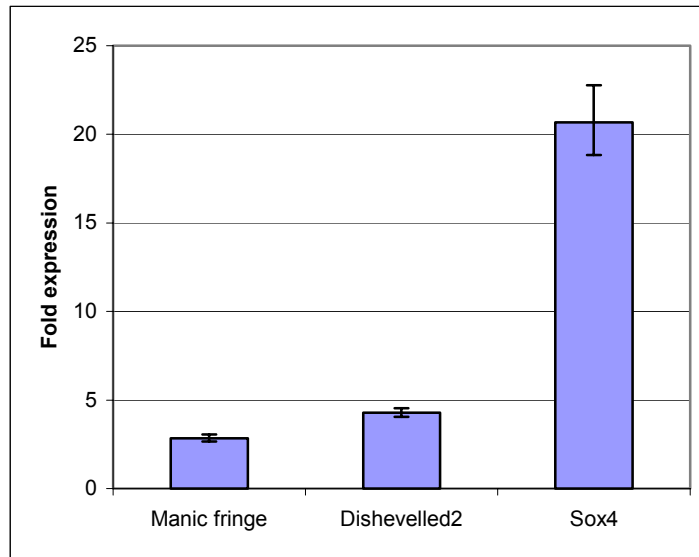


Fig. 9 qPCRs performed for three selected genes with aRNA from PSA<sup>+</sup> cells and ATB. Manic fringe, Dvl2, and Sox4 are upregulated in PSA<sup>+</sup> cells in agreement with the SAGE data.

### 3.3.3 *In situ* hybridizations for selected genes in mouse brain

*In situ* hybridizations with Digoxigenin-labeled RNA probes were performed to study the cellular localization for six selected genes from different functional groups in mouse brain. Sagittal and coronal brain sections showed that the apoptosis inhibitor Survivin/IAP4 was strongly expressed along the SVZ-RMS-OB system (Fig. 10) and localized in cells with the morphology and organization of chain-migrating PSA<sup>+</sup> neuronal precursors in the SVZ except the ependyma (Fig. 10b, d) and in the RMS (Fig. 10e). The sense probe (negative control) produced only background staining (Fig. 10c) confirming the specificity of the antisense hybridization.

*In situ* hybridizations for the transcription factor Sox4 revealed expression in the entire RMS (Fig. 11a, d) and in the SVZ excluding the ependyma (Fig. 11b) (Cheung et al., 2000). The labeling extended to the SVZ in more caudal regions around the third ventricle (data not shown). Hybridization of the sense probe generated no specific staining (Fig. 11c). Immunolabeling for CD24 (Chazal et al., 2000) on top of the Sox4 staining verified the identity of Sox4-expressing cells as neuronal precursors (Fig. 11e).

The Wnt-signaling mediator Dvl2 was shown to be specifically expressed in the RMS (Fig. 12a) and the SVZ (Fig. 12b) in agreement with the individual identification of Dvl2 (Tab. 3)

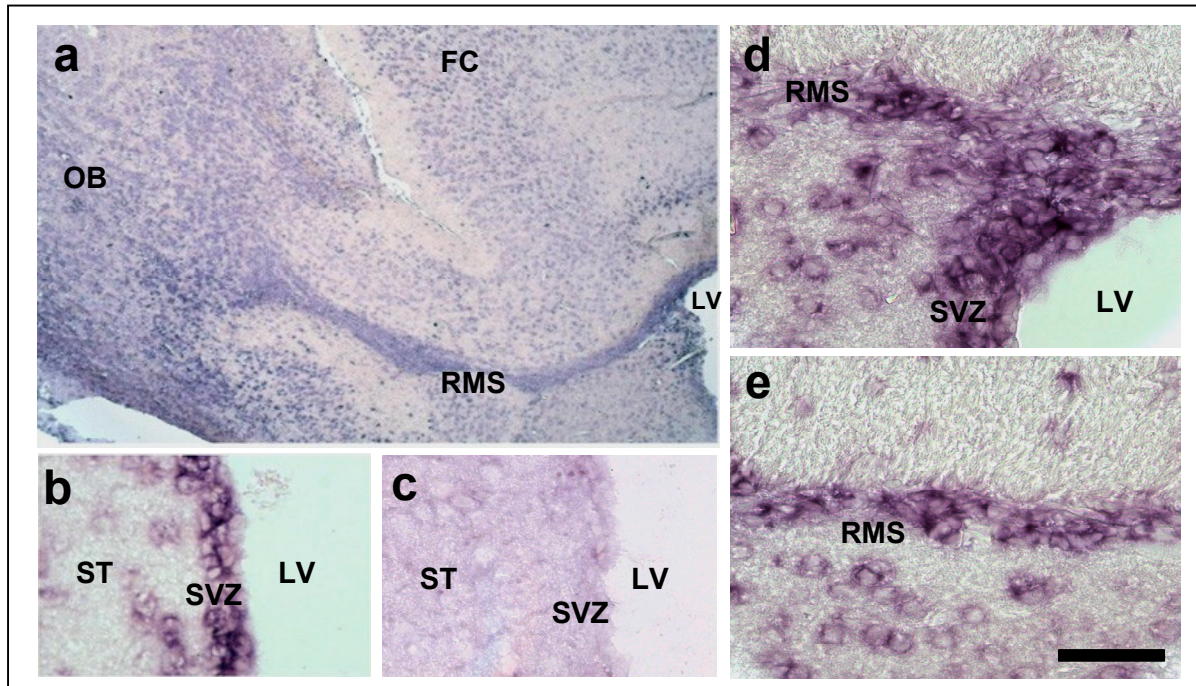


Fig. 10 *In situ* hybridizations for Survivin in mouse brain. Staining of sagittal brains sections of 6-week old mice for Survivin labeled the entire RMS connecting the SVZ with the OB (a). The Survivin antisense probe (b) produced strong staining in the SVZ in a coronal section, the sense probe (c) only background staining. Chain-migrating PSA<sup>+</sup> cells in the SVZ entering the RMS express Survivin (d) and continue to do so during migration in the RMS (e) (sagittal sections). Hybridization conditions: 45°C, 1200 ng/ml. FC: frontal cortex LV: lateral ventricle, OB: olfactory bulb, RMS: rostral migratory stream, ST: striatum, SVZ: subventricular zone. Scale bar: a, 1 mm; b, c, d, e, 70  $\mu$ m.

as well as with the GO clustering analysis of SAGE data (Fig. 8).

Meis2 is a homeodomain protein and expressed by proliferating precursors of striatal neurons as well as in neurons of the adult striatum (Arvidsson et al., 2002; Cecconi et al., 1997; Toresson et al., 2000). The SAGE results indicated that in the adult, strongest expression of the transcription factor is mainly confined to PSA<sup>+</sup> precursor cells. The *in situ* hybridization data was consistent with this observation showing specific labeling for Meis2 in the adult brain in migrating precursors in the RMS (Fig. 12c) and the SVZ (Fig. 12d).

RIKEN cDNA 3110003A17 was prominent among the genes with unknown function counting 30.5 SAGE tags versus 0 tags in ATB. Bioinformatical analysis using a motif search (done by Dr. S. Tomiuk) revealed sequence similarity to the murine protein STARS (striated muscle activator of Rho signaling), an Actin-binding protein which transduces changes in actin dynamics to gene transcription via Rho signaling (Arai et al., 2002). The same conserved motif is also present in the rat protein Ms1, which is also expressed in striated muscle (Mahadeva et al., 2002). In agreement with the SAGE data, specific, strong expression of RIKEN 3110003A17 was found in the RMS (Fig. 12e) and SVZ (Fig. 12f).

The group of chemokines was particularly prominent as individual genes as well as in the clustering analysis. The cellular localization of one member of this group, the G protein-coupled chemokine receptor C3aR1, was investigated. C3aR1 has been shown to bind complement anaphylotoxin C3a and was reported to be present predominantly in cortical and hippocampal neurons, Purkinje cells and also in astrocytes (Davoust et al., 1999). Specific expression was confirmed by *in situ* hybridization in the RMS (Fig. 12g) and in the SVZ (Fig. 12h).

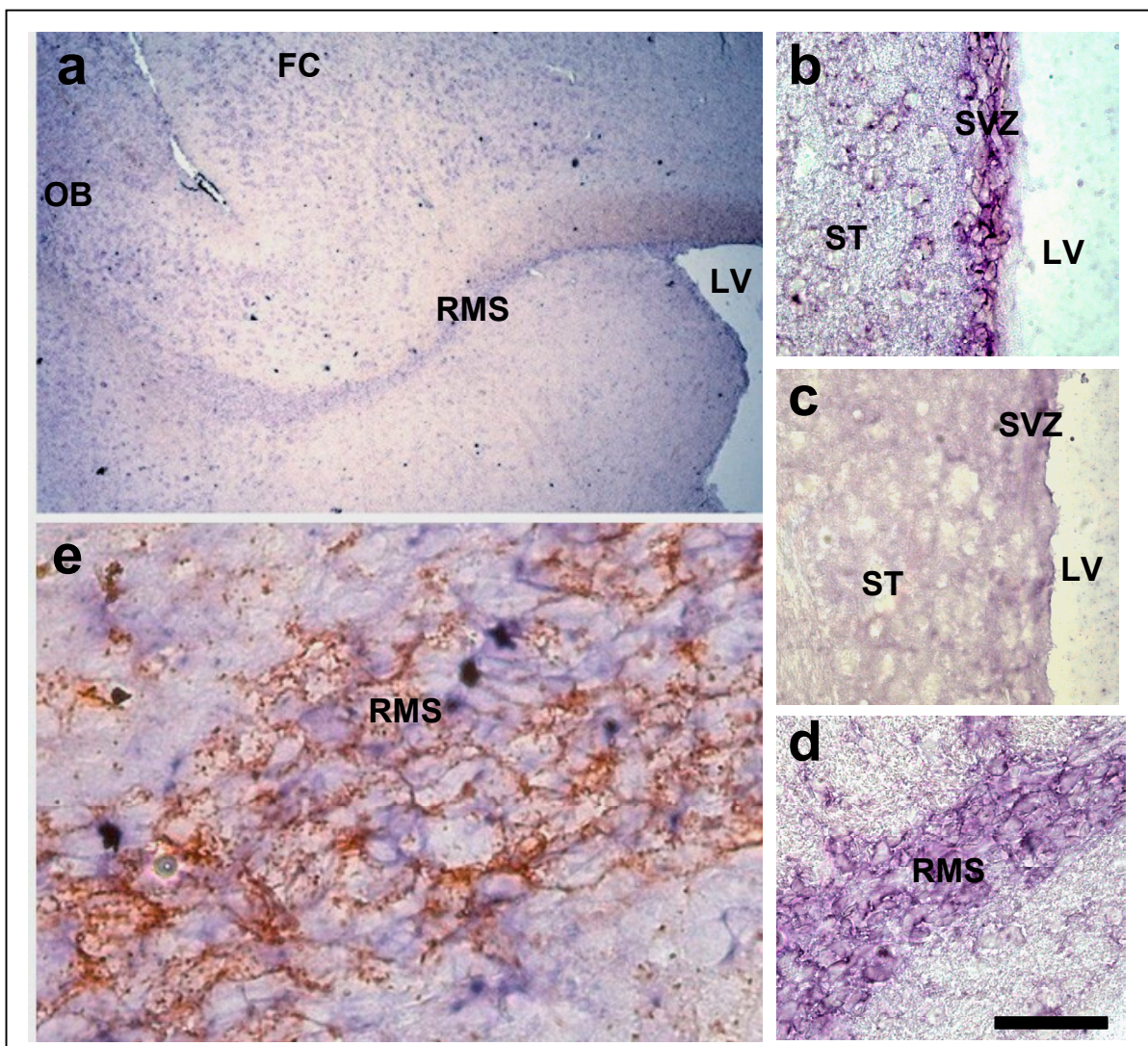


Fig. 11 *In situ* hybridizations for Sox4 in mouse brain. Staining of sagittal brains sections for Sox4 labeled the entire RMS from the SVZ to the OB (a). The SVZ, here in a coronal section, was strongly stained by the Sox4 antisense probe (b), while the sense control (c) showed only background staining. Sox4 expression was observed in the PSA<sup>+</sup> cells in the RMS in sagittal sections (d). The identity of neuronal precursors in the RMS was confirmed by performing *in situ* hybridization for Sox4 in combination with immunocytochemistry against CD24 (e). Hybridization conditions: 45°C, 1200 ng/ml. FC: frontal cortex LV: lateral ventricle, OB: olfactory bulb, RMS: rostral migratory stream, ST: striatum, SVZ: subventricular zone. Scale bar: a, 1 mm; b, c, d, 70  $\mu$ m; e, 15  $\mu$ m.

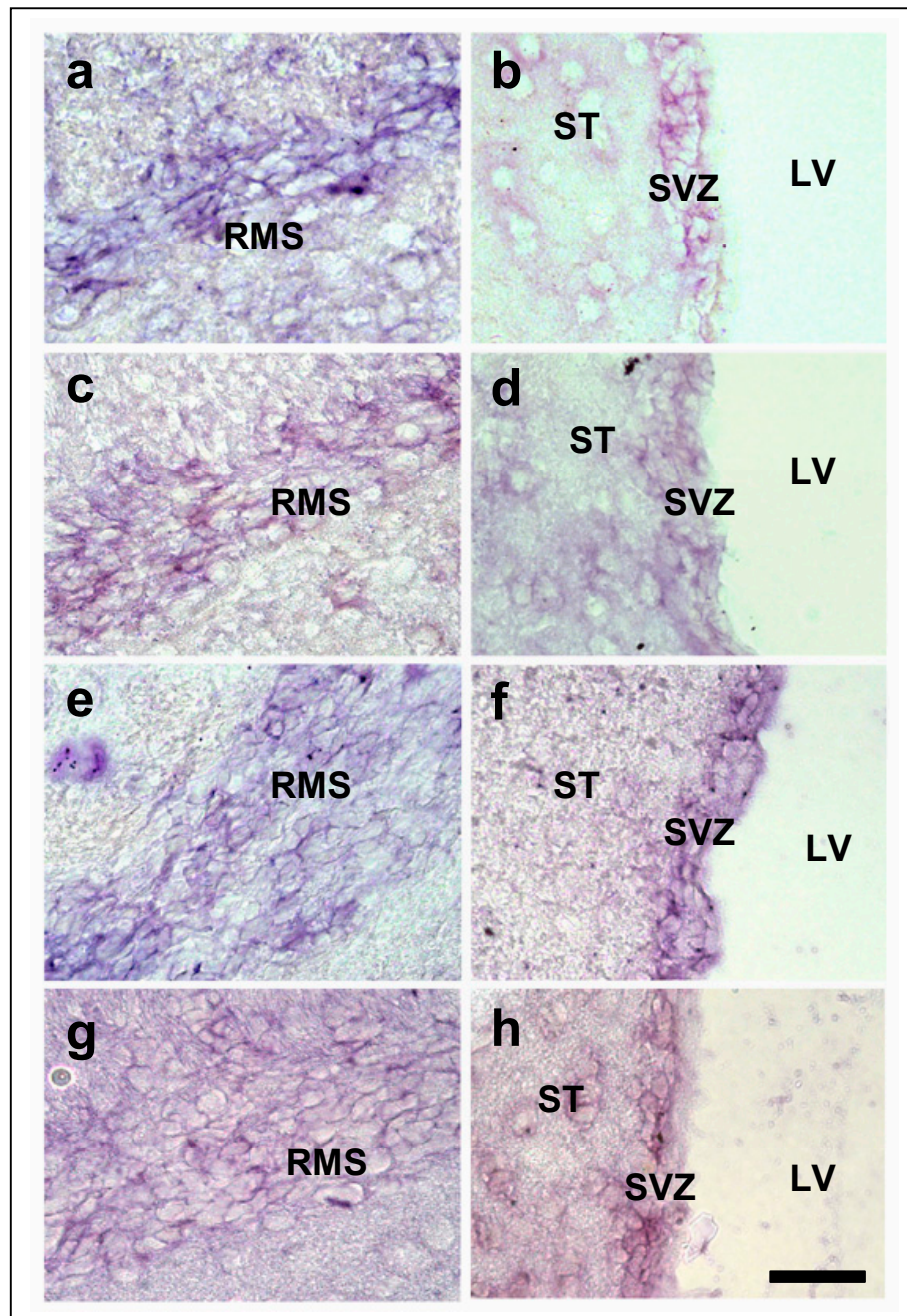


Fig. 12 *In situ* hybridizations for Dvl2, Meis2, RIKEN 3110003A17 and C3aR1 in adult mouse brain. *In situ* hybridizations in the RMS in sagittal sections and in the SVZ in coronal sections confirmed expression of Dvl2 (a, b), Meis2 (c, d), RIKEN 3110003A17 (e, f) and C3aR1 (g, h). Hybridization conditions:(a, b) 55°C, 1000 ng/ml, (c, d) 45°C, 1200 ng/ml, (e, f) 45°C, 1200 ng/ml, (g, h) 45°C, 1200 ng/ml. LV: lateral ventricle, RMS: rostral migratory stream, ST: striatum. Scale bar: 35  $\mu$ m.

### 3.3.4 Analysis of the rostral migratory stream in PlexinA3-deficient mice

According to SAGE and microarray analysis, the semaphorin receptor PlexinA3 was upregulated in PSA<sup>+</sup> cells (13.9 versus 0.7 tags, microarray 13.3-fold). Therefore, in the framework of our collaboration with group of Dr. H. Cremer, we now analyze the role of

---

Semaphorin-Plexin interaction in the control of migration and targeting of the neuronal precursors in the SVZ-RMS-OB system of PlexinA3-deficient mice (Cheng et al., 2001). Preliminary analyses revealed expression of Semaphorin3A and 3F in the mitral cells of the OB. *In vitro* analysis suggests that at least Semaphorin3A shows an attractive function on PSA<sup>+</sup> cells. Finally, the examination of PlexinA3-deficient mice suggests that fewer precursors are present in the mutant RMS and a much smaller number of cells reaches the OB (data not shown; personal communication, Camille Boutin).

### **3.4 Genes identified in ES cells by SAGE**

#### **3.4.1 Characteristic genes for pluripotent cells**

Bruce-4 ES cells were maintained in their original undifferentiated pluripotent state prior to the SAGE. Among ES cell-enriched genes, there should be genes associated with pluripotency and self-renewal and others found predominantly ES cells. In order to identify ES cell-enriched genes, the SAGE data was screened for significantly differentially upregulated ( $p < 0.05$ ) genes showing six-fold expression in ES cells versus PSA<sup>+</sup> cells, ATB, CGCP and Amygdala (Tab. 5).

High transcripts numbers of the pluripotency sustaining factor Nanog (47.8 tags) were present in ES cells but absent in the other four cell types (Chambers et al., 2003; Mitsui et al., 2003). Likewise, expression of the classical pluripotency marker Oct4 (Nichols et al., 1998) was restricted to the ES cell SAGE data (17.2 tags). Other octamer transcription factors are not differentially upregulated. Oct1 was represented by 2.9 and 11.1 tags in ES and PSA<sup>+</sup> cells, respectively, Oct6 by 2.9 and 0 tags, and Pou6f1 (EMB), which is expressed in post-implantation stages and most prominently in the developing CNS, by 0 and 5.5 tags.

The highest number of tags in ES cells was found for Cripto, also known as Teratocarcinoma-derived growth factor, which is expressed in the inner cell mass (Xu et al., 1999). Its interaction partner Nodal was not differentially expressed but solely present in ES cells (8.6 versus 0.0 tags) (Yan et al., 2002). Abundant transcripts of Embryonal stem cell specific gene (Dppa5, Developmental pluripotency associated 5; 137.4 tags) (Bortvin et al., 2003) were found in ES cells. Dppa2 and 4 were the only other two members of this family of Oct4-related genes, which were detected in the ES cells although they were not differentially upregulated (8.6 versus 0 tags in the other libraries, except Dppa4: 1.1 tags in Amygdala). Significant differential expression was observed for Nodal antagonist LeftB (TGF $\beta$ 4,

## Results

Tab. 5 Genes upregulated in Bruce-4 ES cell SAGE data were identified by comparison to other SAGE libraries.

SAGE tag	Tag numbers in...			ATB	CGCP	Amyg- dala	Medullo- blastoma	R1 ES cells	UniGene Number	Annotation
	ES cells	PSA+ cells								
AATATGCACAG	200.3	0.0	0.0	0.0	0.0	0.0	2.5	27.5	Mm.5090	Cripto, Tdglf1 (Manual annotation)
AAGACCCTGGA	137.4	0.0	0.0	0.0	0.0	0.0	0.0	110.2	Mm.139314	Esg1 Embryonal stem cell specific gene (pH34) (Manual annotation)
GTGGACTCAAT	108.7	0.0	0.7	3.5	4.3	2.5	25.3	25.3	Mm.175661	Ifitm1, interferon induced transmembrane protein 1
TTGAATTAATA	80.1	0.0	0.7	5.2	1.1	7.4	4.3	4.3	Mm.3572	RIKEN cDNA 1110033J19
TTTAAGCCTGG (2)	68.7	0.0	0.0	0.0	0.0	0.0	0.0	13.0	Mm.46461	Tdh, L-threonine dehydrogenase
TCCAACCTAGG	57.2	0.0	0.0	1.7	0.0	0.0	0.0	11.6	Mm.347418	Lefib, Tgfb4
CAAACACCGTT (3)	100.2	2.8	4.9	3.5	0.0	0.0	0.0	193.6	Mm.288474	Spp1, Osteopontin
ATGAACCGATG	48.7	0.0	0.0	0.0	0.0	0.0	0.0	14.5	Mm.6047	Nanog
CTGTGTGGCCC	37.2	0.0	2.1	1.7	2.2	0.0	0.0	26.8	Mm.24506	RIKEN cDNA E130012A19
GTGAACTTCA	37.2	0.0	0.0	0.0	0.0	0.0	0.0	0.7	Mm.1297	Trap1a, tumor rejection antigen P1A
AGAGGTGCCC	34.3	0.0	0.7	3.5	0.0	12.3	9.4	9.4	Mm.27134	RIKEN cDNA 2610033C09
GTCAGAGGCTT	34.3	0.0	0.0	0.0	0.0	0.0	4.3	4.3	Mm.24513	Slc25a13 (mitochondrial)
TGCTATGGCAG	34.3	0.0	0.0	0.0	0.0	0.0	43.5	43.5	Mm.4993	Mmp3, matrix metalloproteinase 3
GTGGCTACTA	31.5	0.0	4.2	1.7	3.2	4.9	17.4	17.4	Mm.210638	Adult bone cDNA, RIKEN clone 9830113A02
CAAATGGAGA	28.6	0.0	2.1	0.0	1.1	0.0	8.7	8.7	Mm.312170	Lars, leucyl-tRNA synthetase
TGAGGCAAAGC	28.6	0.0	1.4	3.5	0.0	2.5	5.0	5.0	Mm.57726	Shmt1, serine hydroxymethyl transferase 1
CCCCAGGACTG	25.8	0.0	0.7	1.7	0.0	0.0	7.9	7.9	Mm.234165	RIKEN cDNA 2610318N02
CTGACTTTTCC	25.8	0.0	0.0	0.0	0.0	0.0	8.7	8.7	Mm.302567	Lin28, lin-28 homolog (C. elegans)
TCTGTGCTTTA GATTCTTGTGG (2)	22.9	0.0	0.0	0.0	0.0	0.0	7.9	7.9	Mm.29148	RIKEN cDNA 2400008B06
AGACTTCCT GGAACCTGGA (2)	91.6	5.5	6.3	10.3	15.1	9.9	15.9	15.9	Mm.182927	Mrpl15, mitochondrial ribosomal protein L15
AGACTTCCT GGAACCTGGA (2)	42.9	2.8	0.7	1.7	3.2	0.0	36.2	36.2	Mm.238343	Anxa2, annexin A2
ATGAGTCATAT GTCAAGTTCCC (2)	83.0	5.5	0.7	8.6	4.3	9.9	6.5	6.5	Mm.298300	Dhx16, DEAH (Asp-Glu-Ala-His) box polypeptide 16
AGTCTCGAGGG (2)	20.0	0.0	0.0	1.7	0.0	2.5	0.7	0.7	Mm.21062	Expressed sequence C87860
AGTCTCGAGGG (2)	20.0	0.0	1.4	0.0	0.0	0.0	6.5	6.5	Mm.4325	Klf4, Kruppel-like factor 4
CTGTCTGATAA (2)	37.2	2.8	2.1	0.0	0.0	0.0	6.5	6.5	Mm.1056	ASCT2, Slc1a5
AAGTACAAGGA	37.2	2.8	2.1	3.5	4.3	0.0	2.9	2.9	Mm.29856	RIKEN cDNA 9130022B02
AGTATGTTGGC	17.2	0.0	0.0	1.7	0.0	0.0	2.1	2.1	Mm.246479	RIKEN cDNA D130038B21
CATTCAAACCTG	17.2	0.0	0.7	0.0	1.1	0.0	0.0	0.0	Mm.27536	Similar to FLJ14075 protein
CTCTATGTGGA	17.2	0.0	0.0	0.0	0.0	0.0	9.4	9.4	Mm.17031	Oct4, Pou5f1
GCCCCAGCCCC	17.2	0.0	0.0	0.0	0.0	0.0	0.0	0.0	Mm.31992	RIKEN cDNA 2410003J06
TGTGCTTCAT	17.2	0.0	0.0	0.0	0.0	0.0	25.3	25.3	Mm.12436	Rbpms
TTTGAAAGGAC TTGGCAAGCT (2)	17.2	0.0	0.7	1.7	0.0	0.0	2.9	2.9	Mm.293931	Apba3, amyloid beta precursor protein-binding
TTTGCTCTGGT (2)	17.2	0.0	0.0	1.7	1.1	2.5	0.0	0.0	Mm.34351	Plekhf2
GGATTGGACT (2)	17.2	0.0	0.0	1.7	2.2	7.4	11.6	11.6	Mm.257762	RIKEN cDNA 2610318G08
GGAAGATCCGT (2)	17.2	0.0	0.7	0.0	0.0	4.9	2.9	2.9	Mm.300203	Similar to protein ref:NP_005339.1 heat shock 90kD protein 1, alpha
AACTCTTATTT	17.2	0.0	0.0	1.7	0.0	2.5	4.3	4.3	Mm.57223	Hells, helicase, lymphoid specific
AATCACTGTGT	183.1	16.6	6.3	29.3	29.1	39.5	26.8	26.8	Mm.336245	Rex3, reduced expression 3
AACTACTGTT	14.3	0.0	1.4	1.7	0.0	0.0	2.1	2.1	Mm.16110	Cyclin E1
AACTACTGTT	14.3	0.0	0.7	0.0	0.0	0.0	0.0	0.0	Mm.33240	Eva, epithelial V-like antigen
AACTACTGTT	14.3	0.0	0.0	0.0	0.0	0.0	5.8	5.8	Mm.294740	RIKEN cDNA C330012H03

## Results

Tab. 5. (continued)

SAGE tag	Tag numbers in...				Amygdala	Medulloblastoma	R1 ES cells	UniGene Number	Annotation
	ES cells	PSA+ cells	ATB	CGCP					
ATAATAAAACA	14.3	0.0	0.7	0.0	2.2	<i>4.9</i>	<i>0.0</i>	Mm.10665	Tex292, testis expressed gene 292
CAGGTGTATAT	14.3	0.0	0.0	0.0	1.1	<i>0.0</i>	<i>0.0</i>	Mm.41151	Similar to protein pir:158401protein-tyrosine kinase
CGTATCCTGTC	14.	0.0	0.	0.0	0.0	<i>0.0</i>	<i>0.7</i>	Mm.90003	Gap junction protein beta3, Connexin31
GACCAGTTTAG	14.3	0.0	0.0	0.0	0.0	<i>0.0</i>	<i>7.9</i>	Mm.285710	Dehydrogenase/reductase member 10
GAGAATTTTAT	14.3	0.0	0.0	1.7	0.0	<i>12.3</i>	<i>0.7</i>	Mm.271784	Psph, phosphoserine phosphatase
GCATAGGGTAG	14.3	0.0	0.7	0.0	2.2	<i>0.0</i>	<i>2.9</i>	Mm.215335	Ifrd2, interferon-related developmental regulator 2
TAATGTTGCTA	14.3	0.0	0.0	0.0	0.0	<i>0.0</i>	<i>5.0</i>	Mm.35605	Cadherin 1
TATCCACGCC	28.6	2.8	1.4	3.5	3.2	2.5	85.7	Mm.175848	S100A11, Ca-binding protein Calgizzarin (Manual annotation)
GAGAAGTCCCA (2)	14.3	0.0	2.1	1.7	0.0	<i>0.0</i>	<i>0.7</i>	Mm.28478	RIKEN cDNA 2810475A17
GGATGGGACAG (2)	14.3	0.0	0.7	0.0	1.1	<i>0.0</i>	<i>2.1</i>	Mm.28498	Caspase recruitment domain 4
CAACTTAAGTG (2)	57.2	5.5	4.2	5.2	5.4	<i>4.9</i>	<i>7.2</i>	Mm.3845	Eukaryotic translation termination factor 1
CCTCCCTTTA	186.0	19.4	18.2	25.9	11.9	<i>17.3</i>	<i>31.1</i>	Mm.215667	Heat shock protein 1 (chaperonin 10)
ATAGCACAGTG	25.8	2.8	4.2	1.7	1.1	2.5	<i>4.3</i>	Mm.334789	RIKEN cDNA 1110017C15
CTACCACTCAA	25.8	2.8	0.0	0.0	0.0	<i>0.0</i>	<i>3.6</i>	Mm.44482	Stratifin
TTCTGGGCTCA	25.8	2.8	4.2	0.0	1.1	<i>4.9</i>	<i>10.1</i>	Mm.17932	Purine-nucleoside phosphorylase
TGAATAAATAT (2)	25.8	2.8	4.2	3.5	3.2	<i>0.0</i>	<i>0.0</i>	Mm.273379	Snx5, sorting nexin 5
GGCCAATGTAG (2)	25.8	2.8	1.4	3.5	0.0	<i>0.0</i>	<i>1.4</i>	Mm.87136	Phospholipase A2, group IVB
GAGCTCCAGCG	48.7	5.5	1.4	0.0	0.0	<i>4.9</i>	<i>68.1</i>	Mm.6700	Eukaryotic translation initiation factor 4E binding protein 1
TGAACAGAAAT	42.9	5.5	5.6	1.7	3.2	<i>0.0</i>	<i>5.0</i>	Mm.297862	ES cells cDNA, RIKEN clone C330022M23
GAAAACATTAA	83.0	11.1	7.7	12.1	9.7	<i>4.9</i>	<i>2.1</i>	Mm.289936	Phosphoserine aminotransferase 1
ACGATGATGTA (2)	20.0	2.8	0.7	1.7	2.2	<i>0.0</i>	<i>0.7</i>	Mm.17880	RIKEN cDNA 1700027M01
CATTTGTAA (2)	20.0	2.8	0.7	1.7	1.1	<i>0.0</i>	<i>0.7</i>	Mm.261027	D19Bwg1357e, DNA segment, Chr 19
TGAAATAAACT (4)	540.8	80.4	8.4	70.7	14.0	<i>32.1</i>	<i>83.3</i>	Mm.6343	Nucleophosmin 1

Genes were selected on the basis of significantly differential upregulation ( $p < 0.05$ ) and six-fold expression in ES cells versus PSA<sup>+</sup> cells, ATB, CGCP (publicly available), and Amygdala. The data from the public libraries “Medulloblastoma” and R1 ES cells (data in *Italic style*) was not used for the selection process, only for comparison. Tags without UniGene annotation were removed from the list. In cases, where several tags belong to one transcript, the main tag is shown with the number of different tags indicated in parentheses. Total tag numbers are normalized to 100,000.

Endometrial bleeding factor, Lefty; 57.2 tags), which is required for left-right axis determination, and Osteopontin (Spp1; 100.2 tags) whose expression is activated by Oct4 (Guo et al., 2002). High transcript numbers were found for Lin28 (25.8 tags), which is also highly expressed in human ES cells (Richards et al., 2004). Other genes expected to be expressed in ES cells like the DNA methyltransferases Dnmt3a (14.3 tags) and Dnmt3b (5.7 tags) and Sox2 (14.3 tags) were present but not differentially expressed versus PSA<sup>+</sup> cells (Chen et al., 2003; Richards et al., 2004). In addition, novel genes like RIKEN cDNA 2410003J06 (22.9 versus 0 tags), RIKEN cDNA 2400008B06 (17.2 versus 0 tags) and RIKEN cDNA C330012H03 (14.3 tags) were differentially upregulated in ES cells.



Some of the genes found in ES cells were present on the cDNA microarrays used for validation experiments (3.3.2). Hybridization for ES cells versus ATB and PSA<sup>+</sup> cells versus ES cells gave the following results indicated as x-fold expression: Oct4 28.3, 0.8, respectively; Cripto 314, 0.03; LeftB 99.9, 0.1; Osteopontin 63.6, 0.03; Sox2 7.9, 0.4 (data not shown). The microarray data confirmed the SAGE results. Solely the microarray value 0.8 for Oct4, which equals a 1.3-fold upregulation in ES, cells versus PSA<sup>+</sup> cells seemed too low. Noticeable was -despite a general consistency in terms of present transcripts- the relatively higher expression of several ES cell-characteristic genes in Bruce-4 ES cells as compared to the R1 ES cell SAGE data of Anisimov *et al.* (Anisimov et al., 2002). For example, Nanog, Oct4, Cripto, Dppa2, Sox2 and LeftB were 3.3-, 1.8-, 7.3-, 10.1-, 20.1- and 4.9-fold higher, respectively, in Bruce-4 ES cells (Tab. 5).

#### 3.4.2 Selection of potential NSC marker genes

Criteria were defined for the selection and primary investigation of potential NSC markers (Fig. 13). Provided that the genetic programs of ES cells and NSC overlap, some of the genes that are highly expressed in ES cells and downregulated or absent in PSA<sup>+</sup> cells and ATB should also be expressed by stem cells in the brain (1.2; Fig. 4). The selection of candidate genes from the three SAGE libraries was based on significantly differential upregulation ( $p < 0.05$ ) and 10-fold expression in ES cells versus PSA<sup>+</sup> cells and ATB as well as on cell surface localization (Tab. 6). Genes that code for cell surface proteins represent the most promising potential NSC markers, as antibodies generated against them would allow an one-step isolation of the cells using MACS or FACS.

This selection process led to the identification of Ifitm1 (108.7 tags), an interferon-induced transmembrane protein whose human homologue has been implicated in the control of cell growth (Deblandre et al., 1995) and the uncharacterized RIKEN 2610033C09 (43.3 tags), which possesses eight transmembrane helices with the N and C terminus located inside the cell (personal communication, Dr. S. Tomiuk). Frz7 (34.4 tags), a receptor for Wnt growth factors that is involved in *Xenopus* gastrulation (Winklbauer et al., 2001), was among the candidates as well as the neutral amino acid transporter ASCT2 (37.2 tags) (Utsunomiya-Tate et al., 1996). KIAA0152 (22.8 tags) is a novel transmembrane protein with human, *Xenopus*, *C. elegans* and plant homologues that have not been investigated yet (personal communication, Dr. S. Tomiuk). Gjb3 (Connexin31; 14.3 tags) has already been shown to be expressed in ES cells and the preimplantation embryo and to be essential for early

- Expression pattern: High in ES cells, absent/low in PSA<sup>+</sup> cells and ATB
- Preferably cell surface protein for later cell isolation
- Expression in undifferentiated EBs
- Expression in neurospheres
- Expression in postnatal mouse brain in single cells in the SVZ
- Steady decrease in the number of cells expressing the gene after birth

Fig. 13 Criteria for the selection and primary investigation of a potential NSC marker

Tab. 6 Genes coding for cell surface proteins that represent potential NSC markers.

SAGE tag	Tag number ES cells	Tag number PSA+ cells	Tag number ATB	Microarray fold - expression ES/ATB	UniGene Number	Annotation	Memorec internal number
GTGGACTCAAT	108.7	0.0	0.7	20.3	Mm.175661	Ifitm1, interferon induced transmembrane protein 1	oP219H04
AGAGGTTGCC	34.3	0.0	0.7		Mm.27134	RIKEN 2610033C09	oP237G07
TACAGATCACG	34.4	0.9	0.0		Mm.4770	Frizzled-7	oP015E02
AGTCTCGAGGG (2)	37.2	2.8	2.1	7.3	Mm.1056	ASCT2, Slc1a5	oP011C08
CCCCACCCAC	22.8	0.0	2.2		Mm.153963	KIAA0152 (before CD8 antigen)	oP279A06
CGTATCCTGTC	14.3	0.0	0.0	16.1	Mm.90003	Gap junction protein beta3, Connexin31	oP011D09
AATCACTGTGT	14.3	0.0	0.7	8.6	Mm.33240	Eva, epithelial V-like antigen	oP237H04
TAATGTTGCTA	14.3	0.0	0.0	33.7	Mm.35605	Cadherin 1	oP047B07

The selection of these genes was based on significantly differential upregulation ( $p < 0.05$ ) and 10-fold expression in ES cells versus PSA<sup>+</sup> cells and ATB according to the SAGE data. In cases, where several tags belong to one transcript, the main tag is shown with the number of different tags indicated in parentheses. Total tag numbers are normalized to 100,000. Some of the genes present in the SAGE analysis were also assessed by cDNA microarray experiments. The results for the hybridization of ES cells versus ATB are shown as “fold upregulation”. oP-numbers refer to the Memorec proprietary cDNA collection.

placentation (Flechon et al., 2004; Plum et al., 2002; Plum et al., 2001). Expression of the cell adhesion molecule Eva (epithelial V-like antigen; 14.3 tags) was found in the early embryo and in a number of embryonic and adult epithelial structures of the mouse (Guttinger et al., 1998; Teesalu et al., 1998). The last candidate in this list was Cadherin1 (E-Cadherin; 14.3 tags), which is already present in the zygote, crucial for cell adhesion in the morula and becomes downregulated in the mesoderm and its derivatives during gastrulation while its expression is maintained in all epithelia (Riethmacher et al., 1995; Sefton et al., 1992; Vestweber and Kemler, 1984). The microarray data obtained for these candidates was in agreement with the SAGE data (Tab. 6).

A further criterion for a potential NSC marker gene should be its expression in neurospheres - at least in a subpopulation of cells- since these clonal aggregates grow from NSC in culture (1.1.3; Fig. 13). The initiating neural stem cell keeps dividing symmetrically while other cells derived from asymmetrical divisions go on proliferating and differentiating. As a result, the neurosphere becomes inhomogeneous and contains from less than 1% to about 3-4% NSC according to various estimations (Gritti et al., 1996; Morshead et al., 2002). Capela *et al.* showed that 23% of the cells in neurospheres were LeX-positive (CD15) and concentrated at the neurospheres' periphery (Capela and Temple, 2002).

Embryoid bodies (EBs) were used as a control for *in situ* hybridizations in cryosections of neurospheres. EBs are derived from ES cells (or EC cells) and morphologically similar to neurospheres (Martin, 1980). Because they originated from ES cells and were grown only for a short time, the EBs should express the candidate genes found in ES cells.

In the adult mouse brain, the frequency of NSC is extremely low (Morshead et al., 1998). Rietze *et al.* roughly estimated that only 0.3% of the cells in the small neurogenic area, the SVZ, represent self-renewing, multipotent NSC (Rietze et al., 2001). Consequently, NSC marker genes should label only a subpopulation of cells in the SVZ of adult mice.

Finally, since adult NSC can be viewed as remnants of brain development, a decrease in the number of brain cells expressing a potential marker gene from the time around birth to adulthood would be expected (Cai et al., 2002; Pevny and Rao, 2003).

### 3.4.3 Investigation of potential NSC marker genes

#### 3.4.3.1 Expression in embryoid bodies and neurospheres

*In situ* hybridizations and, in the case of Frz7, immunostainings were used to analyze the expression of the potential NSC markers (Tab. 6) in EBs and secondary neurospheres. Antisense and sense (negative control) Digoxigenin-labeled RNA probes were generated for each candidate by *in vitro* transcription. EBs were grown in culture for 24 h. Primary neurospheres were grown for 5-7 days. To ensure that the neurospheres had the capability of self-renewal, they were dissociated to grow as secondary neurospheres for 5-7 days. EBs and secondary neurospheres were fixed, frozen and cryostat sections were produced.

Immunofluorescence for Frz7 produced a weak staining in EBs and neurospheres (Fig. 14). Because Cadherin1 was suspected to be expressed in ependymal cells, its expression was directly analyzed in mouse brain, but not in EBs and neurospheres (3.4.3.2).

The SAGE tag “CCCCACCCCAC” had initially been assigned to CD8 antigen due to a falsely annotated EMBL sequence within the corresponding UniGene cluster. Recently, the correct UniGene cluster belonging to this tag, namely Mm.153963, KIAA0152, was available. KIAA0152 will be cloned and examined using *in situ* hybridizations in EBs, neurospheres and mouse brain.

So far, the candidate ASCT2 has not been further examined due to a mistake in the SwissProt database, which will be explained below (3.5).

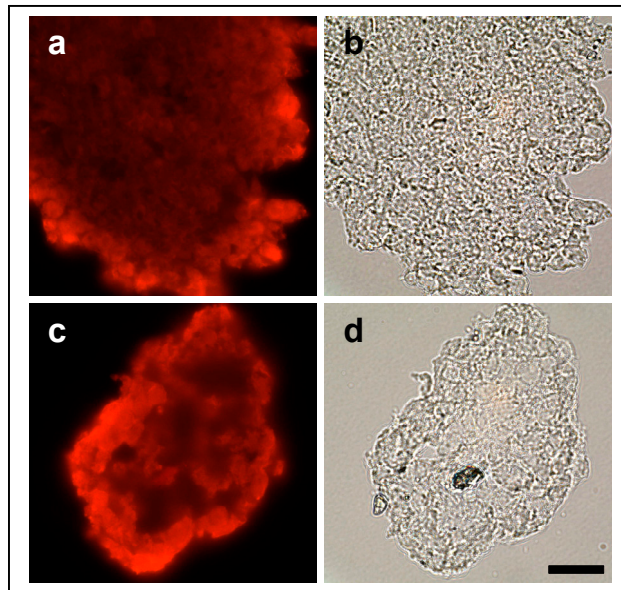


Fig. 14 Immunocytochemical analysis of Frz7 in EBs and secondary neurospheres. Cryostat sections of EBs (a) and neurospheres (c) were stained with anti-Frz7 pAb with 15  $\mu\text{g/ml}$  and 10  $\mu\text{g/ml}$ , respectively. Panels on the right show transmitted light microscopy for the same EBs (b) and neurospheres (d). Scale bar 25  $\mu\text{m}$ .

The remaining candidates were analyzed by means of *in situ* hybridization in EBs and neurospheres. Hybridization of the antisense probe in both, EBs (Fig. 15) and neurospheres (Fig. 16), resulted in a relatively stronger staining than the corresponding sense probe only in the case of RIKEN 2610033C09. The in some cases strong staining of the sense probes might be ascribed to non-specific hybridization due to the shortness of the probes. Different cDNA fragments for new probes could be generated for further analysis. RIKEN 2610033C09 showed the strongest antisense staining among these candidates and was thus further investigated.

#### 3.4.3.2 Expression in mouse brain

*In situ* hybridizations of Cadherin1 in postnatal mouse brain revealed expression in the SVZ only in the entire ependyma (data not shown) rendering the candidate useless for isolation of

NSC. However, no expression was seen in PSA<sup>+</sup> cells confirming the precision of the selection process based on SAGE data.

For RIKEN 2610033C09, staining was observed not only in the SVZ, but also in the entire brain for various hybridization conditions (data not shown). Further optimization might lead to a more specific staining. So far, neither immunofluorescence nor the Vectastain ABC System produced any labeling for Frz7 in postnatal mouse brain cryosections.

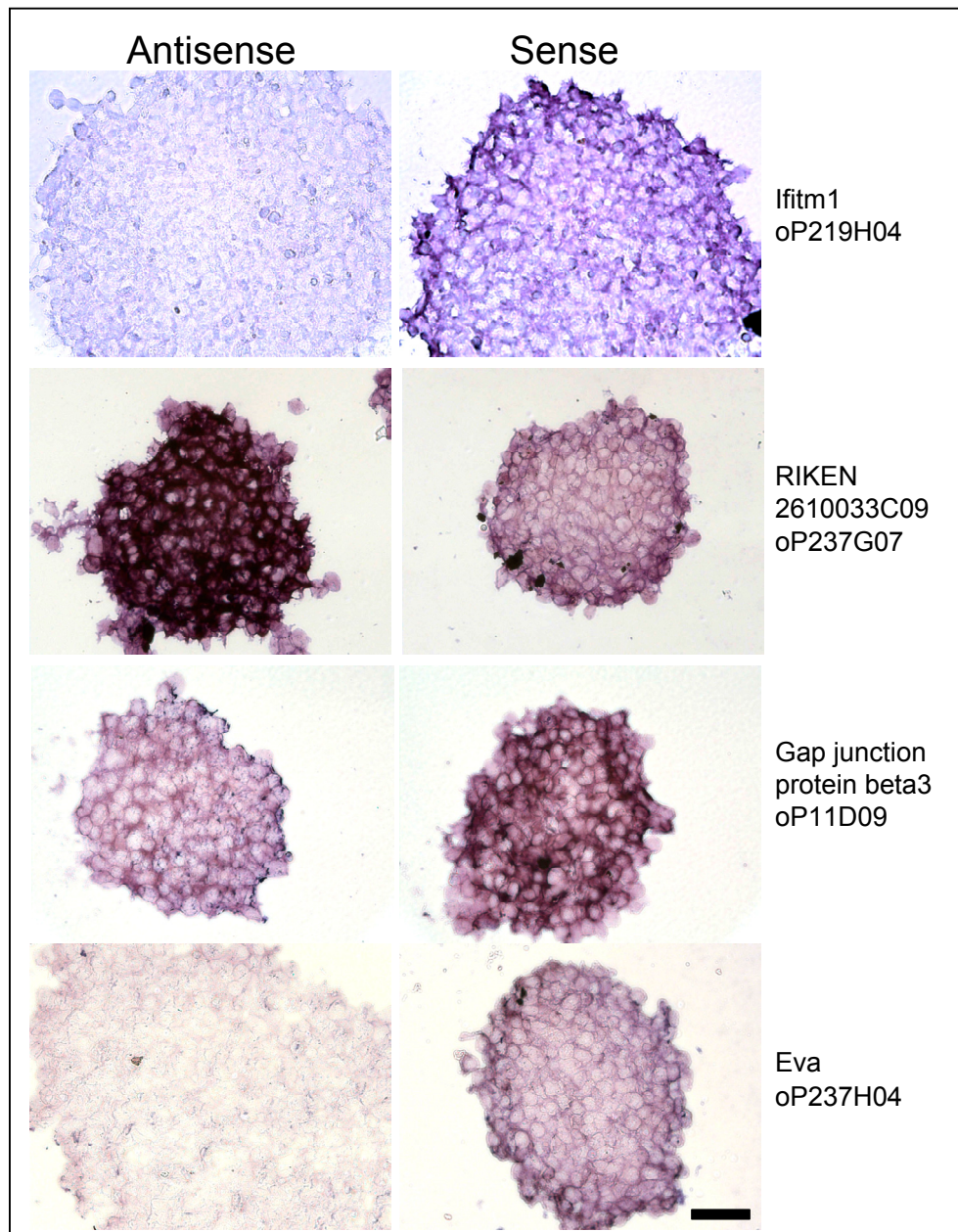


Fig. 15 *In situ* hybridizations with antisense and sense probes for potential NSC markers in 24 h old embryoid bodies. Only for RIKEN 2610033C09 (oP237G07) did the antisense probe produce a stronger staining than the corresponding sense probe. Hybridization conditions: Ifitm1 (oP219H04): 45°C, 1000 ng/ml; RIKEN 2610033C09 (oP237G07), Gap junction protein beta3, Connexin31 (oP11D09), Eva, epithelial V-like antigen (oP237H04): 50°C, 800 ng/ml. oP-numbers refer to the Memorec proprietary cDNA collection (Tab.6). Scale bar 40  $\mu$ m.

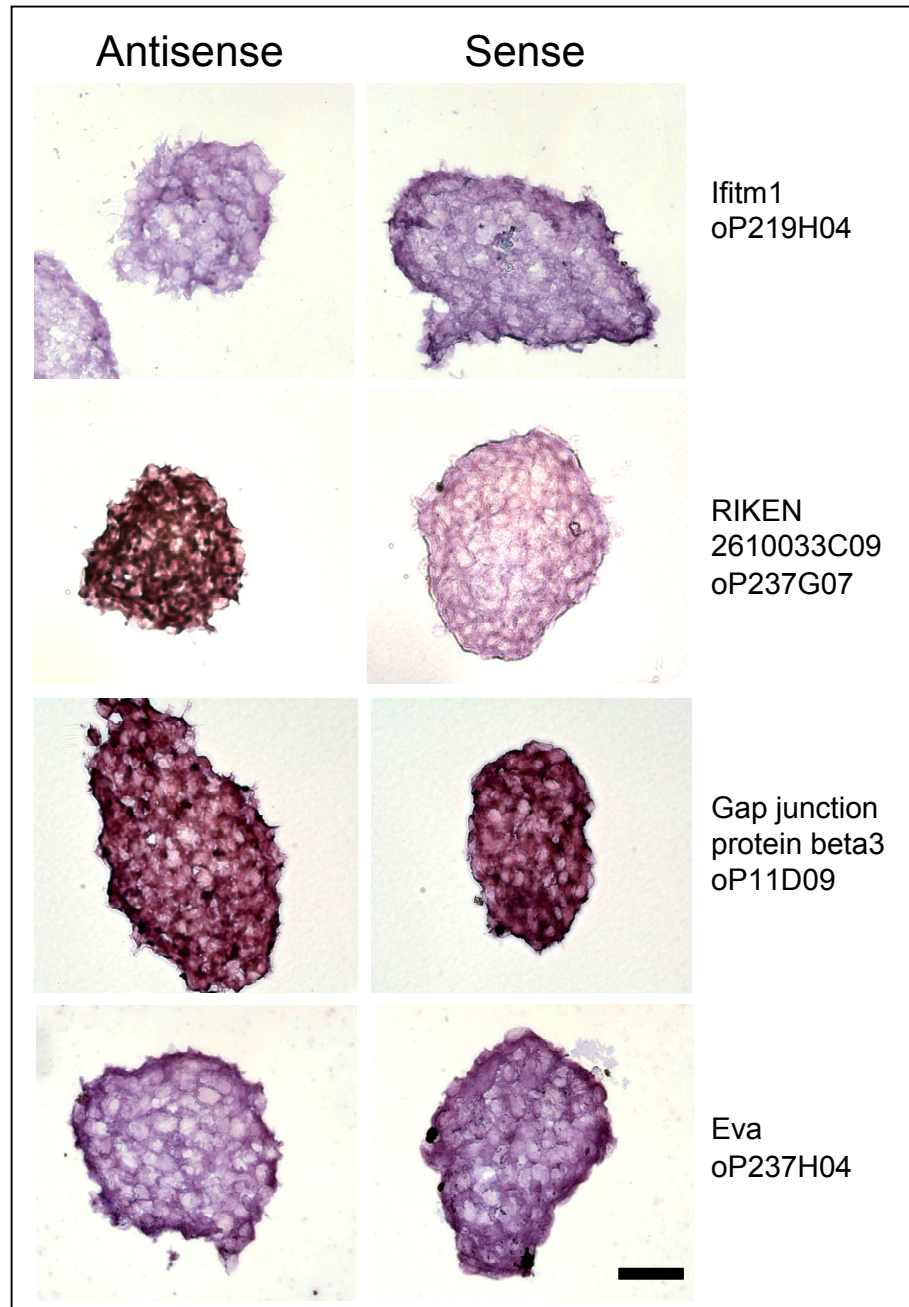


Fig. 16 *In situ* hybridizations with antisense and sense probes for potential NSC markers in secondary neurospheres. The hybridization of the antisense probe resulted in a stronger staining than the corresponding sense probe only in the case of RIKEN 2610033C09 (oP237G07). Hybridization conditions: Ifitm1 (oP219H04): 45°C, 1000 ng/ml; RIKEN 2610033C09 (oP237G07), Gap junction protein beta3, Connexin31 (oP11D09), Eva, epithelial V-like antigen (oP237H04): 50°C, 800 ng/ml. oP-numbers refer to the Memorec proprietary cDNA collection (Tab.6). Scale bar 40  $\mu$ m.

### 3.5 Analysis of *GLT1* expression

A confusion based on a database mistake that can be exactly retraced led to the use of the sequence for *GLT1* (Glutamate transporter 1). The two transporters *ASCT2* and *GLT1* both carry several different gene names and abbreviations as it is the case for many genes.

However, between April 2002 and July 2004, the public database SwissProt listed an identical gene name abbreviation, namely SLC1A2, for the two different genes although it belonged only to GLT1. The automatic search in the SwissProt database with accession numbers for genes identified by SAGE assigned “SLC1A2” to the correct accession number of ASCT2, P51912. This “SLC1A2” was then used to identify the number of the cDNA fragment in Memorec’s proprietary cDNA collection. The annotation for ASCT2 in Memorec’s Laboratory information management system (LIMS) at this time was based on a former database update so that it did not contain “SLC1A2” as alternative name for ASCT2. The changes can also be reconstructed. Only on February 25<sup>th</sup> 2004 the LIMS entry for ASCT2 was changed. Since before “SLC1A2” was not present in the ASCT2 entry, the search led only to the correct “SLC1A2”, also called GLT1 or EAAT2, and its cDNA fragment number oP11E02. The size of the cDNA fragments for ASCT2 and GLT1 are 291 bp and 301 bp, respectively, so that the gel electrophoresis after control digestion did not reveal the confusion. Consequently, *in situ* hybridizations were performed with a probe for the sequence of GLT1 (SLC1A2) instead of ASCT2. The mistake in the SwissProt database was corrected in July 2004.

Databases like SwissProt or Memorec’s LIMS are periodically updated to keep pace with the constantly produced new insights from the genome project.

Hybridization of the GLT1 antisense probe in both, EBs (Fig. 17a) and neurospheres (Fig. 17b), resulted in a relatively stronger staining than the corresponding sense probe. Under more stringent hybridization conditions, the GLT1 antisense probe produced a weaker overall staining in neurospheres while a few cells retained a strong signal (Fig. 18).

*In situ* hybridization for GLT1 in mouse brain generated a remarkable expression pattern (Fig. 19). In P3 and P14 brain, strong labeling was observed in the few cell layers adjacent to the LV. While in P3 brain, the staining extended around the entire ventricle, in P14 brain, it was confined to the striatal side, the SVZ and the initial RMS. In P3 brain, almost all the cells around the ventricle were labeled, though with different intensity, whereas in the older brain relatively less cells were labeled creating a mottled pattern. The number of cells expressing the gene seemed decreased in P14 versus P3 brain. In addition, few other cell types were strongly labeled in the brain. A thin line of individual large cells overlying the corpus callosum was observed in P14 brain (Fig. 20) as well as cells in the hippocampal CA3 region (data not shown). Higher magnifications of the P14 brain showed that only single cells and small groups of cells were labeled in the SVZ and the proximal parts of the RMS (Fig. 21).

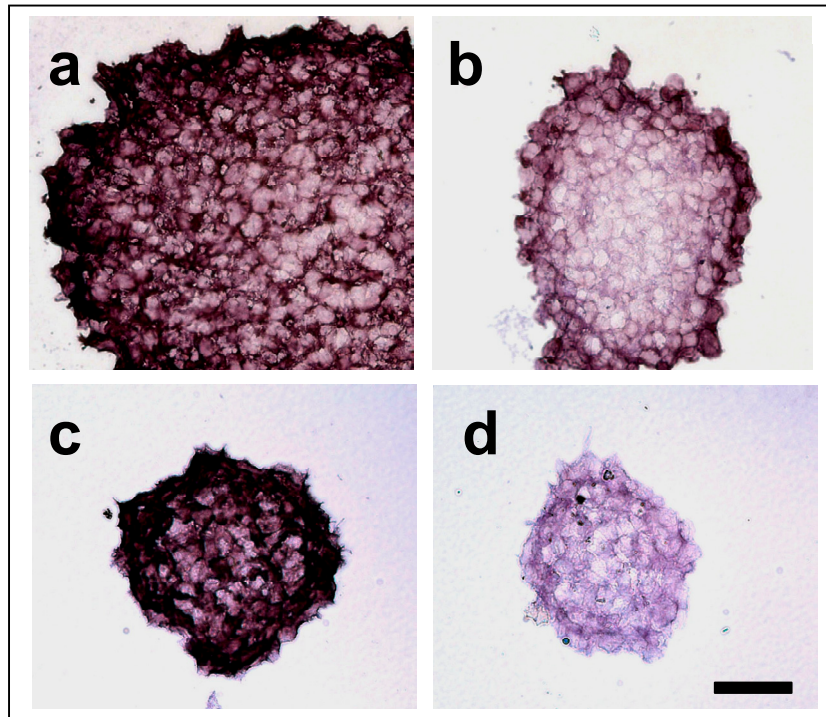


Fig. 17 *In situ* hybridization with antisense (a,c) and sense (b,d) probe for GLUT1 in embryoid bodies (a,b) and secondary neurospheres (c,d). The hybridization of the antisense probe resulted in stronger stainings than the corresponding sense probe. Scale bar 40  $\mu\text{m}$ .

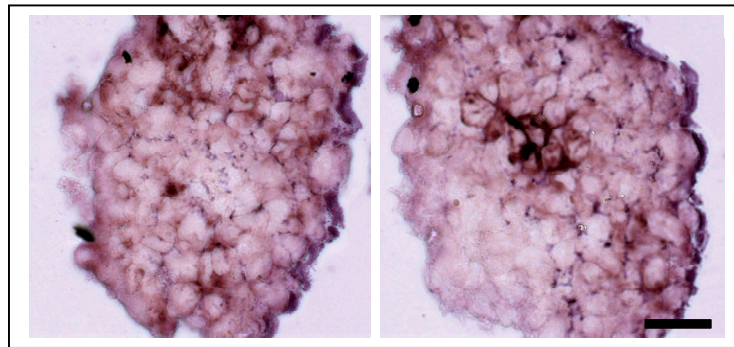


Fig. 18 *In situ* hybridization with the antisense probe for GLUT1 in secondary neurospheres. Under more stringent conditions (50°C, 600 ng/ml), a few cells stand out from the others in the staining. Scale bar 25  $\mu\text{m}$ .

The GLUT1 staining appeared to be restricted to cells within the SVZ excluding the ependyma, the single cell layer bordering the LV. The comparison of *in situ* hybridizations for GLUT1 antisense (Fig. 21) and sense (Fig. 22) probe demonstrates the specificity of the antisense staining. The sense probe produced only background staining. The same specificity was found for P3 and P32 brain (data not shown).



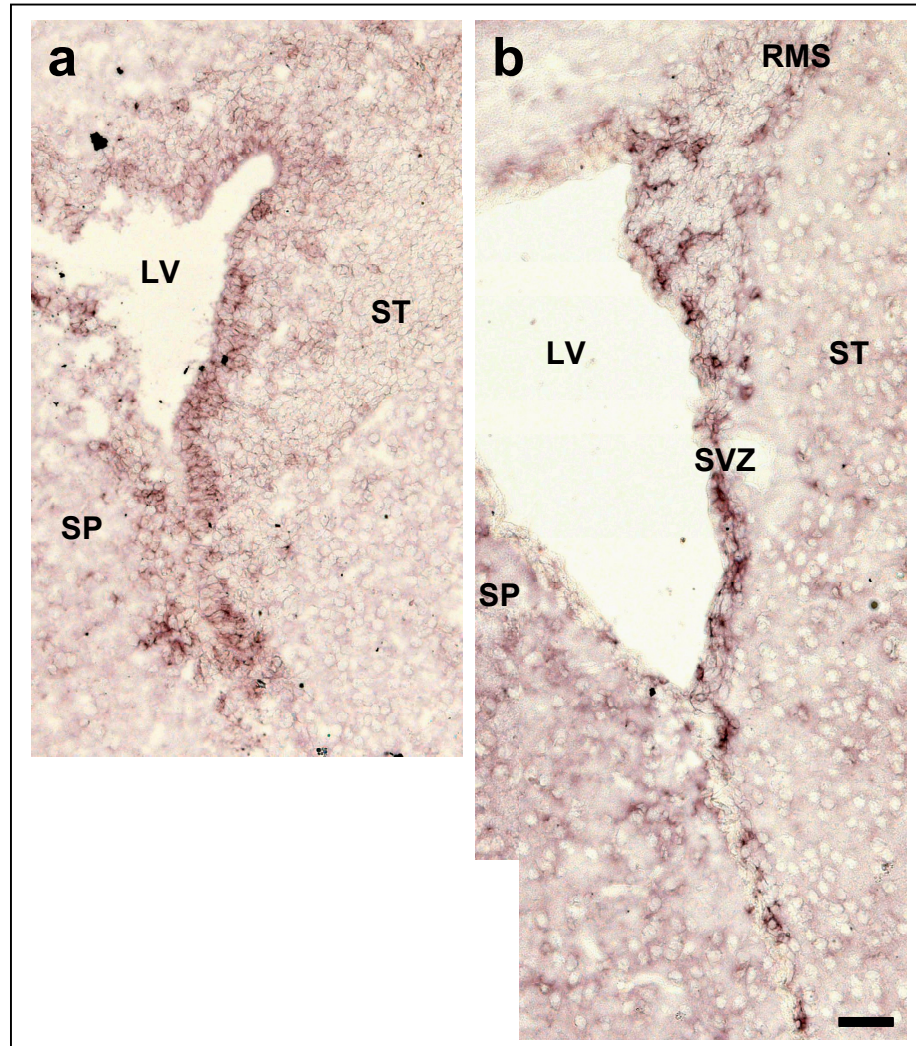


Fig. 19 *In situ* hybridization for GLT1 in postnatal mouse forebrain. The GLT1 antisense probe produced a specific staining in the majority of the cells in the first cell layers surrounding the LV of P3 mice (a). In P14 mice, relatively less cells were labeled creating a patchy staining pattern restricted to the SVZ and the beginning RMS (b). Hybridization conditions: 50°C, 600 ng/ml. LV: lateral ventricle, RMS: rostral migratory stream, SP: septum, ST: striatum. Scale bar 50  $\mu$ m.

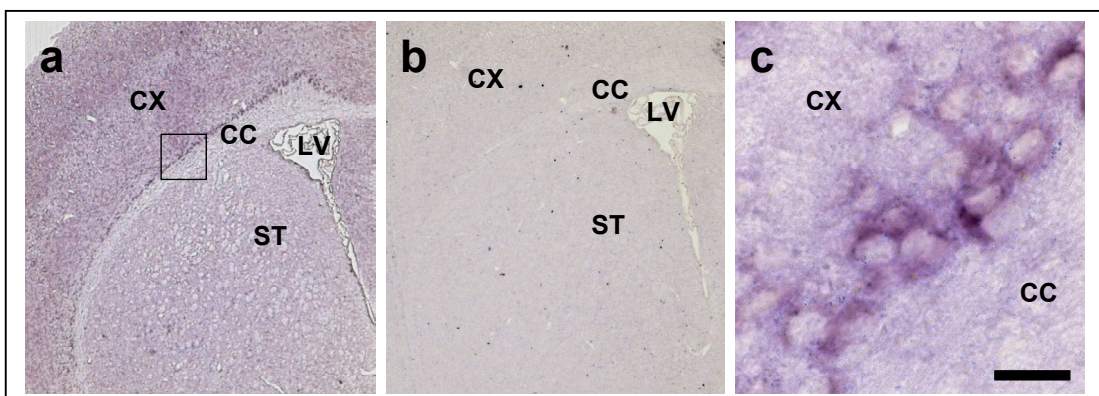


Fig. 20 *In situ* hybridization showing GLT1-labeled cells outside the SVZ. The GLT1 antisense probe labeled a thin line of cells along the corpus callosum in P14 mouse forebrain (a) that were not seen with the sense probe (negative control) (b). (c) shows an enlargement of the boxed area in (a). Hybridization conditions: 50°C, 600 ng/ml. CC: Corpus callosum, CX: Cortex, LV: lateral ventricle, RMS: rostral migratory stream, ST: striatum. Scale bar: a, b, 630  $\mu$ m; c, 25  $\mu$ m.

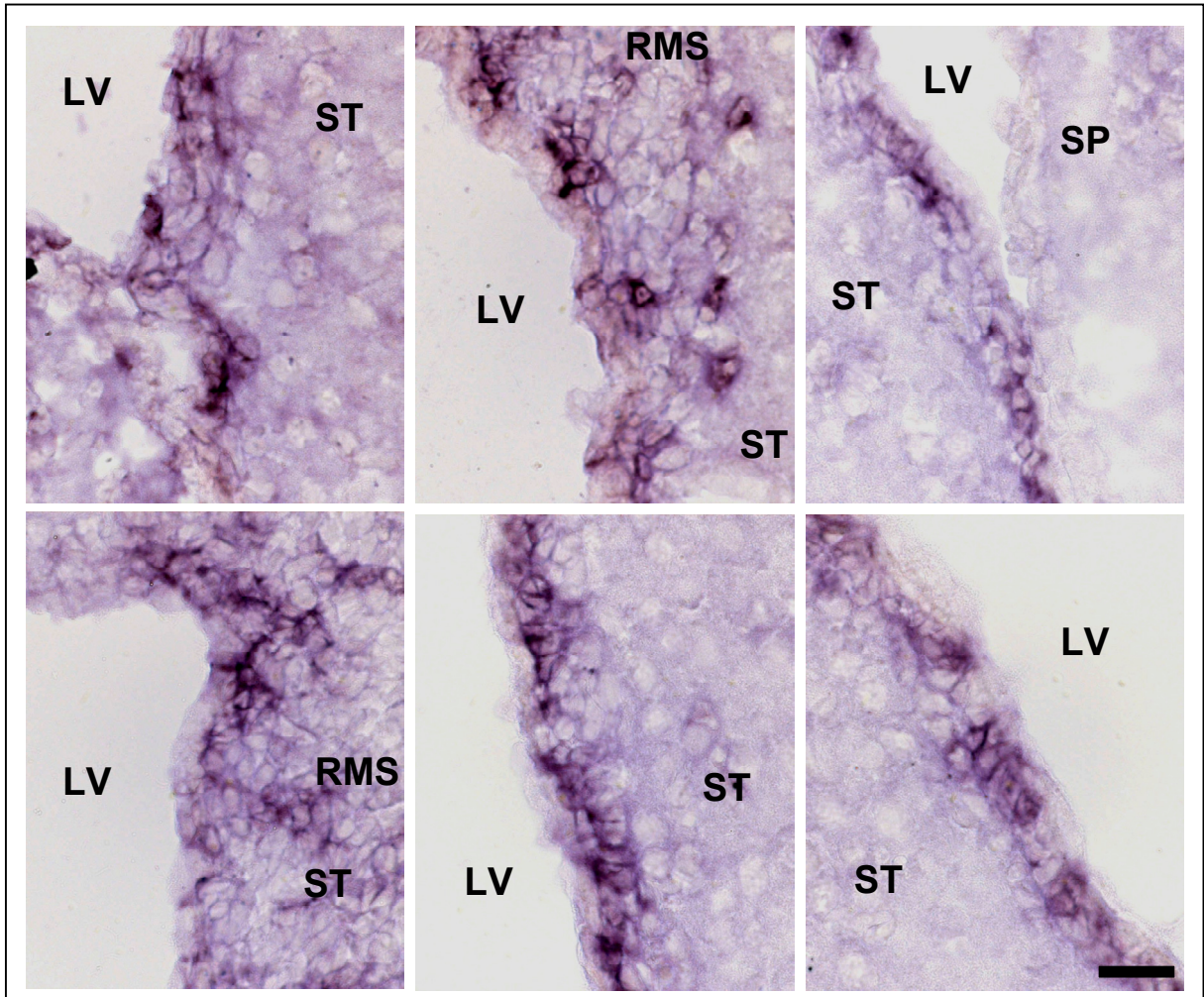


Fig. 21 High magnification of *in situ* hybridization with the GLT1 antisense probe in P14 mouse forebrain. *In situ* hybridization for GLT1 labeled single cells and small groups of cells within the SVZ and the initial RMS while no staining was observed on the septal side of the LV. Hybridization conditions: 50°C, 600 ng/ml. LV: lateral ventricle, RMS: rostral migratory stream, SP: septum, ST: striatum. Scale bar 25  $\mu$ m.

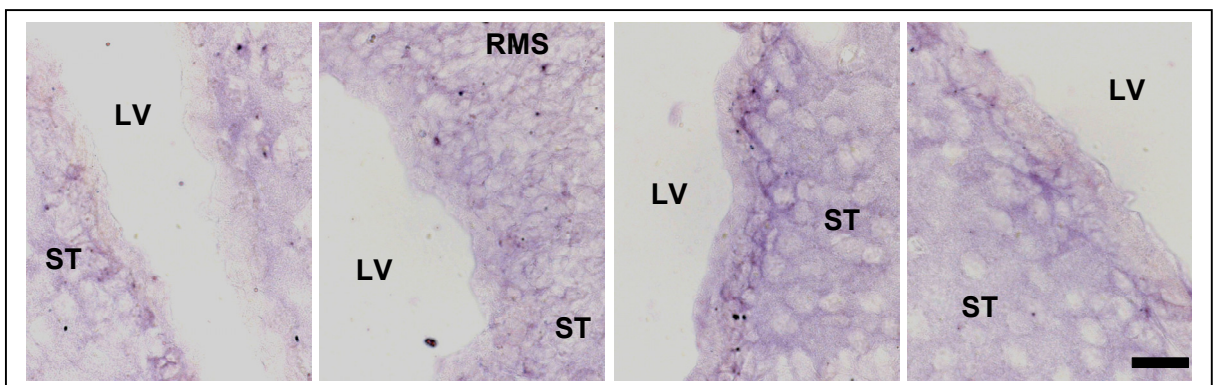


Fig. 22 *In situ* hybridization with the GLT1 sense probe (negative control) in P14 mouse forebrain. The sense probe produced only background staining and thereby confirmed the specificity of the antisense staining. Hybridization conditions: 50°C, 600 ng/ml. LV: lateral ventricle, RMS: rostral migratory stream, ST: striatum. Scale bar 25  $\mu$ m.

*In situ* hybridizations in embryonic brain revealed that GLT1 was not yet expressed at E13, while at E18, weak expression could be observed around the LV in the neuroepithelium and the relatively broad SVZ and weaker expression in the entire brain (Fig. 23).

Similar results like for P14 were seen in P32 mice (Fig. 24) although here staining in the SVZ was observed to be weaker and less distinct. *In situ* hybridizations on embryonic and P32 brain were performed with an independently generated probe

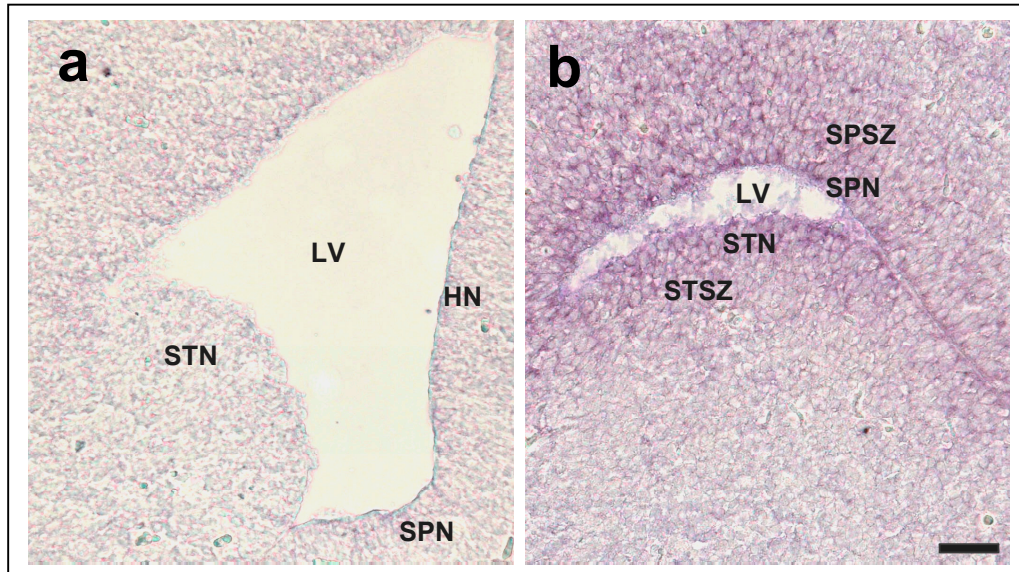


Fig. 23 *In situ* hybridization with the GLT1 antisense probe in embryonic mouse brain. While at an early stage of development, at E13 (a), no cells were labeled, at E18 (b) the entire brain was weakly stained with slightly increased intensity around the LV. Hybridization conditions: 46°C, 500 ng/ml. HN: hippocampal neuroepithelium, LV: lateral ventricle, SPN: septal neuroepithelium, SPSZ: septal subventricular zone, STN: striatal neuroepithelium, SPSZ: striatal subventricular zone. Scale bar 50  $\mu$ m.

Collectively, these experiments demonstrated the presence of GLT1 in the SVZ, the neurogenic area of the postnatal forebrain. A tendency of a decreasing expression in terms of cell number from birth to adulthood was observed.

Although GLT1 has been said to be a typical astrocytic transporter, SAGE tags were also found in PSA<sup>+</sup> cells (19.4 tags). Preliminary results for PSA immunohistochemistry subsequent to GLT1 *in situ* hybridization showed that an overlap of ASCT and PSA labeling is possible (Fig. 25).

Previous studies indicated that NSC should be part of the astrocyte population and thus immunoreactive for GFAP. One analysis claimed that all neurospheres-forming cells from the SVZ are GFAP-positive (Morshead et al., 2003). In order to determine if the strongly GLT1-expressing cells identified here correspond to astrocytes, GFAP immunohistochemistry was

performed after GLT1 *in situ* hybridizations. Apparently, a larger number of cells is GFAP-positive than GLT1-positive, and some GLT1<sup>+</sup> cells might be GFAP-positive (Fig. 26).

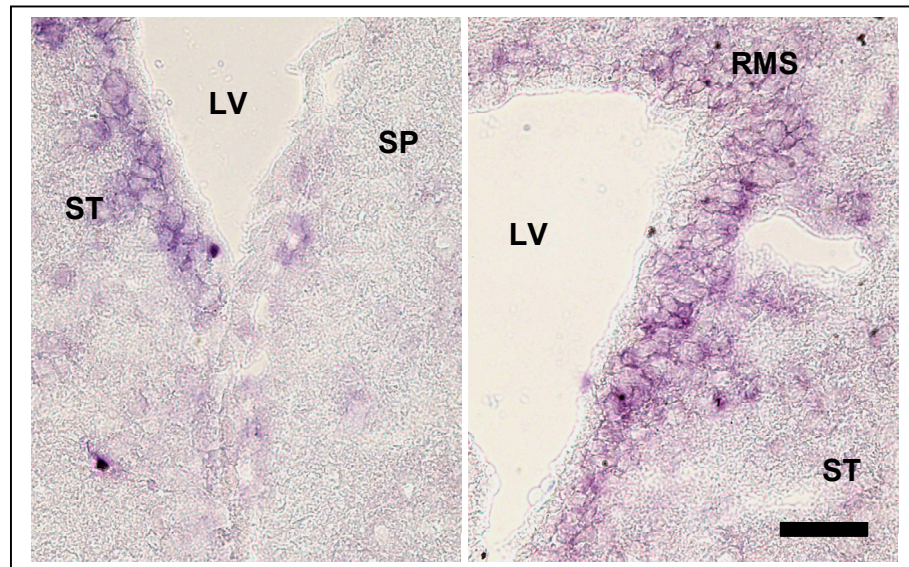


Fig. 24 *In situ* hybridization with the GLT1 antisense probe in P32 mouse forebrain. GLT1 staining is restricted to the SVZ and the beginning RMS in the forebrain, while the septal side of the LV shows no staining. Hybridization conditions: 45°C, 800 ng/ml. LV: lateral ventricle, RMS: rostral migratory stream, SP: septum, ST: striatum. Scale bar 40  $\mu$ m.

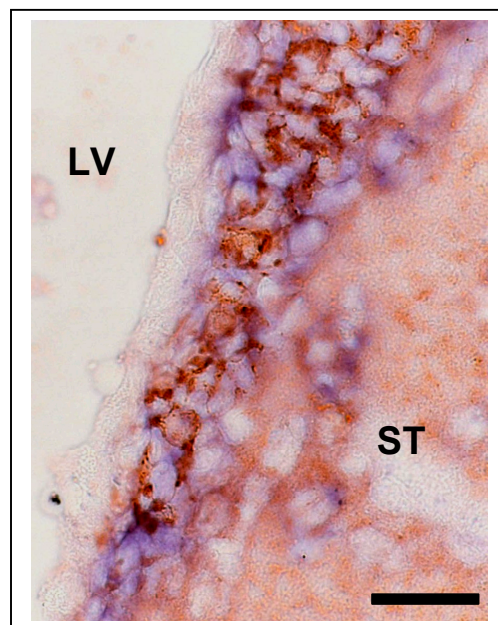


Fig. 25 PSA immunocytochemistry (brown staining) subsequent to GLT1 *in situ* hybridization (blue staining) in P32 brain. PSA staining can be observed next to the GLT1-labeled cells in the SVZ and the beginning RMS. The GLT1<sup>+</sup> cell population seems to be negative for PSA but a co-localization of both signals cannot be excluded on the basis of *in situ* hybridizations for GLT1. Hybridization conditions: 45°C, 800 ng/ml. LV: lateral ventricle, ST: striatum. Scale bar 25  $\mu$ m.

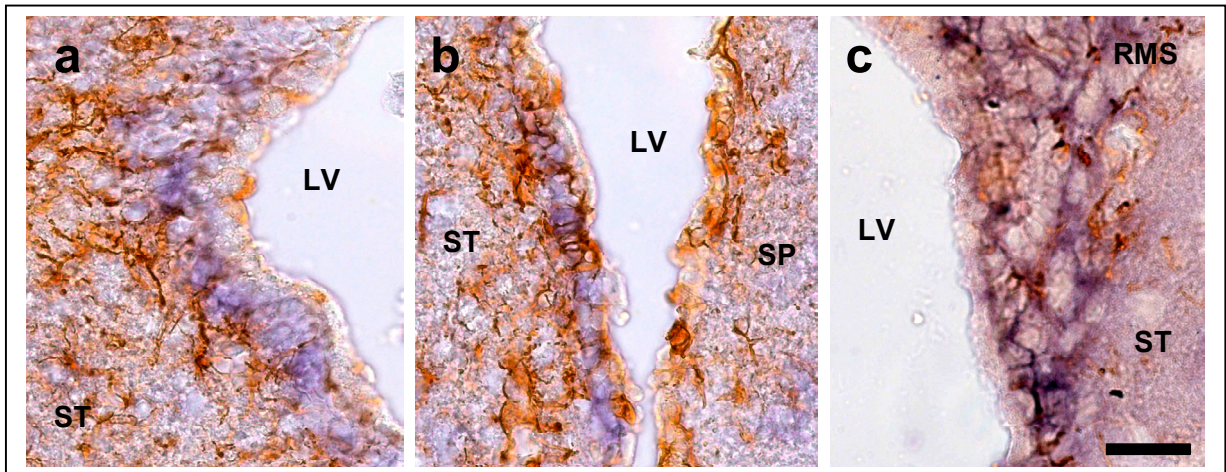


Fig. 26 GFAP immunocytochemistry (brown staining) subsequent to GLUT1 *in situ* hybridization in P14 brain. GFAP labeling can be observed in close vicinity to the GLUT1 *in situ* hybridization staining in the SVZ and the beginning RMS. More cells are positive for GFAP than for GLUT1. A co-localization of both signals is well possible in the case of some cells. Hybridization conditions: 50°C, 600 ng/ml. LV: lateral ventricle, RMS: rostral migratory stream, SP: septum, ST: striatum. Scale bar a, b, 40  $\mu$ m; c, 25  $\mu$ m.

## 4 Discussion

### 4.1 Gene expression analyses

This experimental approach for the identification of genes enriched in PSA<sup>+</sup> neuronal precursors in the adult brain and of genes representing potential NSC markers combines four crucial features. First, instead of bulk tissue or a cell mixture, homogeneous populations of neuronal precursors and ES cells were the basis for the screen. Second, the PSA<sup>+</sup> cells were prevented from undergoing potential modifications by omitting any culture step and directly proceeding to RNA isolation upon FACS. Third, several state-of-the-art gene expression analysis tools were used: SAGE for the initial global screen, cDNA microarrays and qPCR for validation experiments. The RNA samples for the SAGE were not amplified to avoid bias. Fourth, innovative bioinformatical tools were used to analyze the SAGE results for PSA<sup>+</sup> cells and allowed linking the SAGE data to GO annotations and motif databases for clustering.

SAGE has been used with increasing popularity for genome-wide expression analysis and the discovery of novel genes despite its major drawback that experimental repetition is hardly feasible. cDNA microarray technology is appropriate for high throughput analysis of defined gene sets but restricted to the displayed probes. qPCR is ideal for the identification of single genes with high sensitivity. To obtain a most accurate picture of the transcriptome of PSA<sup>+</sup> cells, all three methods were used in combination.

In general, good consistency was observed between SAGE and microarray data, but a few genes known to play a role in the migration process of PSA<sup>+</sup> cells, like, for example, DCC (Murase and Horwitz, 2002), were not detected by SAGE. Likewise, expression of Alkaline phosphatase was absent in ES cells. One reason for missing genes might be the limited size of the two generated SAGE libraries. According to estimations by Velculescu et al. (1999), about 23,500 different transcripts are expressed in an individual cell type of mature brain tissue. 14,754 different transcripts were obtained for PSA<sup>+</sup> precursors after having sequenced 36,093 tags, which is probably insufficient to cover all transcripts expressed at low levels.

One step, which is intrinsic to the SAGE protocol, is the generation of tags in the genetic sequence at the first CATG upstream of the 3' end. In neuronal gene organization, the 3'UTR can span several kilobases. As a consequence, some tags close to the 3' end might be too distant from the coding sequence and thus cannot be assigned to the corresponding gene. For example, Sox11 has a long 3'UTR (Azuma et al., 1999), therefore some tags belonging to this gene had to be annotated manually. Nevertheless, although DCC escaped the SAGE screen,

its expression was demonstrated by microarray hybridization. Manic fringe, Dvl2 and Sox4 could not be validated by the microarray hybridization, although their expression in PSA<sup>+</sup> cells was clearly confirmed by qPCR and *in situ* hybridizations.

## **4.2 Transcriptome analysis of PSA<sup>+</sup> neuronal precursor cells**

### **4.2.1 Already known genes confirm the SAGE results**

Some of the factors characteristic for PSA<sup>+</sup> cells had been characterized previously. The detection of those genes clearly confirms the accuracy of the SAGE analysis, for example, CD24, which negatively regulates the proliferation of the cells (Belvindrah et al., 2002), Doublecortin (Gleeson et al., 1999), which labels migrating neurons in the postnatal brain, the principle sialyltransferase ST8siaII (STX) (Kurosawa et al., 1997), the Reelin receptor ApoER2 (Hack et al., 2002) and the immature neural marker Nestin (Doetsch et al., 1997; Lendahl et al., 1990). Tags for NCAM were also expected to be present in the PSA<sup>+</sup> cell SAGE data since the cells had been isolated by means of PSA-NCAM. However, NCAM expression was not differential versus ATB because it occurs generally without the PSA modification in the brain. These results indicated that the correct cells were isolated in highly purified form and analyzed successfully by SAGE.

### **4.2.2 Novel genes were identified in the PSA<sup>+</sup> cell population**

The role of Sox transcription factor family has been studied in the developing CNS of diverse animals, where members 1, 2, 3, 4, 9, 10, 11 were found to play important roles in developmental neural processes. Sox2 expression is observed throughout the early neuroepithelium and becomes restricted to the VZ at the beginning of neural tube differentiation. It regulates proliferation and differentiation in developing peripheral nervous system (Uwanogho et al., 1995; Wakamatsu et al., 2004). Sox 2 is also expressed in the adult mouse in proliferating progenitors until they exit the cell cycle, and its constitutive expression inhibits neuronal differentiation and maintains progenitor characteristics (Graham et al., 2003). The highly homologous factors Sox4 and Sox11 are expressed simultaneously in early differentiating cells during CNS development (Cheung et al., 2000).

Sox genes were also found in the neural crest. While in *Xenopus* Sox9 expression persists during the migration of cranial crest cells, in zebrafish, Sox9b expression ceases in migrating neural crest cells (Li et al., 2002; Spokony et al., 2002). In chicken, Sox9 was found to be expressed in the VZ and SVZ during development, but not in postmitotic tissues (Szele et al.,

2002). Chicken Sox11 is transiently upregulated in cells leaving the VZ to form the SVZ during embryogenesis (Rex et al., 1998; Uwanogho et al., 1995). In the mouse, Sox11 expression is found in the neuroepithelium and at later developmental stages also in areas of neuronal differentiation (Kuhlbrodt et al., 1998). Expression of all the above Sox genes has not been demonstrated in the PSA<sup>+</sup> cells of the adult SVZ so far. The SAGE data indicated strong expression of Sox11 and Sox4 and lower but still significantly differential expression of Sox2 and Sox9 in the PSA<sup>+</sup> precursors. Sox4 expression was confirmed by qPCR and *in situ* hybridization. Thus, these Sox genes implicated in neural development might have very similar tasks in postnatal neurogenesis, for example, preventing the final differentiation of PSA<sup>+</sup> cells and their exit from the cell cycle.

In one aspect the SAGE data is contradictory to Graham's study, which found that "Sox2 [...] is mutually exclusive with  $\beta$ -tubulin type III" (Graham et al., 2003). For PSA<sup>+</sup> cells, this is not true because, according to the SAGE, they express Sox2 concomitantly with Tubulin $\beta$ III (24.9 tags). Strong Tubulin $\beta$ III expression in PSA<sup>+</sup> cells was already established (Doetsch et al., 1997).

Sox10 is required for the differentiation of melanocytes and glia derived from neural crest cells and has been implicated lately in the maintenance of neural crest stem cells (Kim et al., 2003; Mollaaghababa and Pavan, 2003). According to the SAGE data, Sox10 expression is absent in PSA<sup>+</sup> cells, which is in agreement with the fact that these are committed to the neuronal lineage.

Several studies showed that Dlx transcription factors play an important role in the control of neuronal migration and differentiation during embryogenesis (Panganiban and Rubenstein, 2002), (Eisenstat et al., 1999). Porteus *et al.* observed Dlx2 expression in PSA<sup>+</sup> cells and C cells in the adult brain (Porteus et al., 1994). During embryogenesis, the VZ contains Dlx2-negative cells until, with the onset of neurogenesis, the cells start to consecutively express Dlx2, Dlx1, Dlx5 and Dlx6 whereas Dlx6 is primarily expressed by differentiated cells (Eisenstat et al., 1999). The finding of tags for Dlx2 further confirmed the performance of the SAGE. Likewise, the absence of Dlx6 tags is consistent with the fact that the PSA<sup>+</sup> cells are immature neurons. In addition, the SAGE detected Dlx1 and Dlx5, which have previously been shown to be expressed in embryonic neurogenesis, but not in neuronal precursors in the adult SVZ. This result is in line with a recent study that concludes that Dlx5 is essential for postnatal neurogenesis from the comparison of neurosphere cultures derived from newborn and embryonic Dlx5-null mice (Perera et al., 2004).



---

Notch1, an inhibitor of neuronal differentiation, has been shown to be expressed in the SVZ and RMS (Stump et al., 2002). Notch1 was among the significantly differentially expressed genes in the SAGE data, while other members of the corresponding pathway were weakly expressed (represented by only 2.8 SAGE tags each): Delta-like 1, Hes1, -2, -5, Numb, Numb-like. The glycosyltransferase Manic fringe plays a role in the Notch pathway during mammalian cortical development (Shimizu et al., 2001). Maturing neurons express Manic fringe when they leave the VZ (Ishii et al., 2000). The mitotically active cells outside the VZ are negative for Lunatic fringe, which is expressed prior to neurogenesis, as well as for Radical fringe, which is upregulated when the migrating cortical precursor cells reach the preplate and cease dividing. SAGE and qPCR data both revealed expression of Manic fringe in PSA<sup>+</sup> cells in the SVZ. This finding was confirmed by *in situ* hybridization (data not shown). According to the SAGE, PSA<sup>+</sup> cells are negative for Lunatic and Radical fringe. Thus, the expression of the three fringe genes in PSA<sup>+</sup> precursors in the adult SVZ parallels the expression pattern in cortical precursor cells in the VZ during development.

The transcription factor Pax6 is required for normal brain development and neuronal migration during corticogenesis (Talamillo et al., 2003; Tyas et al., 2003). Pax6 was shown to have a cell-autonomous effect on the adhesiveness of embryonic cortical progenitors and to control their cell cycle length (Estivill-Torres et al., 2002). Pax6 overexpression is sufficient to induce neurogenesis in neurospheres and astrocytes (Hack et al., 2004). The SAGE data demonstrated expression of Pax6 in PSA<sup>+</sup> cells in the adult brain where, according to this information on its function, it is likely to contribute to neuronal differentiation and migration.

Meis2 is a homeobox gene, which was shown to be highly expressed in specific regions of the CNS from E10.5 until birth (Cecconi et al., 1997). It is a marker for proliferating precursors of striatal neurons and is expressed to a lower extent in the adult striatum (Arvidsson et al., 2002; Toresson et al., 2000). The detection of Meis2 in PSA<sup>+</sup> precursors by SAGE was validated by *in situ* hybridizations revealing expression in SVZ and RMS of the adult brain.

In summary, these results reveal striking parallels between embryonic and adult neurogenesis. The expression of Sox and Dlx transcription factors, Manic fringe, genes of the Wnt pathway, Pax6 and Meis2 in PSA<sup>+</sup> cells indicates that the molecular factors that set the course during embryonic development and cease being expressed in the mature adult brain remain active in the postnatal neurogenesis of the SVZ.

The strong caspase expression in PSA<sup>+</sup> cells correlates with the scenario that the majority of the PSA<sup>+</sup> precursors never reaches the OB but dies by apoptosis (Morshead and van der

Kooy, 2000; Morshead and van der Kooy, 1992). On the other hand, the striking upregulation of the clusters “DNA replication” and “Mitosis” is consistent with the notion of proliferating immature cells (Frazier-Cierpial and Brunjes, 1989; Luskin, 1993). Apoptosis and cell division have been suggested to be tightly linked processes and their interplay is essential for correct development as well as tissue homeostasis (Evan et al., 1995; Jacobson et al., 1997). The SAGE data is in agreement with the idea that the number of precursors that is present at a given time point in the adult brain is a result of an equilibrium of cell division and programmed cell death. The cluster analysis mirrors that the CGCP are more strongly proliferating precursors, which do not undergo such extensive cell death as the PSA<sup>+</sup> cells. One of the genes identified by SAGE and *in situ* hybridization as specifically expressed in PSA<sup>+</sup> cells is Survivin. On the one hand, Survivin has been shown to inhibit Caspase-9 (O'Connor et al., 2000) and Caspase-3 (Li et al., 1998; Reed, 2001) and thereby interfere with the apoptotic pathway (Kawamura et al., 2003). On the other hand, Survivin localizes to the mitotic spindle apparatus and is critical for correct mitosis. Disruption of the Survivin gene in mice results in early embryonic lethality due to chromosome segregation and cytokinesis defects (Uren et al., 2000). Thus, Survivin might be a key player in the control of precursor numbers in the adult brain and its impact in the regulation of adult neurogenesis will be further investigated.

The prominent upregulation of individual chemokines and chemokine receptors and their impressive dominance as a whole in the GO cluster “Chemotaxis” in PSA<sup>+</sup> cells was remarkable. Cell guidance based on mechanisms involving chemotactic factors had been reserved to leukocyte interactions for a long time. First evidence that the molecular mechanisms underlying cell migration might apply more generally came from the discovery that the neuronal chemorepellent Slit1 interfered not only with the directed movement of neuronal cells but also with chemokine-induced leukocyte action (Wu et al., 2001). The hypothesis that vice versa chemotaxis-induced movements might be a more universal theme playing a role also in neuronal migration was corroborated in a variety of studies. For example, it has been shown that CXCR4 regulates interneuron migration in the developing neocortex (Stumm et al., 2003). The chemokine SDF-1/Cxcl12 is expressed by meningeal cells and functions as attractant for embryonic cerebellar neurons (Zhu et al., 2002). In accordance with the latter result, the cluster “Chemotaxis” is also elevated in CGCP, even though to a much lesser extent than in PSA<sup>+</sup> cells. Thus, it appears well possible that molecular factors implicated in chemotaxis also serve as guidance cues in the SVZ-RMS-OB

system. Nevertheless, a correlation between the upregulation of chemokines and the disruption of nervous tissue cannot be entirely ruled out. For C3aR1, it has been shown that inflammation does not cause a noteworthy upregulation of neuronal expression (Davoust et al., 1999). Expression of Ccl4/MIP1 beta has been shown following stab wound injury, but in this case the chemokine-secreting cells were evidently astrocytes and macrophages (Ghirnikar et al., 1996). Finally, the *in situ* hybridization for the receptor C3aR1 showed specific expression in the RMS and the SVZ. Although these findings are in support of a specific role of chemotactic factors in this system, further experiments have to ensure that the chemokine expression is intrinsic to the precursor cells and independent of the experimental procedure.

Wu *et al.* reported that the chemorepellent Slit1 is expressed exclusively by cells in the septum and pushes immature neurons away from the SVZ at the onset of their journey in the RMS through a concentration gradient (Wu et al., 1999). The SAGE data was contradictory to these results indicating expression of Slit1 in the PSA<sup>+</sup> cells themselves. This finding was confirmed by a recent study showing Slit1 expression in the neuronal precursors by *in situ* hybridization and by using tau-GFP reporter gene expression under the Slit1 promoter (Nguyen-Ba-Charvet et al., 2004). Abnormal PSA<sup>+</sup> cell migration was observed in Slit1-deficient mice. The SAGE data does not relate to their finding of Slit2 and the Slit receptor Robo3 in the precursors, which might be simply ascribed to a very low expression level and the limited size of the SAGE library. Robo2 was barely detected (2.8 tags).

PSA<sup>+</sup> cells are destined to become predominantly GABAergic interneurons upon arrival in the OB. The SAGE data indicated absence of GABA<sub>A</sub> receptor activity in the precursor cells. Low tag numbers for GABA receptor chains Gabra1, Gabra4, Gabra6, Gabrb1, Gabrg1, Gabrg2, Gabrd, Gabrr2, were detected in ATB but not a single tag in PSA<sup>+</sup> cells. Low expression of the GABA<sub>B</sub> receptor (5.5 tags) was found in the PSA<sup>+</sup> precursors. GAD67, the key enzyme in GABA synthesis, was barely expressed (2.8 tags). Expression of Calretinin, which is used as a marker for GABAergic neurons (Miettinen et al., 1992), was detected in ATB (16.1 tags) but not in PSA<sup>+</sup> cells. A recent study demonstrated depolarization of PSA<sup>+</sup> precursors via the GABA<sub>A</sub> receptor and immunostaining for GABA and GAD67 in a subset of the cell population (Wang et al., 2003). Likewise, Carleton *et al.* showed with electrophysiological analysis that 73% of the migrating precursors in the RMS possess extrasynaptic GABA<sub>A</sub> receptors. The absence of tags for GABA<sub>A</sub> receptor in the SAGE data might be ascribed to a low expression in PSA<sup>+</sup> cells and the small library size. Moreover, the

GABA<sub>A</sub> receptors are only present on part of the cells in the RMS reducing the overall expression level in the population. The PSA<sup>+</sup> cells for the SAGE were isolated primarily from the anterior SVZ where even less cells might have started to express GABA<sub>A</sub> receptor. It is conceivable that, during migration in the RMS, PSA-NCAM expression is decreased in cells that start to produce GABA and to express GABA<sub>A</sub> receptor. Neither one of the above studies combined the electrophysiological investigation with immunostaining against PSA-NCAM.

One of the genes with unknown function discovered by the SAGE was RIKEN 3110003A17. *In situ* hybridizations demonstrated strong expression in RMS and SVZ. RIKEN 3110003A17 shows sequence similarity to the murine Actin-binding protein STARS (striated muscle activator of Rho signaling), which induces polymerization of Actin and activation of Rho GTPase signaling to influence transcription (Arai et al., 2002). RIKEN 3110003A17 might have a similar function and participate in the regulation of the migration process of the PSA<sup>+</sup> precursors.

The significant upregulation of clusters representing properties of differentiated neural cells like “Neurotransmitter secretion”, “Glutamate-gated ion channel activity” and “Angiogenesis” in ATB versus PSA<sup>+</sup> cells confirms the identity of the precursor cells, the purity of their FACS isolation and the quality of the SAGE.

#### 4.2.3 First functional data based on the SAGE results are generated

Many knock-out mice for the precursor-enriched genes identified by SAGE were reported to show lethality in development or shortly after birth (e.g. Sox4, Survivin and Dlx5). PlexinA3-deficient mice were viable and available (Cheng et al., 2001) for the investigation of the SVZ-RMS-OB in the collaborating laboratory of Dr. H. Cremer. Cheng *et al.* showed that PlexinA3 mediates repulsion by class3 semaphorins and that guidance of hippocampal axons is affected in the mutant animals. The Semaphorin signaling system is involved in the development of the mammalian CNS by producing both repulsive and attractive guidance cues (Bagri and Tessier-Lavigne, 2002). In general, PlexinA3 forms a receptor with Neuropilin1 for Semaphorin3A and with Neuropilin2 for Semaphorin3F. However, preliminary data suggests that, in the OB, Semaphorins act as attractive cues for the PSA<sup>+</sup> cells. In line with this idea, we discovered a RMS that was progressively reduced towards the OB in PlexinA3-deficient

mice. This observation could be explained by the inability of the PSA<sup>+</sup> cells to react to attractive cues in the OB.

These preliminary functional data further corroborate the results of the gene expression analysis and prove that the produced candidate list of precursor-enriched genes represents a basis for future projects.

In summary, this study provides the first genome-wide analysis for neuronal precursors FACS-purified from adult brain and contributes to the understanding of the molecular nature of these cells. While previously characterized genes legitimize the SAGE data, new genes fit well into the molecular picture according to what is known for these genes from other settings and according to the notion of migrating immature neuronal cells. Along with completely unknown genes, many of them provide forward passes for functional analyses.

### **4.3 Analysis of ES cell-enriched genes and potential NSC markers**

#### **4.3.1 Characteristic genes confirm pluripotency of ES cells**

The maintenance of a pluripotent and undifferentiated state of the ES cells was an essential prerequisite for the success of the gene expression profiling and the subsequent gene selection process. The pluripotency-sustaining factor Nanog was highly and exclusively expressed in the ES cells, which were used for the SAGE. The homeodomain protein Nanog was shown to be essential for self-renewal and its overexpression sufficient for maintaining pluripotency in the absence of LIF (Chambers et al., 2003; Mitsui et al., 2003; Ying et al., 2003). The octamer transcription factor Oct4 plays an essential role in the control of pluripotency in the preimplantation embryos, epiblast and germ cells and is downregulated during gastrulation when somatic lineages are first defined (Nichols et al., 1998; Niwa et al., 2000). Expression of Nanog and Oct4 clearly proves that the undifferentiated state of the ES cells was conserved. In addition, the SAGE revealed expression of several Oct4-associated genes, e.g. Dppa5 (Embryonal stem cell specific gene), Dppa2, Dppa4 (Bortvin et al., 2003), and the Oct4-activated Osteopontin (Guo et al., 2002). Dppa5 was first described as a cDNA downregulated during embryonic carcinoma cell differentiation (Astigiano et al., 1991). The expression of Dppa5, 4, 2 is in agreement with the results of Ramalho-Santos *et al.* (Ramalho-Santos et al., 2002).

Sox2 was reported to be expressed in the preimplantation embryo, in cultured ES cells, in NSC and neural progenitor cells (Avilion et al., 2003; Miyagi et al., 2004; Tomioka et al., 2002). Sox2 cooperates closely with Oct4 in ES cells to regulate transcription and maintain the pluripotent state, and it interacts likewise with octamer factors in multipotent NSC. Zappone *et al.* discovered that Sox2 expression is not stem cell-specific but occurs also in early precursors devoid of stem cell properties (Zappone et al., 2000). In agreement with this data, the SAGE and microarray experiments revealed equally strong Sox2 expression in ES cells and in PSA<sup>+</sup> neuronal precursors (4.2.2). In ES cells, the enhancer SRR2 (Sox regulatory region 2) was shown to preclude the binding of the Oct1-Sox2 complex but to recruit the Oct6-Sox2 complex as well as the Oct4-Sox2 complex for the stimulation of transcription (Tomioka et al., 2002). The formation of complexes with different octamer factors permits Sox2 to fulfill diverse functions. The divergence of transcript numbers for octamer factors in ES cells and PSA<sup>+</sup> cells probably correlates with the different impacts of Sox2 on the respective cell type. Oct4 and Oct6 are only present in ES cells, while POU6f1 (EMB) is only expressed in PSA<sup>+</sup> cells. Oct1 expression (although not significantly differentially upregulated) is 4-fold higher in PSA<sup>+</sup> cells. Obviously, it is unlikely that in PSA<sup>+</sup> cells Sox2 forms the same Oct6-Sox2 and Oct4-Sox2 complexes that contribute to the ES cells' pluripotency, which is consistent with the lineage commitment of the precursor cells. Octamer factors were shown to play an important role in the regulation of the expression of other neural progenitor-specific genes like Nestin and Brain fatty acid binding protein (Josephson et al., 1998). Graham *et al.* proposed that Sox2 is necessary and sufficient for the maintenance of characteristic neural properties of neural progenitor cells (Graham et al., 2003). It seems that Sox2 more generally, i.e. from ES cells over NSC to restricted PSA<sup>+</sup> neuronal precursors, prevents exit from the cell cycle and thereby differentiation.

Cripto, the most highly expressed gene, according to the SAGE data, was first observed in the inner cell mass (Xu et al., 1999). Cripto was also found in R1 ES cells (Anisimov et al., 2002) and as the second most highly expressed gene in Ramalho-Santos' study. The Cripto-interacting factors Nodal and LeftB (Tgfb4) were also found in the ES cell SAGE data as expected according to Ramalho-Santos' data.

The SAGE data for the Bruce-4 ES cells showed noteworthy consistency with the microarray data of Ramalho-Santos and with the R1 ES cell SAGE data of Anisimov. However, the expression of several ES cell-characteristic genes was considerably higher in Bruce-4 than in R1 ES cells (Tab. 5). This divergence might be due to the different origin of the ES cells. Both this and Ramalho-Santos' study used ES cells derived from C57Bl/6(J) mice while

Anisimov used R1 ES cells. The differences might be ascribed to polymorphisms in the different strains (unpublished observations, Dr. Kay Hofmann).

Taken together, the abundance of ES cell-characteristic and -specific genes demonstrates the pluripotent state of the Bruce-4 ES cells and the efficiency of the SAGE.

The ES cell SAGE data were generated to be used as a screening tool for the search of NSC markers, but, nonetheless, it would be worthwhile to examine the function of unknown genes that have an expression pattern similar to that of Oct4 and Nanog, e.g. RIKEN cDNA 2410003J06, RIKEN cDNA 2400008B06 and RIKEN cDNA C330012H03 (especially considering that, at the end of 2002, this data set already contained the tag for Nanog but without annotation).

#### 4.3.2 Potential NSC markers were selected from the SAGE data

The stringent selection process based on the SAGE data and transmembrane localization led to the identification of eight potential NSC markers. Some of them were known to play a role in preimplantation embryos or in early development.

The interferon-induced transmembrane protein Ifitm1 (Deblandre et al., 1995), the epithelial cell adhesion molecule Eva (Guttinger et al., 1998; Teesalu et al., 1998) and the gap junction protein Connexin31 (Flechon et al., 2004; Plum et al., 2002; Plum et al., 2001) were analyzed for their expression in EBs and neurospheres. The specificity of the resulting weak to medium staining could not be confirmed by the total absence of signal using the corresponding sense probes. Therefore, these genes were not further examined.

It was not surprising to observe expression of the epithelial cell adhesion molecule Cadherin1 only in the ependymal cells of the SVZ since it participates in the composition of all epithelia (Riethmacher et al., 1995; Sefton et al., 1992; Vestweber and Kemler, 1984). This finding eliminated Cadherin1 from the list of potential markers. Weak expression of the Wnt receptor Frz7 (Winklbauer et al., 2001) was found in EBs and neurospheres but not in postnatal brain. Frz7 was already shown to be expressed until E10.5 (Borello et al., 1999). Future analyses will assess expression in late embryonic brain. In any case, according to the present results that do not indicate expression of Frz7 in postnatal brain, it appears to be useless for the identification of adult NSC. The uncharacterized RIKEN 2610033C09 was found in EBs and neurospheres. However, in postnatal brain, this gene stained moderately not only the SVZ but also the entire brain. Unless further optimization of the experimental conditions results in a more defined staining, this candidate will not be followed further.

The novel transmembrane protein KIAA0152, for which the correct annotation was available only recently, remains to be investigated yet.

As mentioned above, a mistake in the gene annotations for ASCT2 in the public database SwissProt led to the assignment of a wrong gene name, SLC1A2, to the correct ASCT2 accession number. As a result, *in situ* hybridizations were performed with a probe for the sequence of the glutamate transporter GLT1 (SLC1A2, EAAT2) (4.4).

Even though the expression in neurospheres or mouse brain has not been analyzed by *in situ* hybridizations yet, the candidate ASCT2 is of interest given the SAGE results and its description in the literature. ASCT2 (also ATB<sup>0</sup>, SLC1A7) is a well-known transporter protein of the EAAT (excitatory amino acid transporters) superfamily (Utsunomiya-Tate et al., 1996). This transporter is part of the ASC system that is responsible for Na<sup>+</sup>-dependent transport of L-alanine, L-serine, and L-cysteine (Palacin et al., 1998). ASCT2 participates in the glutamate-glutamine cycle and exports glutamine out of astrocytes, which is in turn taken up by neurons (Broer and Brookes, 2001). ASCT2 was found to mediate the L-isomer-selective transport of aspartic acid at the blood-brain barrier (Tetsuka et al., 2003). While the transporter gene was originally cloned from mouse testis (Utsunomiya-Tate et al., 1996), a study in rabbits showed expression for ASCT2 in the intestine and in the kidney. More precisely, the protein is confined to the brush-border membrane of the proximal tubular cell as well as of enterocytes and crypt cells (Avissar et al., 2001). While Northern blot analysis readily detected the putative NSC marker TLX (mtll) (Monaghan et al., 1995; Shi et al., 2004), this method failed to detect ASCT2 in adult mouse brain (Utsunomiya-Tate et al., 1996). The low expression level of ASCT2 is consistent with the SAGE results and with the fact that the number of NSC in the adult brain is probably small.

The discovery of weak ASCT2 expression in embryonic brain and strong upregulation in astrocytes cultures by RT-PCR led Bröer *et al.* to the conclusion that ASCT2 might play a role during brain development and its expression might be associated with proliferative astrocytes (Broer and Brookes, 2001).

Immunohistochemical analysis by Tetsuka *et al.* showed that the ASCT2 protein is localized on the abluminal side of the capillary endothelial cells that constitute the blood-brain barrier in the mouse cortex (Tetsuka et al., 2003). Here, GFAP staining did not co-localize with ASCT2 staining, but enclosed it suggesting that astrocytic foot processes that surround each cerebral capillary express the protein. Although Bröer *et al.* reported ASCT2 expression in rat astroglia-rich primary cultures, Tetsuka *et al.* found no significant ASCT2-immunoreactivity in astrocytes in the mouse cortex, which is believed to be a nonneurogenic area.



Signaling through the EGF receptor is known to stimulate SVZ neurogenesis *in vitro* (Gritti et al., 1999; Reynolds and Weiss, 1992) and *in vivo* (Craig et al., 1996; Fallon et al., 2000).

EGF was shown to affect the expression of ASCT2. In rabbit residual gut, EGF in combination with growth hormone was able to reverse the downregulation of system B<sup>0</sup> activity (which comprises ATB<sup>0</sup>/ASCT2) after massive enterectomy (Avissar et al., 2001). Furthermore, exposure of epithelial Caco-2 cells to EGF for 48 h strongly increased the ASCT2 RNA level and the glutamine transporter maximal velocity (Wolfgang et al., 2003). Regarding the expression, ASCT2 exhibits parallels to LeX (Capela and Temple, 2002), which is not NSC-specific but encompasses all neurosphere-forming cells in the adult SVZ. Both are found in pluripotent ES cells, around blood vessels and in some astrocytes. ASCT2 is neither shed into the ECM like LeX nor intracellular like TLX but located on the cell surface. The reported observations and the expression according to SAGE suggest that ASCT2 has the potential to be a NSC marker. The expression in the neurogenic SVZ will be investigated.

#### **4.4 Intense GLT1 expression was found in a neurogenic area**

GLT1 would not have been selected from the SAGE data according to the defined criteria since its expression in PSA<sup>+</sup> cells and ATB was too high. Although its expression pattern was only examined in consequence of a confusion caused by a database mistake and it cannot be considered a potential NSC marker, the results were striking and will be discussed here.

GLT1 (also EAAT2, SLC1A2) is one of five subtypes of glutamate transporters whose primary task is the removal of excess glutamate, a major excitatory neurotransmitter, from the extracellular space to prevent neurotoxic levels (Robinson, 1998). GLT1-deficient mice do not show obvious morphological abnormalities, but suffer from epileptic seizures caused by high glutamate levels (Tanaka et al., 1997).

The expression of GLT1 in EBs and neurospheres is not surprising. The GNF SymAtlas (<http://symatlas.gnf.org/SymAtlas/>) (Su et al., 2002) shows expression of GLT1 in zygote, blastocyst and later embryonic stages. Therefore, the expression in embryoid bodies seems plausible. *In situ* hybridizations for GLT1 specifically labeled a subpopulation of cells within neurospheres. In the brain, GLT1 is primarily found on astrocytes (Rothstein et al., 1994). Since neurospheres are known to contain GFAP<sup>+</sup> cells (Morshead et al., 2003) it is conceivable that these also express GLT1.

In the postnatal brain, GLT1 *in situ* hybridizations produced a striking expression pattern. Shortly after birth, the labeling extended around the entire LV, while two weeks later, the expression was restricted to single cells and small groups of cells in the SVZ at the LV. The latter were distinct from the characteristic chains of cells that are formed by the PSA<sup>+</sup> cells. Only a small number of cells in the brain was strongly labeled outside the SVZ. The SVZ is an area of ongoing neurogenesis in the adult forebrain, where the NSC are known to reside (Gage, 2000). The progressively reduced number of GLT1<sup>+</sup> cells in the SVZ after birth parallels the decline in the number of NSC after termination of primary neurogenesis (Pevny and Rao, 2003). A causal relation between these events, however, remains to be shown.

The expression of GLT1 in the brain has been analyzed in-depth. Increasing expression was observed during development to reach widespread distribution in the rat forebrain and brainstem by P10 and by P24 also in the cerebellum (Furuta et al., 1997). Previous studies describe strong GLT1 expression in proliferative zones of the mouse, namely the pallial VZ and SVZ during development (Shibata et al., 1996; Sutherland et al., 1996). An increase in signal intensity for this pallial SVZ labeling was noticed from P1 to P14 (Chen et al., 2002; Shibata et al., 1996; Sutherland et al., 1996). The line of GLT1<sup>+</sup> cells overlying the corpus callosum in the present *in situ* hybridizations on P14 brain might correspond to the remnants of the pallial SVZ. Sutherland *et al.* observed that postnatally “unexpectedly strong mEAAT2 mRNA expression persists in the subependymal proliferative zone” (here called SVZ). The present data for GLT1 expression in the hippocampus is merely preliminary. Individual labeled cells were observed in the area of the dentate gyrus, while the entire CA3 region was weakly stained. Prior studies also found GLT1 in the hippocampal CA3 region (Chen et al., 2004; Sutherland et al., 1996). At the time, Sutherland did not base her interpretation on today’s theory that NSC are among the SVZ astrocytes but on articles by Morshead and Bayer saying that newly produced cells do not invade the surrounding brain tissue but remain in the SVZ to die and that neurogenesis in the dentate gyrus ceases at P20 (Bayer et al., 1980; Morshead and van der Kooy, 1992; Sutherland et al., 1996). In addition, the autoradiograms for GLT1 were of rather low resolution compared to our Digoxigenin-based *in situ* hybridizations. However, Sutherland associated GLT-1 expression with radial glia and suggested that glutamate transport could contribute to the regulation of cell proliferation and neuronal survival. This observation is interesting considering the recently established hypothesis that a neuroepithelial-radial glia-astrocyte lineage contains the NSC (Alvarez-Buylla et al., 2001; Doetsch, 2003).

For a long time, GLT1 has been thought to be expressed exclusively by astrocytes (Rothstein et al., 1994). In the developing spinal cord, a transient expression on growing axons was observed followed by a switch to astrocytic expression at early postnatal stages (Yamada et al., 1998). Recent analyses revealed two splice variants, GLT1a and GLT1b. Both forms were found in neuronal processes of the CA3 region and in astrocytes of the hippocampal formation with GLT1a being the predominant form (Chen et al., 2002; Chen et al., 2004). The *in situ* probe for GLT1 used in this work hybridizes in the 3' region and probably recognizes GLT1a and GLT1b since only the last 48 nt of GLT1b differ in the region corresponding to the 301 nt probe. Altogether, it is not clear if the type of GLT1<sup>+</sup> SVZ cell in the present work corresponds only to astrocytes. Interestingly, the SAGE data indicated GLT1 expression in PSA<sup>+</sup> precursor cells, the most prominent cell type in SVZ and RMS. No information is available about the expression in another major cell type of the SVZ, the C cells. Since the *in situ* hybridizations show only single labeled cells in SVZ and RMS that consist largely of PSA<sup>+</sup> cells, it is conceivable that only cells with a particularly strong expression of GLT1 were stained. Antibodies against GLT1 are available, but studies have focused on expression in regions other than the SVZ (Chen et al., 2004; Utsumi et al., 2001; Yamada et al., 1998). Several studies showed that NSC are among the SVZ astrocytes and thus should be GFAP-positive (Chiasson et al., 1999; Doetsch et al., 1999a; Imura et al., 2003; Laywell et al., 2000). According to the immunostaining for GFAP after *in situ* hybridization, far more cells are GFAP-positive than GLT1-positive.

In agreement with the present notion that the population of ependymal cells does not contain any GFAP<sup>+</sup> cells, GLT1 staining was excluded from the ependyma and confined to the adjacent SVZ. Very rarely were the processes of individual stained cells observed to penetrate the ependyma. This finding is consistent with the phenomenon that a few SVZ astrocytes contact the ventricle (Doetsch et al., 1999a), provided that the GLT1<sup>+</sup> cells are GFAP-positive.

Swanson *et al.* showed that astrocytes monocultures were negative for GLT1, but astrocytes co-cultured with neurons expressed GLT1. Dibutyryl cAMP (dBcAMP), which is used to mimic neuronal influence on astrocyte cultures, also induced GLT1 expression in astrocytes (Swanson et al., 1997). A link between GFAP and GLT1 expression was established by the discovery that loss of GFAP results in an inability to guide GLT1 to the cell surface following dBcAMP stimulation (Hughes et al., 2004). Since neuron-conditioned medium or neurons separated by a semipermeable membrane likewise induced GLT1 expression in astrocytes the effect might be ascribed to soluble factors (Robinson, 1998).

Later studies found that EGF and TGF- $\alpha$ , which both bind to the EGF receptor, caused a significant increase in GLT1 expression. Astrocytes from striatum but not from cerebellum or spinal cord responded that way (Schluter et al., 2002; Zelenai et al., 2000).

Recently, a relationship between neurogenesis and vasculogenesis within a stem cell “niche” has been suggested (Alvarez-Buylla and Lim, 2004; Palmer et al., 2000). Blood vessel-surrounding basal laminae, which provide inductive microenvironments for adjacent NSC, were discovered in the SVZ (Mercier et al., 2002). The ECM molecules Laminin and Collagen are major components of the basal lamina. Interestingly, both proteins were reported to cause an increase of GLT1 protein but not GLAST in cultured astrocytes (Ye and Sontheimer, 2002).

The higher intensity of GLT1 staining in the SVZ compared to nonneurogenic cortex and the above reported facts suggest that it might be related to neurogenesis. Creating an environment for neuronal survival by preventing high glutamate levels might be particularly important in proliferative zones.

#### 4.4.1 Future experiments for GLT1

Although many studies have been conducted on GLT1, none provided information that would be sufficient to explain the data presented here. Given the interesting expression pattern of GLT1, how is it related to the function of the protein? Double immunolabeling with GFAP, PSA, Dlx2 and LeX, respectively, using confocal microscopy would clarify the identity of the GLT1<sup>+</sup> cells in the SVZ. Furthermore, it might be interesting to examine the postnatal SVZ in GLT1-deficient mice. The impact of EGF on transporter activity and transcription level in the SVZ would be worthwhile to explore.

#### **4.5 Conclusions and outlook**

The analyses described here provide a previously unavailable molecular portrait of neuronal precursor cells from adult brain in the context of neural differentiation. This gene expression study may serve as a reference work to inquire the expression for a gene of interest in migrating neuronal precursors or ES cells. This data and the comparison to further SAGE libraries might allow drawing first conclusions concerning the involvement of a given gene in secondary neurogenesis, neuronal migration and differentiation or self-renewal and pluripotency. Detailed study of individual genes will be necessary to gain progressively deeper insights into the control of neuronal differentiation and migration. The present data

represent an important resource also for research of neural disease and defects and should be exploited in the search of the underlying genes. Despite its humble contribution to ES cell biology, it provides basic information to compare the Bruce-4 cells to other ES cell lines and for the discovery of more “Nanogs”. The function of many novel genes in ES cells and PSA<sup>+</sup> cells remains to be unraveled.

These reliable data sets of homogeneous cell populations have proven to be a powerful selection tool in combination with other SAGE libraries.

---

## 5 References

- Aguirre, A. A., Chittajallu, R., Belachew, S., and Gallo, V. (2004). NG2-expressing cells in the subventricular zone are type C-like cells and contribute to interneuron generation in the postnatal hippocampus. *J Cell Biol* *165*, 575-89.
- Altman, J. (1962). Are new neurons formed in the brains of adult mammals? *Science* *135*, 1127-8.
- Altman, J. (1969). Autoradiographic and histological studies of postnatal neurogenesis. IV. Cell proliferation and migration in the anterior forebrain, with special reference to persisting neurogenesis in the olfactory bulb. *J Comp Neurol* *137*, 433-57.
- Altman, J. (1963). Autoradiographic investigation of cell proliferation in the brains of rats and cats. *Anat. Rec.* *145*, 573-591.
- Alvarez-Buylla, A., Garcia-Verdugo, J. M., and Tramontin, A. D. (2001). A unified hypothesis on the lineage of neural stem cells. *Nat Rev Neurosci* *2*, 287-93.
- Alvarez-Buylla, A., and Lim, D. A. (2004). For the long run: maintaining germinal niches in the adult brain. *Neuron* *41*, 683-6.
- Alvarez-Buylla, A., and Lois, C. (1995). Neuronal stem cells in the brain of adult vertebrates. *Stem Cells* *13*, 263-72.
- Anisimov, S. V., Tarasov, K. V., Tweedie, D., Stern, M. D., Wobus, A. M., and Boheler, K. R. (2002). SAGE Identification of Gene Transcripts with Profiles Unique to Pluripotent Mouse R1 Embryonic Stem Cells. *Genomics* *79*, 169-176.
- Arai, A., Spencer, J. A., and Olson, E. N. (2002). STARS, a striated muscle activator of Rho signaling and serum response factor-dependent transcription. *J Biol Chem* *277*, 24453-9.
- Arvidsson, A., Collin, T., Kirik, D., Kokaia, Z., and Lindvall, O. (2002). Neuronal replacement from endogenous precursors in the adult brain after stroke. *Nat Med* *8*, 963-70.
- Astigiano, S., Barkai, U., Abarzua, P., Tan, S. C., Harper, M. I., and Sherman, M. I. (1991). Changes in gene expression following exposure of nulli-SCC1 murine embryonal carcinoma cells to inducers of differentiation: characterization of a down-regulated mRNA. *Differentiation* *46*, 61-7.
- Audic, S., and Claverie, J. M. (1997). The significance of digital gene expression profiles. *Genome Res* *7*, 986-95.
- Avilion, A. A., Nicolis, S. K., Pevny, L. H., Perez, L., Vivian, N., and Lovell-Badge, R. (2003). Multipotent cell lineages in early mouse development depend on SOX2 function. *Genes Dev* *17*, 126-40.

- Avissar, N. E., Ryan, C. K., Ganapathy, V., and Sax, H. C. (2001). Na(+)-dependent neutral amino acid transporter ATB(0) is a rabbit epithelial cell brush-border protein. *Am J Physiol Cell Physiol* 281, C963-71.
- Azuma, T., Ao, S., Saito, Y., Yano, K., Seki, N., Wakao, H., Masuho, Y., and Muramatsu, M. (1999). Human SOX11, an upregulated gene during the neural differentiation, has a long 3' untranslated region. *DNA Res* 6, 357-60.
- Bagri, A., and Tessier-Lavigne, M. (2002). Neuropilins as Semaphorin receptors: in vivo functions in neuronal cell migration and axon guidance. *Adv Exp Med Biol* 515, 13-31.
- Baker, H., Liu, N., Chun, H. S., Saino, S., Berlin, R., Volpe, B., and Son, J. H. (2001). Phenotypic differentiation during migration of dopaminergic progenitor cells to the olfactory bulb. *J Neurosci* 21, 8505-13.
- Bateman, A., Birney, E., Cerruti, L., Durbin, R., Eddy, S. R., Griffiths-Jones, S., Howe, K. L., Marshall, M., and Sonnhammer, E. L. (2002). The Pfam protein families database. *Nucleic Acids Res* 30, 276-80.
- Bayer, S. A., Yackel, J. W., and Puri, P. S. (1980). Development of the hippocampal region in the rat. I. Neurogenesis examined with 3H-thymidine autoradiography  
Neurons in the rat dentate gyrus granular layer substantially increase during juvenile and adult life. *J Comp Neurol* 190, 87-114.
- Belvindrah, R., Rougon, G., and Chazal, G. (2002). Increased neurogenesis in adult mCD24-deficient mice. *J Neurosci* 22, 3594-607.
- Borello, U., Buffa, V., Sonnino, C., Melchionna, R., Vivarelli, E., and Cossu, G. (1999). Differential expression of the Wnt putative receptors Frizzled during mouse somitogenesis. *Mech Dev* 89, 173-7.
- Bortvin, A., Eggan, K., Skaletsky, H., Akutsu, H., Berry, D. L., Yanagimachi, R., Page, D. C., and Jaenisch, R. (2003). Incomplete reactivation of Oct4-related genes in mouse embryos cloned from somatic nuclei. *Development* 130, 1673-80.
- Bosio, A., Knorr, C., Janssen, U., Gebel, S., Haussmann, H. J., and Muller, T. (2002). Kinetics of gene expression profiling in Swiss 3T3 cells exposed to aqueous extracts of cigarette smoke. *Carcinogenesis* 23, 741-8.
- Bosio, A., Stoffel, M., and Stoffel, W. (1999). Support for the parallel identification and establishment of transcription profiles of polynucleic acids in WO9964623.
- Brazma, A., Hingamp, P., Quackenbush, J., Sherlock, G., Spellman, P., Stoeckert, C., Aach, J., Ansorge, W., Ball, C. A., Causton, H. C., Gaasterland, T., Glenisson, P., Holstege, F. C., Kim, I. F., Markowitz, V., Matese, J. C., Parkinson, H., Robinson, A., Sarkans, U., Schulze-Kremer, S., Stewart, J., Taylor, R., Vilo, J., and Vingron, M. (2001). Minimum information about a microarray experiment (MIAME)-toward standards for microarray data. *Nat Genet* 29, 365-71.

- Broer, S., and Brookes, N. (2001). Transfer of glutamine between astrocytes and neurons. *J Neurochem* *77*, 705-19.
- Bulfone, A., Puellas, L., Porteus, M. H., Frohman, M. A., Martin, G. R., and Rubenstein, J. L. (1993). Spatially restricted expression of *Dlx-1*, *Dlx-2* (*Tes-1*), *Gbx-2*, and *Wnt-3* in the embryonic day 12.5 mouse forebrain defines potential transverse and longitudinal segmental boundaries. *J Neurosci* *13*, 3155-72.
- Burd, G. D., and Nottebohm, F. (1985). Ultrastructural characterization of synaptic terminals formed on newly generated neurons in a song control nucleus of the adult canary forebrain. *J Comp Neurol* *240*, 143-52.
- Cai, J., Wu, Y., Mirua, T., Pierce, J. L., Lucero, M. T., Albertine, K. H., Spangrude, G. J., and Rao, M. S. (2002). Properties of a fetal multipotent neural stem cell (NEP cell). *Dev Biol* *251*, 221-40.
- Cameron, H. A., Woolley, C. S., McEwen, B. S., and Gould, E. (1993). Differentiation of newly born neurons and glia in the dentate gyrus of the adult rat. *Neuroscience* *56*, 337-44.
- Camon, E., Magrane, M., Barrell, D., Binns, D., Fleischmann, W., Kersey, P., Mulder, N., Oinn, T., Maslen, J., Cox, A., and Apweiler, R. (2003). The Gene Ontology Annotation (GOA) project: implementation of GO in SWISS-PROT, TrEMBL, and InterPro. *Genome Res* *13*, 662-72.
- Capela, A., and Temple, S. (2002). *LeX/ssea-1* Is Expressed by Adult Mouse CNS Stem Cells, Identifying Them as Nonependymal. *Neuron* *35*, 865.
- Carleton, A., Petreanu, L. T., Lansford, R., Alvarez-Buylla, A., and Lledo, P. M. (2003). Becoming a new neuron in the adult olfactory bulb. *Nat Neurosci* *6*, 507-18.
- Carleton, A., Rochefort, C., Morante-Oria, J., Desmaisons, D., Vincent, J. D., Gheusi, G., and Lledo, P. M. (2002). Making scents of olfactory neurogenesis. *J Physiol Paris* *96*, 115-22.
- Cecconi, F., Proetzl, G., Alvarez-Bolado, G., Jay, D., and Gruss, P. (1997). Expression of *Meis2*, a Knotted-related murine homeobox gene, indicates a role in the differentiation of the forebrain and the somitic mesoderm. *Dev Dyn* *210*, 184-90.
- Chambers, I., Colby, D., Robertson, M., Nichols, J., Lee, S., Tweedie, S., and Smith, A. (2003). Functional expression cloning of *Nanog*, a pluripotency sustaining factor in embryonic stem cells. *Cell* *113*, 643-55.
- Chazal, G., Durbec, P., Jankovski, A., Rougon, G., and Cremer, H. (2000). Consequences of neural cell adhesion molecule deficiency on cell migration in the rostral migratory stream of the mouse. *J Neurosci* *20*, 1446-57.
- Chen, T., Ueda, Y., Dodge, J. E., Wang, Z., and Li, E. (2003). Establishment and maintenance of genomic methylation patterns in mouse embryonic stem cells by *Dnmt3a* and *Dnmt3b*. *Mol Cell Biol* *23*, 5594-605.



- Chen, W., Aoki, C., Mahadomrongkul, V., Gruber, C. E., Wang, G. J., Blitzblau, R., Irwin, N., and Rosenberg, P. A. (2002). Expression of a variant form of the glutamate transporter GLT1 in neuronal cultures and in neurons and astrocytes in the rat brain. *J Neurosci* 22, 2142-52.
- Chen, W., Mahadomrongkul, V., Berger, U. V., Bassan, M., DeSilva, T., Tanaka, K., Irwin, N., Aoki, C., and Rosenberg, P. A. (2004). The glutamate transporter GLT1a is expressed in excitatory axon terminals of mature hippocampal neurons. *J Neurosci* 24, 1136-48.
- Cheng, H. J., Bagri, A., Yaron, A., Stein, E., Pleasure, S. J., and Tessier-Lavigne, M. (2001). Plexin-A3 mediates semaphorin signaling and regulates the development of hippocampal axonal projections. *Neuron* 32, 249-63.
- Cheung, M., Abu-Elmagd, M., Clevers, H., and Scotting, P. J. (2000). Roles of Sox4 in central nervous system development. *Brain Res Mol Brain Res* 79, 180-91.
- Chiaramello, A., Soosaar, A., Neuman, T., and Zuber, M. X. (1995). Differential expression and distinct DNA-binding specificity of ME1a and ME2 suggest a unique role during differentiation and neuronal plasticity. *Brain Res Mol Brain Res* 29, 107-18.
- Chiasson, B. J., Tropepe, V., Morshead, C. M., and van der Kooy, D. (1999). Adult mammalian forebrain ependymal and subependymal cells demonstrate proliferative potential, but only subependymal cells have neural stem cell characteristics. *J Neurosci* 19, 4462-71.
- Ciccolini, F. (2001). Identification of two distinct types of multipotent neural precursors that appear sequentially during CNS development. *Mol Cell Neurosci* 17, 895-907.
- Clarke, D. L., Johansson, C. B., Wilbertz, J., Veress, B., Nilsson, E., Karlstrom, H., Lendahl, U., and Frisen, J. (2000). Generalized potential of adult neural stem cells. *Science* 288, 1660-3.
- Collinson, J. M., Quinn, J. C., Hill, R. E., and West, J. D. (2003). The roles of Pax6 in the cornea, retina, and olfactory epithelium of the developing mouse embryo. *Dev Biol* 255, 303-12.
- Conover, J. C., Doetsch, F., Garcia-Verdugo, J. M., Gale, N. W., Yancopoulos, G. D., and Alvarez-Buylla, A. (2000). Disruption of Eph/ephrin signaling affects migration and proliferation in the adult subventricular zone. *Nat Neurosci* 3, 1091-7.
- Craig, C. G., Tropepe, V., Morshead, C. M., Reynolds, B. A., Weiss, S., and van der Kooy, D. (1996). In vivo growth factor expansion of endogenous subependymal neural precursor cell populations in the adult mouse brain. *J Neurosci* 16, 2649-58.
- Cremer, H., Lange, R., Christoph, A., Plomann, M., Vopper, G., Roes, J., Brown, R., Baldwin, S., Kraemer, P., Scheff, S., and et al. (1994). Inactivation of the N-CAM gene in mice results in size reduction of the olfactory bulb and deficits in spatial learning. *Nature* 367, 455-9.
- Davoust, N., Jones, J., Stahel, P. F., Ames, R. S., and Barnum, S. R. (1999). Receptor for the C3a anaphylatoxin is expressed by neurons and glial cells. *Glia* 26, 201-11.

- Deblandre, G. A., Marinx, O. P., Evans, S. S., Majaj, S., Leo, O., Caput, D., Huez, G. A., and Wathélet, M. G. (1995). Expression cloning of an interferon-inducible 17-kDa membrane protein implicated in the control of cell growth. *J Biol Chem* *270*, 23860-6.
- Doetsch, F. (2003). The glial identity of neural stem cells. *Nat Neurosci* *6*, 1127-34. Epub 2003 Oct 28.
- Doetsch, F. (2003). A niche for adult neural stem cells. *Curr Opin Genet Dev* *13*, 543-50.
- Doetsch, F., and Alvarez-Buylla, A. (1996). Network of tangential pathways for neuronal migration in adult mammalian brain. *Proc Natl Acad Sci U S A* *93*, 14895-900.
- Doetsch, F., Caille, I., Lim, D. A., Garcia-Verdugo, J. M., and Alvarez-Buylla, A. (1999a). Subventricular zone astrocytes are neural stem cells in the adult mammalian brain. *Cell* *97*, 703-16.
- Doetsch, F., Garcia-Verdugo, J. M., and Alvarez-Buylla, A. (1997). Cellular composition and three-dimensional organization of the subventricular germinal zone in the adult mammalian brain. *J Neurosci* *17*, 5046-61.
- Doetsch, F., Garcia-Verdugo, J. M., and Alvarez-Buylla, A. (1999b). Regeneration of a germinal layer in the adult mammalian brain. *Proc Natl Acad Sci U S A* *96*, 11619-24.
- Doetsch, F., Petreanu, L., Caille, I., Garcia-Verdugo, J. M., and Alvarez-Buylla, A. (2002). EGF converts transit-amplifying neurogenic precursors in the adult brain into multipotent stem cells. *Neuron* *36*, 1021-34.
- Durbec, P., and Cremer, H. (2001). Revisiting the function of PSA-NCAM in the nervous system. *Mol Neurobiol* *24*, 53-64.
- Eckhardt, M., Bukalo, O., Chazal, G., Wang, L., Goridis, C., Schachner, M., Gerardy-Schahn, R., Cremer, H., and Dityatev, A. (2000). Mice deficient in the polysialyltransferase ST8SiaIV/PST-1 allow discrimination of the roles of neural cell adhesion molecule protein and polysialic acid in neural development and synaptic plasticity. *J Neurosci* *20*, 5234-44.
- Eisenstat, D. D., Liu, J. K., Mione, M., Zhong, W., Yu, G., Anderson, S. A., Ghattas, I., Puelles, L., and Rubenstein, J. L. (1999). DLX-1, DLX-2, and DLX-5 expression define distinct stages of basal forebrain differentiation. *J Comp Neurol* *414*, 217-37.
- Eriksson, P. S., Perfilieva, E., Bjork-Eriksson, T., Alborn, A. M., Nordborg, C., Peterson, D. A., and Gage, F. H. (1998). Neurogenesis in the adult human hippocampus. *Nat Med* *4*, 1313-7.
- Estivill-Torrus, G., Pearson, H., van Heyningen, V., Price, D. J., and Rashbass, P. (2002). Pax6 is required to regulate the cell cycle and the rate of progression from symmetrical to asymmetrical division in mammalian cortical progenitors. *Development* *129*, 455-66.
- Evan, G. I., Brown, L., Whyte, M., and Harrington, E. (1995). Apoptosis and the cell cycle. *Curr Opin Cell Biol* *7*, 825-34.

- Fallon, J., Reid, S., Kinyamu, R., Opole, I., Opole, R., Baratta, J., Korc, M., Endo, T. L., Duong, A., Nguyen, G., Karkehabadhi, M., Twardzik, D., Patel, S., and Loughlin, S. (2000). In vivo induction of massive proliferation, directed migration, and differentiation of neural cells in the adult mammalian brain. *Proc Natl Acad Sci U S A* *97*, 14686-91.
- Falquet, L., Pagni, M., Bucher, P., Hulo, N., Sigrist, C. J., Hofmann, K., and Bairoch, A. (2002). The PROSITE database, its status in 2002. *Nucleic Acids Res* *30*, 235-8.
- Flechon, J. E., Degrouard, J., Flechon, B., Lefevre, F., and Traub, O. (2004). Gap junction formation and connexin distribution in pig trophoblast before implantation. *Placenta* *25*, 85-94.
- Frazier-Cierpial, L., and Brunjes, P. C. (1989). Early postnatal cellular proliferation and survival in the olfactory bulb and rostral migratory stream of normal and unilaterally odor-deprived rats. *J Comp Neurol* *289*, 481-92.
- Furuta, A., Rothstein, J. D., and Martin, L. J. (1997). Glutamate transporter protein subtypes are expressed differentially during rat CNS development. *J Neurosci* *17*, 8363-75.
- Gage, F. H. (2000). Mammalian neural stem cells. *Science* *287*, 1433-8.
- Gage, F. H., Coates, P. W., Palmer, T. D., Kuhn, H. G., Fisher, L. J., Suhonen, J. O., Peterson, D. A., Suhr, S. T., and Ray, J. (1995). Survival and differentiation of adult neuronal progenitor cells transplanted to the adult brain. *Proc Natl Acad Sci U S A* *92*, 11879-83.
- Garcia-Verdugo, J. M., Ferron, S., Flames, N., Collado, L., Desfilis, E., and Font, E. (2002). The proliferative ventricular zone in adult vertebrates: a comparative study using reptiles, birds, and mammals. *Brain Res Bull* *57*, 765-75.
- Gheusi, G., Cremer, H., McLean, H., Chazal, G., Vincent, J. D., and Lledo, P. M. (2000). Importance of newly generated neurons in the adult olfactory bulb for odor discrimination. *Proc Natl Acad Sci U S A* *97*, 1823-8.
- Ghirnikar, R. S., Lee, Y. L., He, T. R., and Eng, L. F. (1996). Chemokine expression in rat stab wound brain injury. *J Neurosci Res* *46*, 727-33.
- Gleeson, J. G., Lin, P. T., Flanagan, L. A., and Walsh, C. A. (1999). Doublecortin is a microtubule-associated protein and is expressed widely by migrating neurons. *Neuron* *23*, 257-71.
- Goldman, S. A., and Nottebohm, F. (1983). Neuronal production, migration, and differentiation in a vocal control nucleus of the adult female canary brain. *Proc Natl Acad Sci U S A* *80*, 2390-4.
- Goodell, M. A., Brose, K., Paradis, G., Conner, A. S., and Mulligan, R. C. (1996). Isolation and functional properties of murine hematopoietic stem cells that are replicating in vivo. *J Exp Med* *183*, 1797-806.

- Graham, V., Khudyakov, J., Ellis, P., and Pevny, L. (2003). SOX2 functions to maintain neural progenitor identity. *Neuron* 39, 749-65.
- Gray, G. E., and Sanes, J. R. (1991). Migratory paths and phenotypic choices of clonally related cells in the avian optic tectum. *Neuron* 6, 211-25.
- Gritti, A., Bonfanti, L., Doetsch, F., Caille, I., Alvarez-Buylla, A., Lim, D. A., Galli, R., Verdugo, J. M., Herrera, D. G., and Vescovi, A. L. (2002). Multipotent neural stem cells reside into the rostral extension and olfactory bulb of adult rodents. *J Neurosci* 22, 437-45.
- Gritti, A., Frolichsthal-Schoeller, P., Galli, R., Parati, E. A., Cova, L., Pagano, S. F., Bjornson, C. R., and Vescovi, A. L. (1999). Epidermal and fibroblast growth factors behave as mitogenic regulators for a single multipotent stem cell-like population from the subventricular region of the adult mouse forebrain. *J Neurosci* 19, 3287-97.
- Gritti, A., Parati, E. A., Cova, L., Frolichsthal, P., Galli, R., Wanke, E., Faravelli, L., Morassutti, D. J., Roisen, F., Nickel, D. D., and Vescovi, A. L. (1996). Multipotential stem cells from the adult mouse brain proliferate and self-renew in response to basic fibroblast growth factor. *J Neurosci* 16, 1091-100.
- Groszer, M., Erickson, R., Scripture-Adams, D. D., Lesche, R., Trumpp, A., Zack, J. A., Kornblum, H. I., Liu, X., and Wu, H. (2001). Negative regulation of neural stem/progenitor cell proliferation by the Pten tumor suppressor gene in vivo. *Science* 294, 2186-9. Epub 2001 Nov 1.
- Gunnarsen, J. M., Augustine, C., Spirkoska, V., Kim, M., Brown, M., and Tan, S. S. (2002). Global analysis of gene expression patterns in developing mouse neocortex using serial analysis of gene expression. *Mol Cell Neurosci* 19, 560-73.
- Guo, Y., Costa, R., Ramsey, H., Starnes, T., Vance, G., Robertson, K., Kelley, M., Reinbold, R., Scholer, H., and Hromas, R. (2002). The embryonic stem cell transcription factors Oct-4 and FoxD3 interact to regulate endodermal-specific promoter expression. *Proc Natl Acad Sci U S A* 99, 3663-7. Epub 2002 Mar 12.
- Guttinger, M., Sutti, F., Panigada, M., Porcellini, S., Merati, B., Mariani, M., Teesalu, T., Consalez, G. G., and Grassi, F. (1998). Epithelial V-like antigen (EVA), a novel member of the immunoglobulin superfamily, expressed in embryonic epithelia with a potential role as homotypic adhesion molecule in thymus histogenesis. *J Cell Biol* 141, 1061-71.
- Hack, I., Bancila, M., Loulier, K., Carroll, P., and Cremer, H. (2002). Reelin is a detachment signal in tangential chain-migration during postnatal neurogenesis. *Nat Neurosci* 5, 939-45.
- Hack, M. A., Sugimori, M., Lundberg, C., Nakafuku, M., and Gotz, M. (2004). Regionalization and fate specification in neurospheres: the role of Olig2 and Pax6. *Mol Cell Neurosci* 25, 664-78.
- Hogan, B., Beddington, R., Costantini, F., and Lacy, E. (1994). *Manipulating the mouse embryo.*, 2nd Ed. Edition: Cold Spring Harbor Laboratory Press).

- Hu, H. (1999). Chemorepulsion of neuronal migration by Slit2 in the developing mammalian forebrain. *Neuron* 23, 703-11.
- Hu, H. (2000). Polysialic acid regulates chain formation by migrating olfactory interneuron precursors. *J Neurosci Res* 61, 480-92.
- Hughes, E. G., Maguire, J. L., McMinn, M. T., Scholz, R. E., and Sutherland, M. L. (2004). Loss of glial fibrillary acidic protein results in decreased glutamate transport and inhibition of PKA-induced EAAT2 cell surface trafficking. *Brain Res Mol Brain Res* 124, 114-23.
- Imura, T., Kornblum, H. I., and Sofroniew, M. V. (2003). The predominant neural stem cell isolated from postnatal and adult forebrain but not early embryonic forebrain expresses GFAP. *J Neurosci* 23, 2824-32.
- Ishii, Y., Nakamura, S., and Osumi, N. (2000). Demarcation of early mammalian cortical development by differential expression of fringe genes. *Brain Res Dev Brain Res* 119, 307-20.
- Ivanova, N. B., Dimos, J. T., Schaniel, C., Hackney, J. A., Moore, K. A., and Lemischka, I. R. (2002). A Stem Cell Molecular Signature. *Science* 12, 12.
- Jacobson, M. D., Weil, M., and Raff, M. C. (1997). Programmed cell death in animal development. *Cell* 88, 347-54.
- Jin, K., Minami, M., Lan, J. Q., Mao, X. O., Bateur, S., Simon, R. P., and Greenberg, D. A. (2001). Neurogenesis in dentate subgranular zone and rostral subventricular zone after focal cerebral ischemia in the rat. *Proc Natl Acad Sci U S A* 98, 4710-5.
- Johansson, C. B., Momma, S., Clarke, D. L., Risling, M., Lendahl, U., and Frisen, J. (1999). Identification of a neural stem cell in the adult mammalian central nervous system. *Cell* 96, 25-34.
- Josephson, R., Muller, T., Pickel, J., Okabe, S., Reynolds, K., Turner, P. A., Zimmer, A., and McKay, R. D. (1998). POU transcription factors control expression of CNS stem cell-specific genes. *Development* 125, 3087-100.
- Kawamura, K., Sato, N., Fukuda, J., Kodama, H., Kumagai, J., Tanikawa, H., Shimizu, Y., and Tanaka, T. (2003). Survivin acts as an antiapoptotic factor during the development of mouse preimplantation embryos. *Dev Biol* 256, 331-41.
- Kee, N. J., Preston, E., and Wojtowicz, J. M. (2001). Enhanced neurogenesis after transient global ischemia in the dentate gyrus of the rat. *Exp Brain Res* 136, 313-20.
- Kempermann, G. (2002). Why new neurons? Possible functions for adult hippocampal neurogenesis. *J Neurosci* 22, 635-8.
- Kim, J., Lo, L., Dormand, E., and Anderson, D. J. (2003). SOX10 maintains multipotency and inhibits neuronal differentiation of neural crest stem cells. *Neuron* 38, 17-31.

- Kim, M., and Morshead, C. M. (2003). Distinct populations of forebrain neural stem and progenitor cells can be isolated using side-population analysis. *J Neurosci* 23, 10703-9.
- Knoepfler, P. S., Cheng, P. F., and Eisenman, R. N. (2002). N-myc is essential during neurogenesis for the rapid expansion of progenitor cell populations and the inhibition of neuronal differentiation. *Genes Dev* 16, 2699-712.
- Kontgen, F., Suss, G., Stewart, C., Steinmetz, M., and Bluethmann, H. (1993). Targeted disruption of the MHC class II Aa gene in C57BL/6 mice. *Int Immunol* 5, 957-64.
- Kuhlbrodt, K., Herbarth, B., Sock, E., Enderich, J., Hermans-Borgmeyer, I., Wegner, M., Uwanogho, D., Rex, M., Cartwright, E. J., Pearl, G., Healy, C., Scotting, P. J., and Sharpe, P. T. (1998). Cooperative function of POU proteins and SOX proteins in glial cells  
Embryonic expression of the chicken Sox2, Sox3 and Sox11 genes suggests an interactive role in neuronal development. *J Biol Chem* 273, 16050-7.
- Kurosawa, N., Yoshida, Y., Kojima, N., and Tsuji, S. (1997). Polysialic acid synthase (ST8Sia II/STX) mRNA expression in the developing mouse central nervous system. *J Neurochem* 69, 494-503.
- Laywell, E. D., Rakic, P., Kukekov, V. G., Holland, E. C., and Steindler, D. A. (2000). Identification of a multipotent astrocytic stem cell in the immature and adult mouse brain. *Proc Natl Acad Sci U S A* 97, 13883-8.
- Lazarini, F., Tham, T. N., Casanova, P., Arenzana-Seisdedos, F., and Dubois-Dalcq, M. (2003). Role of the alpha-chemokine stromal cell-derived factor (SDF-1) in the developing and mature central nervous system. *Glia* 42, 139-48.
- Lendahl, U., Zimmerman, L. B., and McKay, R. D. (1990). CNS stem cells express a new class of intermediate filament protein. *Cell* 60, 585-95.
- Li, F., Ambrosini, G., Chu, E. Y., Plescia, J., Tognin, S., Marchisio, P. C., and Altieri, D. C. (1998). Control of apoptosis and mitotic spindle checkpoint by survivin. *Nature* 396, 580-4.
- Li, M., Zhao, C., Wang, Y., Zhao, Z., and Meng, A. (2002). Zebrafish sox9b is an early neural crest marker. *Dev Genes Evol* 212, 203-6.
- Lie, D. C., Song, H., Colamarino, S. A., Ming, G. L., and Gage, F. H. (2004). Neurogenesis in the adult brain: new strategies for central nervous system diseases. *Annu Rev Pharmacol Toxicol* 44, 399-421.
- Lim, D. A., and Alvarez-Buylla, A. (1999). Interaction between astrocytes and adult subventricular zone precursors stimulates neurogenesis. *Proc Natl Acad Sci U S A* 96, 7526-31.
- Lim, D. A., Fishell, G. J., and Alvarez-Buylla, A. (1997). Postnatal mouse subventricular zone neuronal precursors can migrate and differentiate within multiple levels of the developing neuraxis. *Proc Natl Acad Sci U S A* 94, 14832-6.

- Lim, D. A., Tramontin, A. D., Trevejo, J. M., Herrera, D. G., Garcia-Verdugo, J. M., and Alvarez-Buylla, A. (2000). Noggin antagonizes BMP signaling to create a niche for adult neurogenesis. *Neuron* *28*, 713-26.
- Livingston, B. D., and Paulson, J. C. (1993). Polymerase chain reaction cloning of a developmentally regulated member of the sialyltransferase gene family. *J Biol Chem* *268*, 11504-7.
- Lois, C., and Alvarez-Buylla, A. (1994). Long-distance neuronal migration in the adult mammalian brain. *Science* *264*, 1145-8.
- Lois, C., Garcia-Verdugo, J. M., and Alvarez-Buylla, A. (1996). Chain migration of neuronal precursors. *Science* *271*, 978-81.
- Lovell-Badge, R. (2001). The future for stem cell research. *Nature* *414*, 88-91.
- Lowe, G. (2003). Electrical signaling in the olfactory bulb. *Curr Opin Neurobiol* *13*, 476-81.
- Luskin, M. B. (1993). Restricted proliferation and migration of postnatally generated neurons derived from the forebrain subventricular zone. *Neuron* *11*, 173-89.
- Mahadeva, H., Brooks, G., Lodwick, D., Chong, N. W., and Samani, N. J. (2002). ms1, a novel stress-responsive, muscle-specific gene that is up-regulated in the early stages of pressure overload-induced left ventricular hypertrophy. *FEBS Lett* *521*, 100-4.
- Martin, G. R. (1980). Teratocarcinomas and mammalian embryogenesis. *Science* *209*, 768-76.
- Menezes, J. R., Smith, C. M., Nelson, K. C., and Luskin, M. B. (1995). The division of neuronal progenitor cells during migration in the neonatal mammalian forebrain. *Mol Cell Neurosci* *6*, 496-508.
- Mercier, F., Kitasako, J. T., and Hatton, G. I. (2002). Anatomy of the brain neurogenic zones revisited: fractones and the fibroblast/macrophage network. *J Comp Neurol* *451*, 170-88.
- Miettinen, R., Gulyas, A. I., Baimbridge, K. G., Jacobowitz, D. M., and Freund, T. F. (1992). Calretinin is present in non-pyramidal cells of the rat hippocampus-II. Co-existence with other calcium binding proteins and GABA. *Neuroscience* *48*, 29-43.
- Mitsui, K., Tokuzawa, Y., Itoh, H., Segawa, K., Murakami, M., Takahashi, K., Maruyama, M., Maeda, M., and Yamanaka, S. (2003). The homeoprotein Nanog is required for maintenance of pluripotency in mouse epiblast and ES cells. *Cell* *113*, 631-42.
- Miyagi, S., Saito, T., Mizutani, K., Masuyama, N., Gotoh, Y., Iwama, A., Nakauchi, H., Masui, S., Niwa, H., Nishimoto, M., Muramatsu, M., and Okuda, A. (2004). The Sox-2 regulatory regions display their activities in two distinct types of multipotent stem cells. *Mol Cell Biol* *24*, 4207-20.
- Mollaaghababa, R., and Pavan, W. J. (2003). The importance of having your SOX on: role of SOX10( dagger ) in the development of neural crest-derived melanocytes and glia. *Oncogene* *22*, 3024-34.

- Monaghan, A. P., Grau, E., Bock, D., and Schutz, G. (1995). The mouse homolog of the orphan nuclear receptor *tailless* is expressed in the developing forebrain. *Development* *121*, 839-53.
- Morshead, C. M., Benveniste, P., Iscove, N. N., and van der Kooy, D. (2002). Hematopoietic competence is a rare property of neural stem cells that may depend on genetic and epigenetic alterations. *Nat Med* *8*, 268-73.
- Morshead, C. M., Craig, C. G., and van der Kooy, D. (1998). In vivo clonal analyses reveal the properties of endogenous neural stem cell proliferation in the adult mammalian forebrain. *Development* *125*, 2251-61.
- Morshead, C. M., Garcia, A. D., Sofroniew, M. V., and van Der Kooy, D. (2003). The ablation of glial fibrillary acidic protein-positive cells from the adult central nervous system results in the loss of forebrain neural stem cells but not retinal stem cells. *Eur J Neurosci* *18*, 76-84.
- Morshead, C. M., Reynolds, B. A., Craig, C. G., McBurney, M. W., Staines, W. A., Morassutti, D., Weiss, S., and van der Kooy, D. (1994). Neural stem cells in the adult mammalian forebrain: a relatively quiescent subpopulation of subependymal cells. *Neuron* *13*, 1071-82.
- Morshead, C. M., and van der Kooy, D. (2000). A cell-survival factor (N-acetyl-L-cysteine) alters the in vivo fate of constitutively proliferating subependymal cells in the adult forebrain. *J Neurobiol* *42*, 338-46.
- Morshead, C. M., and van der Kooy, D. (2004). Disguising adult neural stem cells. *Curr Opin Neurobiol* *14*, 125-31.
- Morshead, C. M., and van der Kooy, D. (1992). Postmitotic death is the fate of constitutively proliferating cells in the subependymal layer of the adult mouse brain. *J Neurosci* *12*, 249-56.
- Murase, S., and Horwitz, A. F. (2002). Deleted in colorectal carcinoma and differentially expressed integrins mediate the directional migration of neural precursors in the rostral migratory stream. *J Neurosci* *22*, 3568-79.
- Murayama, A., Matsuzaki, Y., Kawaguchi, A., Shimazaki, T., and Okano, H. (2002). Flow cytometric analysis of neural stem cells in the developing and adult mouse brain. *J Neurosci Res* *69*, 837-47.
- Nait-Oumesmar, B., Decker, L., Lachapelle, F., Avellana-Adalid, V., Bachelin, C., and Van Evercooren, A. B. (1999). Progenitor cells of the adult mouse subventricular zone proliferate, migrate and differentiate into oligodendrocytes after demyelination. *Eur J Neurosci* *11*, 4357-66.
- Nakatomi, H., Kuriu, T., Okabe, S., Yamamoto, S., Hatano, O., Kawahara, N., Tamura, A., Kirino, T., and Nakafuku, M. (2002). Regeneration of hippocampal pyramidal neurons after ischemic brain injury by recruitment of endogenous neural progenitors. *Cell* *110*, 429-41.



- Nguyen-Ba-Charvet, K. T., Picard-Riera, N., Tessier-Lavigne, M., Baron-Van Evercooren, A., Sotelo, C., and Chedotal, A. (2004). Multiple roles for slits in the control of cell migration in the rostral migratory stream. *J Neurosci* 24, 1497-506.
- Nichols, J., Zevnik, B., Anastassiadis, K., Niwa, H., Klewe-Nebenius, D., Chambers, I., Scholer, H., and Smith, A. (1998). Formation of pluripotent stem cells in the mammalian embryo depends on the POU transcription factor Oct4. *Cell* 95, 379-91.
- Niwa, H., Miyazaki, J., and Smith, A. G. (2000). Quantitative expression of Oct-3/4 defines differentiation, dedifferentiation or self-renewal of ES cells. *Nat Genet* 24, 372-6.
- O'Connor, D. S., Grossman, D., Plescia, J., Li, F., Zhang, H., Villa, A., Tognin, S., Marchisio, P. C., and Altieri, D. C. (2000). Regulation of apoptosis at cell division by p34cdc2 phosphorylation of survivin. *Proc Natl Acad Sci U S A* 97, 13103-7.
- Ong, E., Nakayama, J., Angata, K., Reyes, L., Katsuyama, T., Arai, Y., Fukuda, M., Kurosawa, N., Yoshida, Y., Kojima, N., and Tsuji, S. (1998). Developmental regulation of polysialic acid synthesis in mouse directed by two polysialyltransferases, PST and STX Polysialic acid synthase (ST8Sia II/STX) mRNA expression in the developing mouse central nervous system. *Glycobiology* 8, 415-24.
- Ono, K., Tomasiewicz, H., Magnuson, T., and Rutishauser, U. (1994). N-CAM mutation inhibits tangential neuronal migration and is phenocopied by enzymatic removal of polysialic acid. *Neuron* 13, 595-609.
- Palacin, M., Estevez, R., Bertran, J., and Zorzano, A. (1998). Molecular biology of mammalian plasma membrane amino acid transporters. *Physiol Rev* 78, 969-1054.
- Palmer, T. D., Markakis, E. A., Willhoite, A. R., Safar, F., and Gage, F. H. (1999). Fibroblast growth factor-2 activates a latent neurogenic program in neural stem cells from diverse regions of the adult CNS. *J Neurosci* 19, 8487-97.
- Palmer, T. D., Willhoite, A. R., Gage, F. H., Markakis, E. A., and Safar, F. (2000). Vascular niche for adult hippocampal neurogenesis
- Panganiban, G., and Rubenstein, J. L. (2002). Developmental functions of the Distal-less/Dlx homeobox genes. *Development* 129, 4371-86.
- Pennartz, S., Belvindrah, R., Tomiuk, S., Zimmer, C., Hofmann, K., Conradt, M., Bosio, A., and Cremer, H. (2004). Purification of neuronal precursors from the adult mouse brain: comprehensive gene expression analysis provides new insights into the control of cell migration, differentiation, and homeostasis. *Mol Cell Neurosci* 25, 692-706.
- Perera, M., Merlo, G. R., Verardo, S., Paleari, L., Corte, G., and Levi, G. (2004). Defective neurogenesis in the absence of Dlx5. *Mol Cell Neurosci* 25, 153-61.
- Petreanu, L., and Alvarez-Buylla, A. (2002). Maturation and death of adult-born olfactory bulb granule neurons: role of olfaction. *J Neurosci* 22, 6106-13.
- Pevny, L., and Rao, M. S. (2003). The stem-cell menagerie. *Trends Neurosci* 26, 351-9.

- Plum, A., Hallas, G., and Willecke, K. (2002). Expression of the mouse gap junction gene *Gjb3* is regulated by distinct mechanisms in embryonic stem cells and keratinocytes. *Genomics* 79, 24-30.
- Plum, A., Winterhager, E., Pesch, J., Lautermann, J., Hallas, G., Rosentreter, B., Traub, O., Herberhold, C., and Willecke, K. (2001). Connexin31-deficiency in mice causes transient placental dysmorphogenesis but does not impair hearing and skin differentiation. *Dev Biol* 231, 334-47.
- Porteus, M. H., Bulfone, A., Liu, J. K., Puelles, L., Lo, L. C., and Rubenstein, J. L. (1994). DLX-2, MASH-1, and MAP-2 expression and bromodeoxyuridine incorporation define molecularly distinct cell populations in the embryonic mouse forebrain. *J Neurosci* 14, 6370-83.
- Rakic, P. (1972). Mode of cell migration to the superficial layers of fetal monkey neocortex. *J Comp Neurol* 145, 61-83.
- Rakic, P. (2004). Neuroscience: immigration denied. *Nature* 427, 685-6.
- Ramalho-Santos, M., Yoon, S., Matsuzaki, Y., Mulligan, R. C., and Melton, D. A. (2002). "Stemness": transcriptional profiling of embryonic and adult stem cells. *Science* 298, 597-600.
- Reed, J. C. (2001). The Survivin saga goes in vivo. *J Clin Invest* 108, 965-9.
- Rex, M., Church, R., Tointon, K., Ichihashi, R. M., Mokhtar, S., Uwanogho, D., Sharpe, P. T., and Scotting, P. J. (1998). Granule cell development in the cerebellum is punctuated by changes in Sox gene expression. *Brain Res Mol Brain Res* 55, 28-34.
- Reynolds, B. A., and Weiss, S. (1996). Clonal and population analyses demonstrate that an EGF-responsive mammalian embryonic CNS precursor is a stem cell. *Dev Biol* 175, 1-13.
- Reynolds, B. A., and Weiss, S. (1992). Generation of neurons and astrocytes from isolated cells of the adult mammalian central nervous system. *Science* 255, 1707-10.
- Richards, M., Tan, S. P., Tan, J. H., Chan, W. K., and Bongso, A. (2004). The transcriptome profile of human embryonic stem cells as defined by SAGE. *Stem Cells* 22, 51-64.
- Riethmacher, D., Brinkmann, V., and Birchmeier, C. (1995). A targeted mutation in the mouse E-cadherin gene results in defective preimplantation development. *Proc Natl Acad Sci U S A* 92, 855-9.
- Rietze, R. L., Valcanis, H., Brooker, G. F., Thomas, T., Voss, A. K., and Bartlett, P. F. (2001). Purification of a pluripotent neural stem cell from the adult mouse brain. *Nature* 412, 736-9.
- Robinson, M. B. (1998). The family of sodium-dependent glutamate transporters: a focus on the GLT-1/EAAT2 subtype. *Neurochem Int* 33, 479-91.

- Rothstein, J. D., Martin, L., Levey, A. I., Dykes-Hoberg, M., Jin, L., Wu, D., Nash, N., and Kunch, R. W. (1994). Localization of neuronal and glial glutamate transporters. *Neuron* *13*, 713-25.
- Rougon, G., Alterman, L. A., Dennis, K., Guo, X. J., and Kinnon, C. (1991). The murine heat-stable antigen: a differentiation antigen expressed in both the hematolymphoid and neural cell lineages. *Eur J Immunol* *21*, 1397-402.
- Rougon, G., Dubois, C., Buckley, N., Magnani, J. L., and Zollinger, W. (1986). A monoclonal antibody against meningococcus group B polysaccharides distinguishes embryonic from adult N-CAM. *J Cell Biol* *103*, 2429-37.
- Rousselot, P., Lois, C., and Alvarez-Buylla, A. (1995). Embryonic (PSA) N-CAM reveals chains of migrating neuroblasts between the lateral ventricle and the olfactory bulb of adult mice. *J Comp Neurol* *351*, 51-61.
- Rutishauser, U., and Landmesser, L. (1996). Polysialic acid in the vertebrate nervous system: a promoter of plasticity in cell-cell interactions. *Trends Neurosci* *19*, 422-7.
- Saghatelian, A., de Chevigny, A., Schachner, M., and Lledo, P. M. (2004). Tenascin-R mediates activity-dependent recruitment of neuroblasts in the adult mouse forebrain. *Nat Neurosci* *7*, 347-56. Epub 2004 Mar 14.
- Sakakibara, S., Nakamura, Y., Satoh, H., and Okano, H. (2001). Rna-binding protein Musashi2: developmentally regulated expression in neural precursor cells and subpopulations of neurons in mammalian CNS. *J Neurosci* *21*, 8091-107.
- Sambrook, J., Fritsch, E. F., and Maniatis, T. (1989). *Molecular cloning. A laboratory manual.*, 2nd edition Edition: Cold Spring Harbor Laboratory Press,).
- Sanai, N., Tramontin, A. D., Quinones-Hinojosa, A., Barbaro, N. M., Gupta, N., Kunwar, S., Lawton, M. T., McDermott, M. W., Parsa, A. T., Manuel-Garcia Verdugo, J., Berger, M. S., and Alvarez-Buylla, A. (2004). Unique astrocyte ribbon in adult human brain contains neural stem cells but lacks chain migration. *Nature* *427*, 740-4.
- Schaeren-Wiemers, N., and Gerfin-Moser, A. (1993). A single protocol to detect transcripts of various types and expression levels in neural tissue and cultured cells: in situ hybridization using digoxigenin-labelled cRNA probes. *Histochemistry* *100*, 431-40.
- Scharenberg, C. W., Harkey, M. A., and Torok-Storb, B. (2002). The ABCG2 transporter is an efficient Hoechst 33342 efflux pump and is preferentially expressed by immature human hematopoietic progenitors. *Blood* *99*, 507-12.
- Schluter, K., Figiel, M., Rozyczka, J., and Engele, J. (2002). CNS region-specific regulation of glial glutamate transporter expression. *Eur J Neurosci* *16*, 836-42.
- Seaberg, R. M., and van der Kooy, D. (2002). Adult rodent neurogenic regions: the ventricular subependyma contains neural stem cells, but the dentate gyrus contains restricted progenitors. *J Neurosci* *22*, 1784-93.

- Sefton, M., Johnson, M. H., and Clayton, L. (1992). Synthesis and phosphorylation of uvomorulin during mouse early development. *Development* *115*, 313-8.
- Serafini, T. (1999). Of neurons and gene chips. *Curr Opin Neurobiol* *9*, 641-4.
- Seri, B., Garcia-Verdugo, J. M., McEwen, B. S., and Alvarez-Buylla, A. (2001). Astrocytes give rise to new neurons in the adult mammalian hippocampus. *J Neurosci* *21*, 7153-60.
- Shen, Q., Goderie, S. K., Jin, L., Karanth, N., Sun, Y., Abramova, N., Vincent, P., Pumiglia, K., and Temple, S. (2004). Endothelial cells stimulate self-renewal and expand neurogenesis of neural stem cells. *Science* *304*, 1338-40. Epub 2004 Apr 1.
- Shi, Y., Chichung Lie, D., Taupin, P., Nakashima, K., Ray, J., Yu, R. T., Gage, F. H., and Evans, R. M. (2004). Expression and function of orphan nuclear receptor TLX in adult neural stem cells. *Nature* *427*, 78-83.
- Shibata, T., Watanabe, M., Tanaka, K., Wada, K., and Inoue, Y. (1996). Dynamic changes in expression of glutamate transporter mRNAs in developing brain. *Neuroreport* *7*, 705-9.
- Shimizu, K., Chiba, S., Saito, T., Kumano, K., Takahashi, T., and Hirai, H. (2001). Manic fringe and lunatic fringe modify different sites of the Notch2 extracellular region, resulting in different signaling modulation. *J Biol Chem* *276*, 25753-8.
- Simeone, A., Acampora, D., Pannese, M., D'Esposito, M., Stornaiuolo, A., Gulisano, M., Mallamaci, A., Kastury, K., Druck, T., Huebner, K., and et al. (1994). Cloning and characterization of two members of the vertebrate Dlx gene family. *Proc Natl Acad Sci U S A* *91*, 2250-4.
- Song, H., Stevens, C. F., and Gage, F. H. (2002). Astroglia induce neurogenesis from adult neural stem cells. *Nature* *417*, 39-44.
- Song, H. J., Stevens, C. F., and Gage, F. H. (2002). Neural stem cells from adult hippocampus develop essential properties of functional CNS neurons. *Nat Neurosci* *5*, 438-45.
- Soosaar, A., Chiaramello, A., Zuber, M. X., and Neuman, T. (1994). Expression of basic-helix-loop-helix transcription factor ME2 during brain development and in the regions of neuronal plasticity in the adult brain. *Brain Res Mol Brain Res* *25*, 176-80.
- Spokony, R. F., Aoki, Y., Saint-Germain, N., Magner-Fink, E., and Saint-Jeannet, J. P. (2002). The transcription factor Sox9 is required for cranial neural crest development in *Xenopus*. *Development* *129*, 421-32.
- Spradling, A., Drummond-Barbosa, D., and Kai, T. (2001). Stem cells find their niche. *Nature* *414*, 98-104.
- St Croix, B., Rago, C., Velculescu, V., Traverso, G., Romans, K. E., Montgomery, E., Lal, A., Riggins, G. J., Lengauer, C., Vogelstein, B., and Kinzler, K. W. (2000). Genes expressed in human tumor endothelium. *Science* *289*, 1197-202.

- Stewart, R. R., Zigova, T., and Luskin, M. B. (1999). Potassium currents in precursor cells isolated from the anterior subventricular zone of the neonatal rat forebrain. *J Neurophysiol* *81*, 95-102.
- Stumm, R. K., Zhou, C., Ara, T., Lazarini, F., Dubois-Dalcq, M., Nagasawa, T., Holtt, V., and Schulz, S. (2003). CXCR4 regulates interneuron migration in the developing neocortex. *J Neurosci* *23*, 5123-30.
- Stump, G., Durrer, A., Klein, A., Lutolf, S., Suter, U., and Taylor, V. (2002). Notch1 and its ligands Delta-like and Jagged are expressed and active in distinct cell populations in the postnatal mouse brain. *Mech Dev* *114*, 153.
- Su, A. I., Cooke, M. P., Ching, K. A., Hakak, Y., Walker, J. R., Wiltshire, T., Orth, A. P., Vega, R. G., Sapinoso, L. M., Moqrich, A., Patapoutian, A., Hampton, G. M., Schultz, P. G., and Hogenesch, J. B. (2002). Large-scale analysis of the human and mouse transcriptomes. *Proc Natl Acad Sci U S A* *99*, 4465-70. Epub 2002 Mar 19.
- Suhonen, J. O., Peterson, D. A., Ray, J., and Gage, F. H. (1996). Differentiation of adult hippocampus-derived progenitors into olfactory neurons in vivo. *Nature* *383*, 624-7.
- Sutherland, M. L., Delaney, T. A., and Noebels, J. L. (1996). Glutamate transporter mRNA expression in proliferative zones of the developing and adult murine CNS. *J Neurosci* *16*, 2191-207.
- Swanson, R. A., Liu, J., Miller, J. W., Rothstein, J. D., Farrell, K., Stein, B. A., and Longuemare, M. C. (1997). Neuronal regulation of glutamate transporter subtype expression in astrocytes. *J Neurosci* *17*, 932-40.
- Szele, F. G., Chin, H. K., Rowson, M. A., and Cepko, C. L. (2002). Sox-9 and cDachsund-2 expression in the developing chick telencephalon. *Mech Dev* *112*, 179-82.
- Talamillo, A., Quinn, J. C., Collinson, J. M., Caric, D., Price, D. J., West, J. D., and Hill, R. E. (2003). Pax6 regulates regional development and neuronal migration in the cerebral cortex. *Dev Biol* *255*, 151-63.
- Tanaka, K., Watase, K., Manabe, T., Yamada, K., Watanabe, M., Takahashi, K., Iwama, H., Nishikawa, T., Ichihara, N., Kikuchi, T., Okuyama, S., Kawashima, N., Hori, S., Takimoto, M., Wada, K., Shibata, T., and Inoue, Y. (1997). Epilepsy and exacerbation of brain injury in mice lacking the glutamate transporter GLT-1  
Dynamic changes in expression of glutamate transporter mRNAs in developing brain. *Science* *276*, 1699-702.
- Teesalu, T., Grassi, F., and Guttinger, M. (1998). Expression pattern of the epithelial v-like antigen (Eva) transcript suggests a possible role in placental morphogenesis. *Dev Genet* *23*, 317-23.
- Tetsuka, K., Takanaga, H., Ohtsuki, S., Hosoya, K., and Terasaki, T. (2003). The l-isomer-selective transport of aspartic acid is mediated by ASCT2 at the blood-brain barrier. *J Neurochem* *87*, 891-901.

- Tiveron, M. C., Hirsch, M. R., and Brunet, J. F. (1996). The expression pattern of the transcription factor Phox2 delineates synaptic pathways of the autonomic nervous system. *J Neurosci* *16*, 7649-60.
- Tomioka, M., Nishimoto, M., Miyagi, S., Katayanagi, T., Fukui, N., Niwa, H., Muramatsu, M., and Okuda, A. (2002). Identification of Sox-2 regulatory region which is under the control of Oct-3/4-Sox-2 complex. *Nucleic Acids Res* *30*, 3202-13.
- Tomiuk, S., and Hofmann, K. (2001). Microarray probe selection strategies. *Brief Bioinform* *2*, 329-40.
- Toresson, H., Parmar, M., and Campbell, K. (2000). Expression of Meis and Pbx genes and their protein products in the developing telencephalon: implications for regional differentiation. *Mech Dev* *94*, 183-7.
- Tyas, D. A., Pearson, H., Rashbass, P., and Price, D. J. (2003). Pax6 regulates cell adhesion during cortical development. *Cereb Cortex* *13*, 612-9.
- Uchida, N., Buck, D. W., He, D., Reitsma, M. J., Masek, M., Phan, T. V., Tsukamoto, A. S., Gage, F. H., and Weissman, I. L. (2000). Direct isolation of human central nervous system stem cells. *Proc Natl Acad Sci U S A* *97*, 14720-5.
- Uren, A. G., Wong, L., Pakusch, M., Fowler, K. J., Burrows, F. J., Vaux, D. L., and Choo, K. H. (2000). Survivin and the inner centromere protein INCENP show similar cell-cycle localization and gene knockout phenotype. *Curr Biol* *10*, 1319-28.
- Utsumi, M., Ohno, K., Onchi, H., Sato, K., and Tohyama, M. (2001). Differential expression patterns of three glutamate transporters (GLAST, GLT1 and EAAC1) in the rat main olfactory bulb. *Brain Res Mol Brain Res* *92*, 1-11.
- Utsunomiya-Tate, N., Endou, H., Kanai, Y., Avissar, N. E., Ryan, C. K., Ganapathy, V., Sax, H. C., Tetsuka, K., Takanaga, H., Ohtsuki, S., Hosoya, K., and Terasaki, T. (1996). Cloning and functional characterization of a system ASC-like Na<sup>+</sup>-dependent neutral amino acid transporter. *J Biol Chem* *271*, 14883-90.
- Uwanogho, D., Rex, M., Cartwright, E. J., Pearl, G., Healy, C., Scotting, P. J., and Sharpe, P. T. (1995). Embryonic expression of the chicken Sox2, Sox3 and Sox11 genes suggests an interactive role in neuronal development. *Mech Dev* *49*, 23-36.
- Van Gelder, R. N., von Zastrow, M. E., Yool, A., Dement, W. C., Barchas, J. D., and Eberwine, J. H. (1990). Amplified RNA synthesized from limited quantities of heterogeneous cDNA. *Proc Natl Acad Sci U S A* *87*, 1663-7.
- van Praag, H., Christie, B. R., Sejnowski, T. J., and Gage, F. H. (1999). Running enhances neurogenesis, learning, and long-term potentiation in mice. *Proc Natl Acad Sci U S A* *96*, 13427-31.
- van Praag, H., Schinder, A. F., Christie, B. R., Toni, N., Palmer, T. D., and Gage, F. H. (2002). Functional neurogenesis in the adult hippocampus. *Nature* *415*, 1030-4.

- Velculescu, V. E., Zhang, L., Vogelstein, B., and Kinzler, K. W. (1995). Serial analysis of gene expression [see comments]. *Science* *270*, 484-7.
- Vestweber, D., and Kemler, R. (1984). Rabbit antiserum against a purified surface glycoprotein decompacts mouse preimplantation embryos and reacts with specific adult tissues. *Exp Cell Res* *152*, 169-78.
- Voigt, T. (1989). Development of glial cells in the cerebral wall of ferrets: direct tracing of their transformation from radial glia into astrocytes. *J Comp Neurol* *289*, 74-88.
- Wakamatsu, Y., Endo, Y., Osumi, N., and Weston, J. A. (2004). Multiple roles of Sox2, an HMG-box transcription factor in avian neural crest development. *Dev Dyn* *229*, 74-86.
- Wang, D. D., Krueger, D. D., and Bordey, A. (2003). GABA depolarizes neuronal progenitors of the postnatal subventricular zone via GABAA receptor activation. *J Physiol* *13*, 13.
- Wichterle, H., Garcia-Verdugo, J. M., and Alvarez-Buylla, A. (1997). Direct evidence for homotypic, glia-independent neuronal migration. *Neuron* *18*, 779-91.
- Winklbauer, R., Medina, A., Swain, R. K., and Steinbeisser, H. (2001). Frizzled-7 signalling controls tissue separation during *Xenopus* gastrulation. *Nature* *413*, 856-60.
- Wolfgang, C. L., Lin, C., Meng, Q., Karinch, A. M., Vary, T. C., and Pan, M. (2003). Epidermal growth factor activation of intestinal glutamine transport is mediated by mitogen-activated protein kinases. *J Gastrointest Surg* *7*, 149-56.
- Wu, J. Y., Feng, L., Park, H. T., Havlioglu, N., Wen, L., Tang, H., Bacon, K. B., Jiang, Z., Zhang, X., and Rao, Y. (2001). The neuronal repellent Slit inhibits leukocyte chemotaxis induced by chemotactic factors. *Nature* *410*, 948-52.
- Wu, W., Wong, K., Chen, J., Jiang, Z., Dupuis, S., Wu, J. Y., and Rao, Y. (1999). Directional guidance of neuronal migration in the olfactory system by the protein Slit. *Nature* *400*, 331-6.
- Xu, C., Liguori, G., Persico, M. G., and Adamson, E. D. (1999). Abrogation of the *Cripto* gene in mouse leads to failure of postgastrulation morphogenesis and lack of differentiation of cardiomyocytes. *Development* *126*, 483-94.
- Yamada, K., Watanabe, M., Shibata, T., Nagashima, M., Tanaka, K., and Inoue, Y. (1998). Glutamate transporter GLT-1 is transiently localized on growing axons of the mouse spinal cord before establishing astrocytic expression. *J Neurosci* *18*, 5706-13.
- Yan, Y. T., Liu, J. J., Luo, Y., E, C., Haltiwanger, R. S., Abate-Shen, C., and Shen, M. M. (2002). Dual roles of *Cripto* as a ligand and coreceptor in the nodal signaling pathway. *Mol Cell Biol* *22*, 4439-49.
- Ye, Z. C., and Sontheimer, H. (2002). Modulation of glial glutamate transport through cell interactions with the extracellular matrix. *Int J Dev Neurosci* *20*, 209-17.

- Ying, Q. L., Nichols, J., Chambers, I., and Smith, A. (2003). BMP induction of Id proteins suppresses differentiation and sustains embryonic stem cell self-renewal in collaboration with STAT3. *Cell* *115*, 281-92.
- Yokoi, M., Mori, K., and Nakanishi, S. (1995). Refinement of odor molecule tuning by dendrodendritic synaptic inhibition in the olfactory bulb. *Proc Natl Acad Sci U S A* *92*, 3371-5.
- Yoshida, Y., Kojima, N., and Tsuji, S. (1995). Molecular cloning and characterization of a third type of N-glycan alpha 2,8-sialyltransferase from mouse lung. *J Biochem (Tokyo)* *118*, 658-64.
- Zappone, M. V., Galli, R., Catena, R., Meani, N., De Biasi, S., Mattei, E., Tiveron, C., Vescovi, A. L., Lovell-Badge, R., Ottolenghi, S., and Nicolis, S. K. (2000). Sox2 regulatory sequences direct expression of a (beta)-geo transgene to telencephalic neural stem cells and precursors of the mouse embryo, revealing regionalization of gene expression in CNS stem cells. *Development* *127*, 2367-82.
- Zelenaia, O., Schlag, B. D., Gochenauer, G. E., Ganel, R., Song, W., Beesley, J. S., Grinspan, J. B., Rothstein, J. D., and Robinson, M. B. (2000). Epidermal growth factor receptor agonists increase expression of glutamate transporter GLT-1 in astrocytes through pathways dependent on phosphatidylinositol 3-kinase and transcription factor NF-kappaB. *Mol Pharmacol* *57*, 667-78.
- Zhu, Y., Yu, T., Zhang, X. C., Nagasawa, T., Wu, J. Y., and Rao, Y. (2002). Role of the chemokine SDF-1 as the meningeal attractant for embryonic cerebellar neurons. *Nat Neurosci* *5*, 719-20.
- Zimmer, C., Tiveron, M. C., Bodmer, R., and Cremer, H. (2004). Dynamics of Cux2 Expression Suggests that an Early Pool of SVZ Precursors is Fated to Become Upper Cortical Layer Neurons. *Cereb Cortex* *6*, 6.



## Acknowledgment

I am very grateful to Prof. Dr. Sigrun Korsching who supported this work through her supervision and her kind and helpful advice. I would like to thank Dr. Boris Stoffel for providing me with the opportunity to perform this doctoral thesis at Memorec Biotec GmbH, Cologne, and permitting its continuation also during uncertain times.

I am sincerely grateful to my supervisor at Memorec, Dr. Andreas Bosio, for “adopting” my PhD project. I thank Andreas very much for being such a competent, accurate and demanding supervisor, for his critical comments, useful advice and the continuous support.

I especially thank Dr. Harold Cremer for initiating this project and thereby the fruitful collaboration between Memorec and the Developmental Biology Institute of Marseille (IBDM). I am very grateful to Harold for constantly encouraging and motivating me, for his unshakable optimism, for the interesting scientific discussions and for -often daily- answering my questions via email and telephone. I would like to thank Harold’s group, namely Dr. Céline Zimmer, Dr. Marie-Catherine Tiveron, Dr. Ralph Seidenfaden, Damien Rei, Camille Boutin and Angelique Desoeuvre for welcoming me warmly at the IBDM and teaching me several experimental methods. I appreciate especially Céline’s hospitality. I thank Dr. Richard Belvindrah for the great teamwork. Thanks to Marc Barad for assistance with FACS experiments.

I would like to thank Dr. Stefan Tomiuk and Dr. Kay Hofmann at Memorec for bioinformatical support and Michael Birth for his help during the SAGE. My thanks go out to my initial supervisor at Memorec, Dr. Marcus Conradt, who made an effort to get the project accepted at first. I thank Daniel Küsters and Sebastian Knöbel for giving me a hand with the Taqman experiments and the generation of EBs, respectively. I thank Prof. Dr. W. Stoffel and Christian Frie from the Biochemistry Institute, Cologne, for making vibratome and cryostat available to me. Thanks to Dr. Graeme Lowe for the permission to use his illustration of the olfactory system.

I am grateful to Dr. Stefan Tomiuk, Harmut Scheel, Alena Benschik, Dr. Frank Schacherer among others for enjoyable time-outs at lunch, jokes, discussions and advice. I appreciate the kindness and helpfulness of the Memorec colleagues.

I would like to thank everybody who encouraged me; notably Assunta Croce for exchanging many thoughts via email. Very special thanks go out to the Simmons family.

Ich danke von Herzen Christian, meinen Eltern, meinen Großeltern und meinem Bruder David, deren aller Beitrag durch ihre unendliche Unterstützung, starken Rückhalt, große Geduld, Trost, Ratschläge und ständige Aufmunterung hier mit den wenigen Worten nicht genug gewürdigt werden kann.

## Erklärung

Ich versichere, dass ich die von mir vorgelegte Dissertation selbständig angefertigt, die benutzten Quellen und Hilfsmittel vollständig angegeben und die Stellen der Arbeit - einschließlich Tabellen, Karten und Abbildungen -, die anderen Werken im Wortlaut oder dem Sinn nach entnommen sind, in jedem Einzelfall als Entlehnung kenntlich gemacht habe; dass diese Dissertation noch keiner anderen Fakultät oder Universität zur Prüfung vorgelegen hat; dass sie - abgesehen von unten angegebenen Teilpublikationen - noch nicht veröffentlicht worden ist sowie, dass ich eine solche Veröffentlichung vor Abschluss des Promotionsverfahrens nicht vornehmen werde. Die Bestimmungen dieser Promotionsordnung sind mir bekannt. Die von mir vorgelegte Dissertation ist von Frau Prof. Dr. Sigrun Korsching betreut worden.

Köln, September 2004

Sandra Pennartz

### Teilpublikationen:

Pennartz, S., Belvindrah, R., Tomiuk, S., Zimmer, C., Hofmann, K., Conradt, M., Bosio, A., and Cremer, H. (2004). Purification of neuronal precursors from the adult mouse brain: comprehensive gene expression analysis provides new insights into the control of cell migration, differentiation, and homeostasis. *Mol Cell Neurosci* 25, 692-706.

## Lebenslauf

### Persönliche Daten

Name: Sandra Pennartz  
Geburtsdaten: 2. Januar 1977 in Krefeld  
Familienstand: ledig

### Schule

08/87-06/96 Bischöfliche Maria-Montessori-Gesamtschule, Krefeld  
07/93-06/94 Morro Bay, Kalifornien, Stipendium des deutschen Bundestages,  
Parlamentarischen Patenschaftsprogramm, *High School Diploma*  
06/96 Abitur, Krefeld

### Hochschulausbildung

09/96-03/01 Studium der Biologie mit den Schwerpunkten Genetik, Biochemie und  
Botanik, Universität zu Köln  
07/98 Vordiplom in Biologie  
08/98 Praktikum im LFI der Uniklinik Köln  
10/98 Praktikum im Institut für Genetik, Prof. Rajewsky, Köln  
07-10/99 Neapel, Italien, Leonardo da Vinci-Stipendium, Praktikum im *Istituto  
Internazionale di Genetica e Biofisica*, CNR; Bearbeitung eines eigenen  
Projektes im Rahmen des Genetik-Praktikums der Universität zu Köln:  
“Molecular genetics of cuticulin genes in *C. elegans*: Analysis of the secretion  
process of CUT-1 using the reporter GFP“  
04/00 Diplomarbeit in der Memorec Biotec GmbH, Köln: „Biochemische und  
molekularbiologische Charakterisierung von hSAS10“; Betreuer der  
Universität zu Köln: Prof. Dr. A. Tarakhovsky  
03/01 Abschluss als Diplom-Biologin  
06/01-11/04 Promotionsarbeit in der Memorec Biotec GmbH, “Gene expression analysis of  
neuronal precursor from adult mouse brain and differential screen for neural  
stem cell markers”, Betreuerin der Universität zu Köln: Prof. Dr. S.  
Korsching, Kollaboration mit dem *Developmental Biology Institute of  
Marseille*, Frankreich  
11/04 Voraussichtlicher Abschluss der Promotion an der Universität zu Köln  
Köln, 4. Juli 2004